METC/SP-79/3
Distribution Category UC-92a

THE APPLICATION OF FRACTOGRAPHY TO CORE AND OUTCROP FRACTURE INVESTIGATIONS

Prepared by:

B.R. Kulander, C.C. Barton and S.L. Dean

March 1979

Prepared for:

UNITED STATES DEPARTMENT OF ENERGY
Morgantown Energy Technology Center
Morgantown, West Virginia

Under
Purchase Order No. EY-77-Y-21-1391

METC/SP-79/3
Distribution Category UC-92a

THE APPLICATION OF FRACTOGRAPHY TO CORE AND OUTCROP FRACTURE INVESTIGATIONS

Prepared by:

B.R. Kulander, C.C. Barton and S.L. Dean

March 1979

Prepared for:

UNITED STATES DEPARTMENT OF ENERGY
Morgantown Energy Technology Center
Morgantown, West Virginia

Under
Purchase Order No. EY-77-Y-21-1391

CONTENTS

LIST OF ILLUSTRATIONS

FRACTOGRAPHY IN HYDROCARBON EXPLORATION AND DEVELOPMENT

As prime drilling areas disappear, hydrocarbon companies must seriously consider prospects that have proved to be unsuccessful or marginally successful in the past. Often production from these reservoirs is primarily controlled by fracture permeability. Thorough fracture investigations of well cores and outcrops are essential to any complete evaluation of these reservoirs -- and any complete examination must be based on fractographic principles.

Fractography can assist in the solution of problems inherent in any surface or subsurface fracture investigation. It is known that at some critical propagation velocity a fracture may bifurcate, also in a rapidly changing stress field a fracture might break into twist hackle. Can this knowledge, along with other mechanisms that may increase fracture surface area, be applied to artificial fracture stimulation procedures, specifically secondary porosity and permeability? The application of fractographic principles should prove to be a valuable tool for geologists who have for too long been overly dependent on geometrical implications when interpreting fracture genesis and trends. In this vein fractography can assist in determining the following items all of which are related to secondary natural or induced porosity and permeability.

1) regional fracture trends
2) relative fracture chronology
3) intrastratum stress distribution during fracturing
4) fracture propagation directions
5) fracture origin
6) changes in fracture velocity
7) singular fracture events
8) fracture density

The mastery of fractographic terminology and proper application of fractographic principles also permits recognition of regional as well as local fracturing stress distributions and resulting leading portions of a fracture front at any time past. For example if a given fracture set has propagated from the basement up then fracture surface morphology on a given stratum should reflect this stress distribution. To assist the application of fractography to rocks the authors propose a fractographic reclassification of fracture surface structures.

Geologists involved in basin investigations can appreciate the value of a meaningful fracture analysis. The determination of fracture sets, coupled with an appreciation of their spatial and genetic relationship with other structures can give valuable information on changes in principal stress directions through time. It is also possible, by applying fractographic principles, to identify regional fracture trends that may be unrelated to, and pre or post date, surrounding structures. Such a pervasive fracture trend may prove to be a prime factor in development of directional permeability and thus hydrocarbon migration.

The Department of Energy - Morgantown Energy Technology Center, is pleased to offer this professional paper for your examination. The report will assist individuals engaged in academic and energy-related field and laboratory fracture research. The paper describes the morphology and inception mechanics of fracture surface features observed in well cores and outcrop. A chapter discussing selected basic mechanical aspects of the fracture process supports these sections. Other chapters suggest fractographic field and laboratory investigation procedures.

THE APPLICATION OF FRACTOGRAPHY TO CORE AND OUTCROP FRACTURE INVESTIGATIONS

By

Byron R. Kulander1/, Christopher C. Barton2/, Stuart L. Dean3/

CHAPTER 1

INTRODUCTION

Individuals working in the fields of structural geology and rock mechanics today are generally aware of the often cited failure hypotheses applied to rock fractures propounded by Coulomb (1773), Mohr (1882), Griffith (1920, 1925), McClintock and Walsh (1962). However, the application of basic fractographic principles to the study of rock fractures has not been recognized by many geologists engaged in field and laboratory investigations. This unfortunate situation persists even though the theories basic to the correct interpretations of fracture surface structures have been available in ceramic, glass science, and metallurgical journals for decades. Therefore, the major purpose of this paper will be to introduce geologists to the principles of fractography, especially those principles that govern the formation of fracture surface structures commonly observed in rocks.

A knowledge of the inception mechanics governing the formation of a fracture's tendential and transient structures should accomplish the following goals, each elaborated upon in appropriate sections of the text:

- provide geologists with a method to distinguish natural from coring-induced and handling-induced fractures in oriented core samples;
- show how coring-induced fractures may be assisted in their formation by stresses that can be attributed to the drilling process;
- provide a sound basis for the planning of proposed outcrop fracture studies;

1/ Department of Geology, Wright State University, Dayton, Ohio 45435
2/ Department of Geology and Geophysics, Yale University, New Haven, Conn., 06502
3/ Department of Geology, University of Toledo, Toledo, Ohio 43606

- simplify local and regional fracture investigations by eliminating the time-consuming collection of meaningless data;

- stress the importance of determining singular fracture events and their sequential development, and provide the basis for determining these events;

- increase the awareness of fracture information that should be obtained to facilitate a meaningful interpretation of field data -- including any statistical analysis procedure, and fracture relationships, both genetic and geometrical, to other anisotropies and adjacent structures;

- provide constraining stress parameters that any quantitative stress analysis must satisfy in order to be valid;

- provide information that will permit the cause of rock failure and the conditions under which it occurred to be ascertained.

The paper also includes:

- a number of descriptive examples illustrating the qualitative and quantitative application of fractography to geological problems;

- a review of several important concepts pertaining to fracture inception and propagation mechanics;

- a genetic reclassification of Hodgson's (1961) classification of joint surface structures.

If geologists engaged in any investigation relying upon the proper interpretation of fracture events are aware of the applications of and principles governing the topics mentioned above, it may be possible to base the interpretation of any given outcrop fracture set on something other than its geometrical relationship to adjacent fractures and surrounding structures. This worthwhile goal carries over to the investigation of fractures present in oriented core samples. Here, where only a small area of any natural fracture plane is extracted for observation, fractography is the only reliable tool available for distinguishing natural fractures cut by the drill from coring-induced and handling fractures.

It is emphasized that any single fracture does not form at the same instant, throughout the fractured rock body. A fracture develops at varying propagation velocities. Its path and behavior, from inception at a discrete origin to conclusion, is governed by changing static and dynamic stresses and the chemical and mechanical properties of the rock itself. Any brittle fracture is propagated in a plane perpendicular to the greatest effective tension, and any transient or tendential variation of that fracture plane occurs in response to a change in the principal tension direction. Conjugate

"shear" fracture sets, easily produced in plastic clay or in rocks under compression at elevated confining pressures and temperatures, should not be regionally common in undeformed foreland rocks that were never deeply buried or subjected to elevated temperatures. Any strike-slip or shear movement made evident by offsets or slickensides occurred after the fracture surface formed. The distinctive fracture characteristics of certain minerals (conchoidal fracture), fractures initiated artificially in natural fuel or water reservoir rocks, and the myriad of brittle fractures (flow features excluded) evident in intensely folded and faulted strata are all attributed to the same mechanical principles that are responsible for regionally developed joint sets. A joint is a fracture; it has formed in direct response to a mechanical stress just like any other fracture. Therefore, the term "fracture" is used throughout this paper for any failure plane along which no appreciable movement has occurred.

CHAPTER 2

ACKNOWLEDGEMENTS

This report was written under a contract issued by the Department of Energy - Morgantown Energy Technology Center (DOE). Individuals presently employed at DOE-METC who have been of assistance are William Overbey and Claude Dean. The authors also thank Rick Williams, a friend and co-worker who has generated any number of ideas (and arguments) in countless fracture discussions. Rick also donated several of the illustrations used in the text.

Dr. Claude Dean suggested the adopted terms for various coring-induced fractures (petal-centerline, disc, knife edge spall) and the term "handling-induced fractures." In fact, unbeknown to the authors, Claude's early research on the origin and classification of core fractures proceeded concurrently with ours.

The authors would like to express their appreciation to Dr. VanDerck Frechette, professor of ceramic science at the New York State College of Ceramics at Alfred University. Professor Frechette, along with being a recognized expert in the field of fractography, also possesses a firm grasp of geological principles. Through this unusual combination of knowledge he was able to introduce the authors to fractographic principles and their geological application. This fractographic education was delightfully administered both in the classroom and through many informative discussions.

Dr. Eugene Moores, a geologist with Sunmark Exploration Company, read the manuscript and offered valuable advice based on a petroleum geologist's point of view. The one-page summary titled "Fractography in Hydrocarbon Exploration and Development" was written at his suggestion.

An early draft of this paper was read by Dr. Russell Wheeler. His suggestions and constructive criticism were very helpful.

CHAPTER 3
SELECTED MECHANICAL ASPECTS OF FRACTURE

Joints as fractures

Joints are defined as fractures. While this definition may seem geologically specific, in reality, it places broad limits around what can be considered 'fracture.' This becomes more apparent when an attempt is made to determine whether a particular fracture represents brittle failure or ductile failure, fracture mode I, II, or III or some combination of modes, etc. (The three fracture modes are illustrated in figure 1.) One fracture feature that may be particularly useful in narrowing down these possibilities is the presence of specific fracture surface structures discussed in ensuing sections of this text. These structures have been experimentally produced by mode I fracturing of brittle solids. However, it is not clear whether these kinds of structures are limited to mode I fractures. It is possible that this fracture surface morphology may also be found on combined mode and semi-brittle fracture surfaces. From experiment it is known that modes II and III can give rise to completely different kinds of surface structures. In addition, ductile fracture produces a characteristic fracture surface morphology, regardless of mode. So, where present, specific types of fracture surface structures might be considered indicative of brittle or semibrittle fracture by a process dominantly mode I. On the other hand, the absence of these structures on a fracture surface can not be taken to infer anything about the mode or material state at the time of jointing. Considering all joint types, columnar joints, sheeting joints and perhaps the ac and bc systematic joints most closely approach mode I fracture of brittle rock. Most of the disk fractures discussed in other parts of this text are also of this type.

Mode I fracturing of brittle solids has been selected for elaboration because this mode most likely applies to common fracture types. Also, these fracture conditions are fundamental, for they form the initial evidence from which fracture theory was developed.

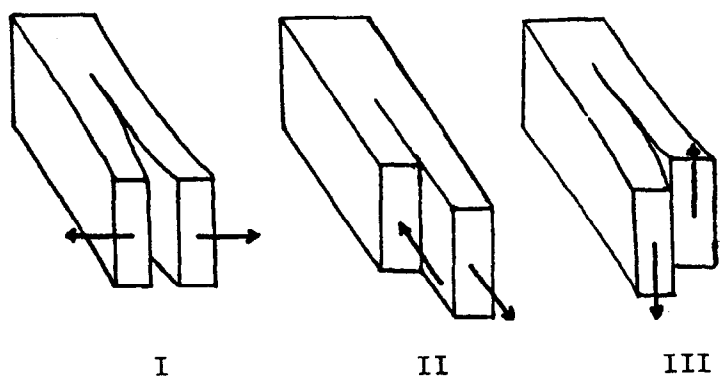

Figure 1, the three modes of fracture:

I - opening mode
II - sliding mode
III - tearing mode

Fracture theory

Concomitant with the industrial revolution, man began to build large girdered structures which placed the component materials under considerable stress. The engineers erecting such structures quickly recognized the need to stay within the elastic limits of the component members. It followed that the theory of elasticity and the sophistication of deformation experiments to determine the elastic properties of materials advanced rapidly in response to engineering needs. For example, it was known that the behavior of materials within their elastic limits could be evaluated from measurable material constants. Therefore, a reasonable extension of these ideas was the concept of a 'critical stress constant' for a material, at which failure would occur. However, early laboratory experiments and the failure (sometimes spectacular) of engineering structures indicated that the fracture strength of a material was not highly reproducible. In fact, the failure stress could vary several orders of magnitude even under the same loading conditions! It was equally well known that the tensile strength of a material was generally much lower than the theoretical strength. Not until the second and third decade of this century were reasonable explanations offered for what appeared to be highly variable material properties.

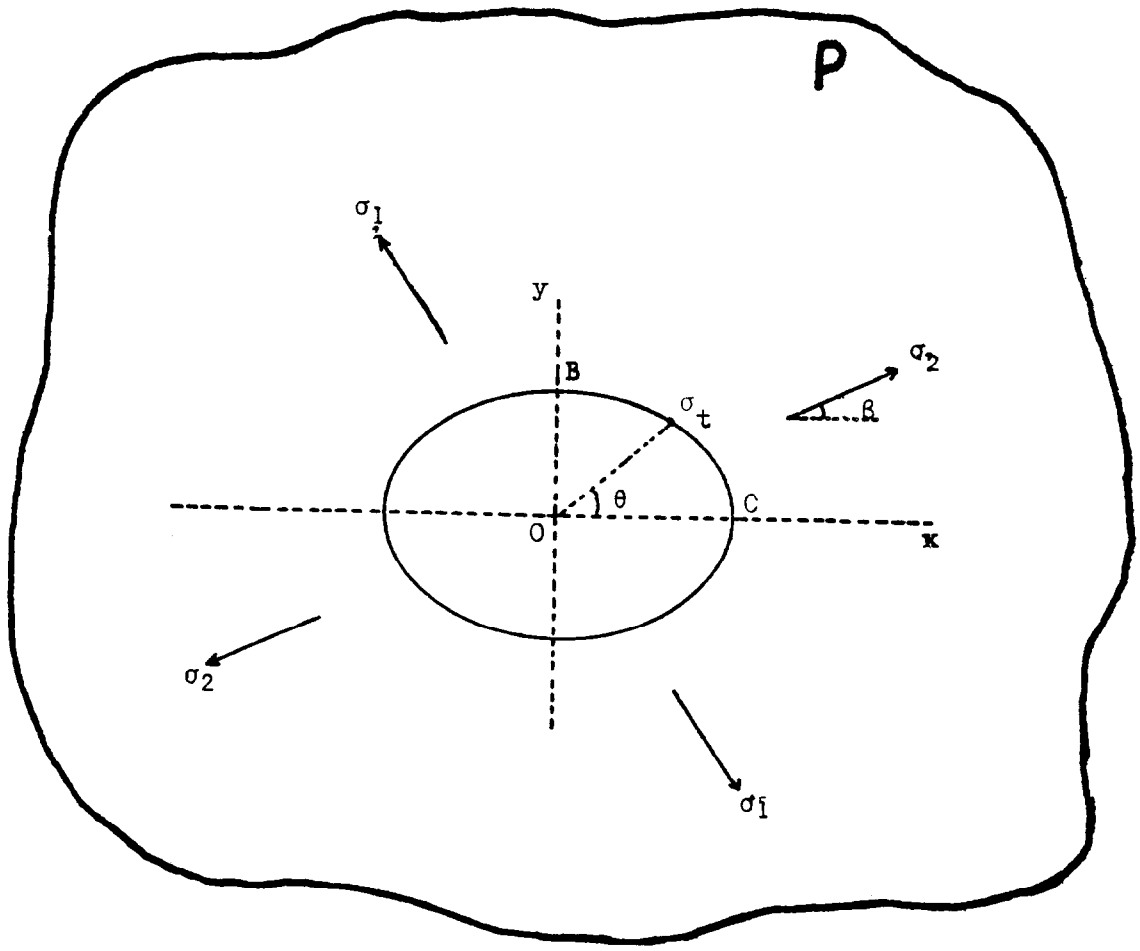

Figure 2, plate P containing an elliptical hole with stresses σ_1 and σ_2 at infinity and tangental surface stress σ_t located by polar angle θ.

Inglis and the stress concentration factor

The first step forward in understanding the variability of fracture strength was the work of Inglis (1913) on the effect of notches and elliptical holes on the internal stress distribution within a uniformly stressed plate. Inglis' stress analysis shows that local stresses at sharp corners can in fact be several times higher than the uniform stress applied at the outer boundaries. Thus, as Inglis recognized, small flaws could be a potential source of weakness in solids, and the Inglis solutions, taken to the limiting case of an infinitesimal narrow ellipse, could be considered as a model crack.

The modification of the stress distribution in the region of an elliptical hole in an infinite plate has become a classic problem in the study of elasticity theory. The problem was first solved by Inglis in the following manner. Consider, as in figure 2, an infinite plate P containing an elliptical hole with major axis of length 2C and minor axis of length 2B. Now establish a Cartesian coordinate system with the origin O in the center of the ellipse, semi-axis C along the x axis and semi-axis B along the y axis. The principal stresses at infinity are σ_2 inclined at angle β to OX and σ_1 inclined at angle $1/2\pi + \beta$ to OX. For the analysis, assume: (1) Hooke's law holds everywhere in the plate, i.e, the plate is linear elastic material ; (2) the boundary of the hole is stress free (a requirement of equilibrium); (3) the axes of the ellipse are small compared to the dimensions of the plate. With these assumptions, the problem reduces to a relatively straightforward exercise in linear elasticity. The mathematical treatment, however, becomes somewhat unwieldy. The most important quantity to emerge from the analysis is the stress tangential to the surface of the hole, σ_t. The general result is:

$$\sigma_t = \frac{2CB\,(\sigma_1 + \sigma_2) + (\sigma_1 - \sigma_2)\,[(C + B)^2 \cos 2\,(\beta-\eta) - (C^2 - B^2)\cos 2\beta\,]}{C^2 + B^2 - (C^2-B^2)\cos 2\eta} \qquad (1\text{-}1)$$

(see Jaeger and Cook, 1976 §§10.11)

where C and B are the major and minor semi-axis of the ellipse, σ_1 and σ_2 are the principal stresses at infinity. β is the angle between OX and σ_2. The elliptical coordinate is related to the polar angle θ of polar coordinates $x = r\cos\theta$, $y = r\sin\theta$ by $\tan\theta = y/x = B/C\tan\eta$.

The form of this equation can be examined where $\sigma_1 = 0$ for two cases of interest. In case 1: σ_2 is at right angles to the major axis of the ellipse, and in case 2: σ_2 is parallel to the major axis of the ellipse.

With $\sigma_1 = 0$ equation (1-1) reduces to:

$$\sigma_t = \sigma_2\left[\frac{2BC + (C^2-B^2)\cos 2\beta - (C+B)^2\cos 2(\beta-\eta)}{C^2 + B^2 - (C^2-B^2)\cos 2\eta}\right] \qquad (1\text{-}2)$$

Case 1

The geometry of case 1 is set out in figure 3a. Here $\beta = 90°$. Figure 4 is a plot of the solution for the ellipse where C = 3B as θ varies from 0 to 180°. Note that the greatest stress concentration occurs at the point C, the point of maximum curvature. At C equation (1-2) further reduces to:

$$\sigma_t(C,0) = \sigma_2(1 + 2C/B) \qquad (1-3)$$

Note that for an ellipse where $B << C$ equation (1-3) reduces to:

$$\sigma_t(C,0) \simeq \sigma_2(2C/B) \qquad (1-4)$$

The ratio 2C/B is commonly referred to as an elastic stress concentration factor.

At the end of the minor axis, point B, $\theta = 90$ and equation (1-2) reduces to $\sigma_t = -\sigma_2$, that is, equal to σ_2 but opposite in sense.

Case 2

The geometry of Case 2 is set out in figure 3b. Here $\beta = 0$. Examination of the plot of equation (1-2) for the ellipse C = 3B, as θ varies from 0 to 180°, shows that at point C, $\sigma_t = -\sigma_2$. At point B, equation (1-2) reduces to:

$$\sigma_t = \sigma_2 (1 + 2B/C) \qquad (1-5)$$

Note that for both cases the maximum stress concentration is parallel to the direction of applied stress, but that the stress concentration factor is much smaller for a larger radius of curvature. Also note that when σ_2 is tensile, a greater magnification of that tensile stress occurs at point C in case 1 than at point B in case 2. In fact the greatest magnification occurs at C when the loading stress is directed perpendicular to the major axis of the ellipse. So for a material full of randomly oriented elliptical flaws, those flaws oriented with long axes perpendicular to the applied stress will act as the greatest stress concentrators.

Another aspect worth considering is the stress variation along OX away from C for the loading geometry shown in figure 3a. Figure 5 is a plot of the stresses σ_{yy} and σ_{xx} for the ellipse where C = 3B. Note that σ_{yy} drops off quickly from its maximum value and approaches asymptotically the value of σ_2. σ_{xx} on the other hand rises rapidly from a value of zero, to peak and then approaches zero asymptotically at approximately the same rate that σ_{yy} approaches σ_2. So we see that the high stress gradients are within a distance $\simeq \rho$ (the radius of curvature at C) from C, and that the concentration diminishes within a distance $\simeq$ C from C.

Inglis's analysis proves that the stress at the tip of a highly curved region can actually be many times the value of some distantly applied uniform stress. However, in extending this analysis by considering an ellipse as a model crack system, the analysis falls short of a complete explanation of crack properties. By Inglis's analysis, the stress concentration factor is dependent only on hole

shape and is size independent. Therefore, the Inglis treatment does not account for the fact that large cracks propagate more easily than small ones. Nor does it account for the fact that large flaws in the vicinity of small flaws serve as fracture origins. It was the incorporation of Inglis's analysis within the framework of an energy balance concept by A.A. Griffith (1920) that resulted in a criterion of failure.

The Griffith criterion of failure

The Griffith criterion of failure is based on reversible thermodynamics and the conservation of energy. Griffith's result for the boundary conditions within which it applies will now be derived. Consider the following system: assume an infinite plate of unit thickness. The plate is made of a material that is linearly elastic up to the point of failure. In this plate there exists an elliptical hole with its major axis oriented horizontally as in figure 3. With the plate clamped at the top, a load (L) is applied evenly across the bottom edge of the plate as shown in figure 6.

Now consider the following component energy terms for this system.

U_L is the work done by the load (L) in deforming the plate.

U_E is the strain potential energy stored in the plate during deformation.

U_S is the surface energy of the newly created fracture surface.

The total energy of the system U_{Total} is equal to some combination of U_L, U_E, and U_S. To determine how these energies are related, consider the system at two times: t_1 when the system is as described above, and t_2 after the crack has lengthened.

Consider now how crack propagation affects each term.

	U_L	U_E	U_S
At time t_1	0	U_{E_1}	U_{S_1}
At time t_2	U_{L_2}	U_{E_2}	U_{S_2}

The difference in each energy term from t_1 to t_2 is:

$$U_L = U_{L_2} - 0$$

$$U_E = U_{E_2} - U_{E_1}$$

$$U_S = U_{S_2} - U_{S_1}$$

Energy balance concept

The work done U_L contributes to an increase in U_E and U_S. Therefore, the work done must equal the sum of strain energy and surface energy increases; so it can be said that:

$$U_L = U_E + U_S \tag{2-1}$$

With the relation of U_L, U_E, and U_S known, the total energy for the system can be defined as:

$$U_T = -U_L + U_E + U_S \tag{2-2}$$

Now, remembering that fracture is here considered to be an equilibrium process, impose the constraint that $\partial U_T / \partial C = 0$ onto equation (2-2) so that:

$$0 = -U_L + U_E + U_S$$

or

$$U_L = U_E + U_S \tag{2-3}$$

Evaluation of energy terms

Two powerful concepts have emerged, (1) the stress concentration factor of Inglis and (2) the energy balance concept of Griffith. The concepts can be combined by using Inglis's solutions to evaluate each of the energy terms in equation (2-3). Consider, as Griffith did, the case of a narrow elliptical crack of length 2C, remote in an infinite plate with a uniaxial tensile stress field.

The mechanical energy term U_L, the work done by loading, is equal to twice the strain energy, equation (3-1). This relationship is a result derived from linear elastic theory for a body under constant applied stress during crack extension. To see this solved see Jaeger and Cook (1976, §§ 120, 121).

$$U_L = 2U_E \tag{3-1}$$

The strain energy term U_E can be calculated from Inglis's solution of the stress and strain fields for each volume element about the crack, and then integrated over dimensions large compared with the length of the crack. The result for a crack of unit width is:

$$U_E = \pi C^2 \sigma_L^{\,2}/E \qquad \text{(3-2a) for plane stress, i.e. for a thin plate, lateral boundaries unclamped (not restrained).}$$

and

$$U_E = \pi(1-\upsilon^2)\, C^2\sigma_L{}^2/E \qquad \text{(3-2b) for plane strain, i.e. lateral boundaries clamped (restrained).}$$

where σ_L is the applied tension normal to the crack plane,

E is Young's modulus,

υ is Poisson's ratio,

2C is the length of the internal crack.

To see how equations (3-2a & b) were derived, see Jaeger and Cook (1976,§§ 12.2).

The surface energy term per unit width of crack is:

$$U_S = 4C\gamma \qquad (3\text{-}3)$$

where γ is the free surface energy per unit area,

2C is the length of an internal crack.

Substituting the above values for U_L, U_E and U_S into equation (2-2), it is apparent that the total energy of the system U_T is:

$$U_T = -\pi C^2\, \sigma_L{}^2/E + 4C\gamma \qquad \text{(3-4a) for plane stress}$$

and

$$U_T = -\pi C^2\sigma_L{}^2\,(1-\upsilon^2)/E + 4C\,\gamma \qquad \text{(3-4b) for plane strain.}$$

Now by invoking the equilibrium constraint that $\partial U_T/\partial C = 0$ equations (3-4 a & b) reduce to:

$$0 = -2\,\pi C\sigma_L{}^2/E + 4\gamma$$

or

$$\sigma_L = (2E\gamma/\pi C)^{1/2} \qquad \text{(3-5a) for plane stress}$$

and

$$0 = -2\pi C\sigma_L{}^2(1-\upsilon^2)/E + 4\gamma$$

or

$$\sigma_L = [2E\gamma/\pi C\,(1-\upsilon^2)]^{1/2} \qquad \text{(3-5b) for plane strain.}$$

Equations (3-5) comprise the Griffith criterion for failure. So given Young's modulus and a crack length C one can calculate the load stress σ_L at which the crack will grow. Likewise given a load stress σ_L one can calculate the maximum flaw size that can be tolerated. The elegance of the Griffith result is that it is founded

on the principle of energy balance and conservation. The limitations are that the result applies only to mode I constant loading of a remote elliptical crack in an infinite Hookean plate. Finally, Griffith did not include all the probable energy terms. There should undoubtedly be energy terms for plastic processes in the region of the crack tip, for the energy dissipated in shock waves, and for chemical effects. There should also be a kinetic energy term to account for the dynamic aspects of the fracture process.

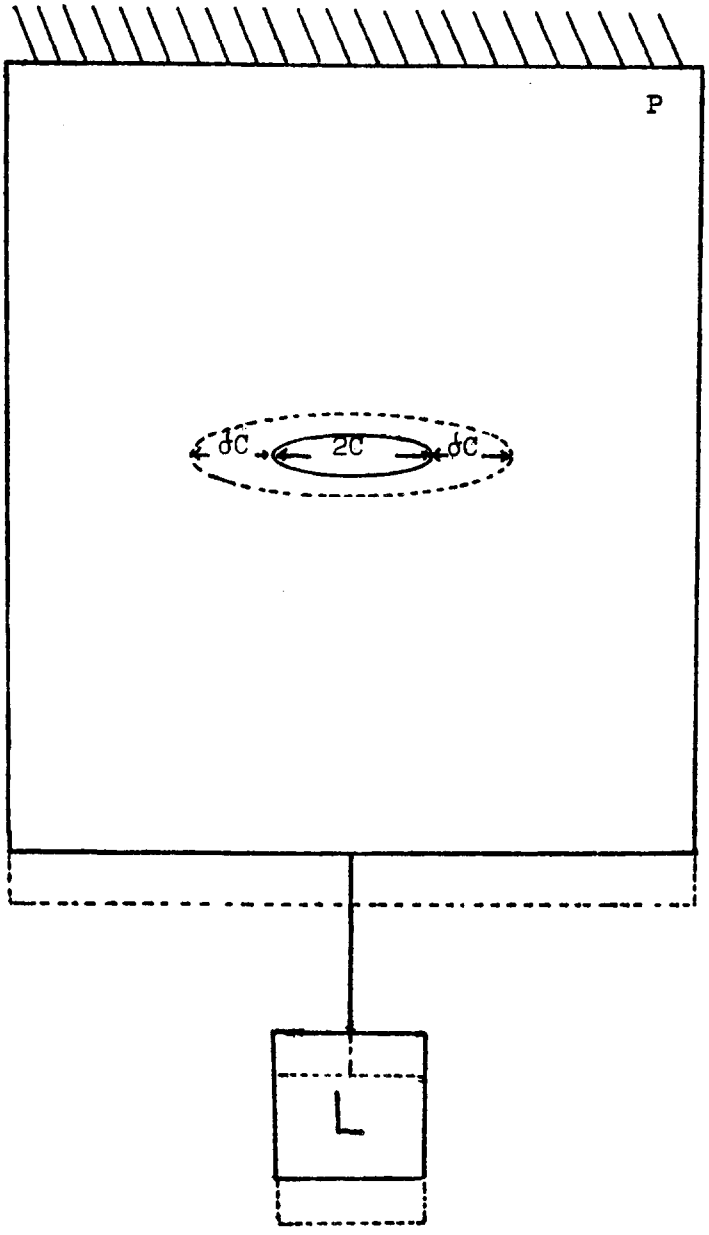

Figure 6, plate P clamped at top, with load L applied at bottom. Solid lines at time t_1 before crack extension. Dotted lines at time t_2 after crack extension δC.

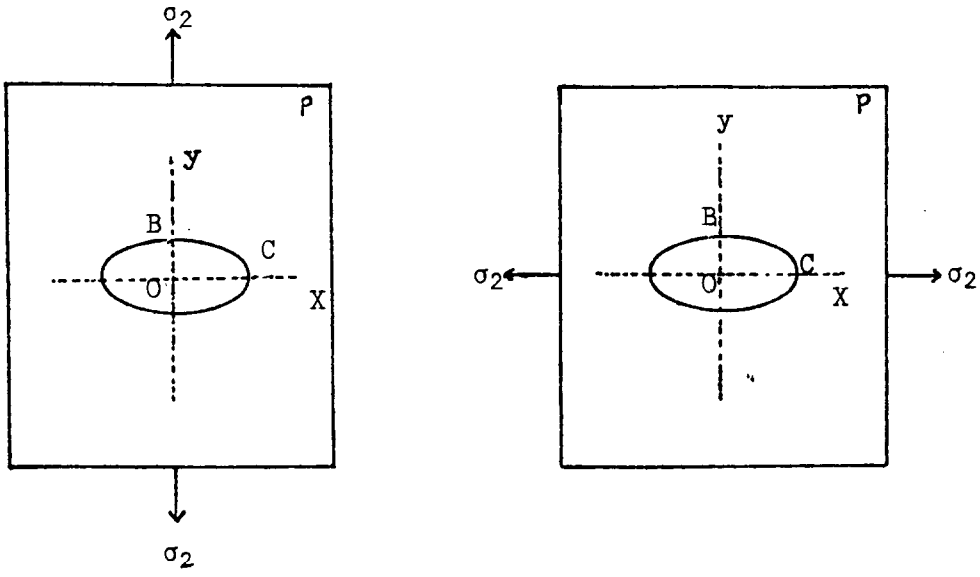

Figure 3, plates P containing elliptical holes, major axis 2C parallel to OX, subjected to uniform applied tension σ_2 oriented (a) $\beta = 90°$, (b) $\beta = 0°$.

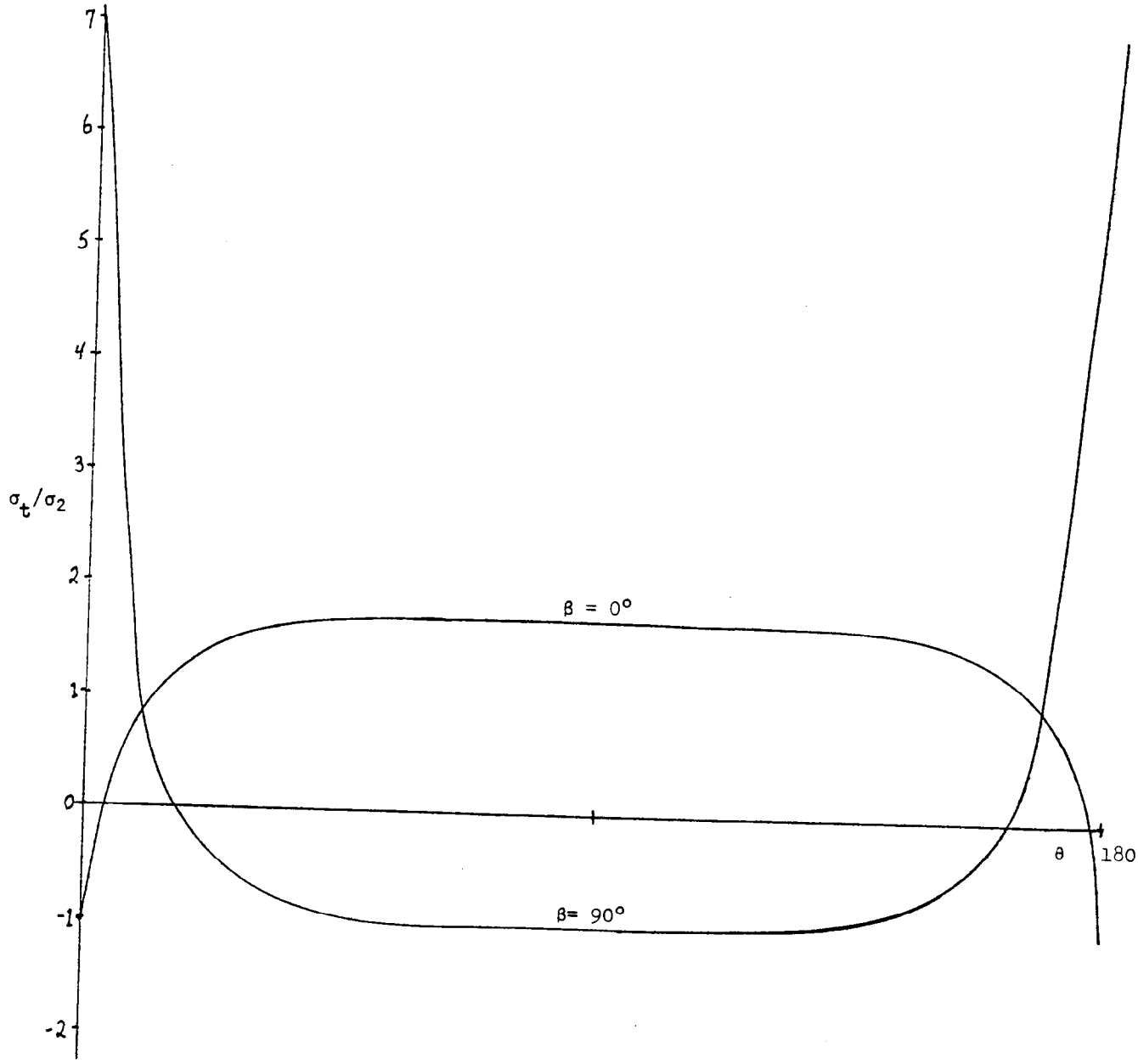

Figure 4, variation of the tangental surface stress σ_t with polar angle θ, for C = 3B.

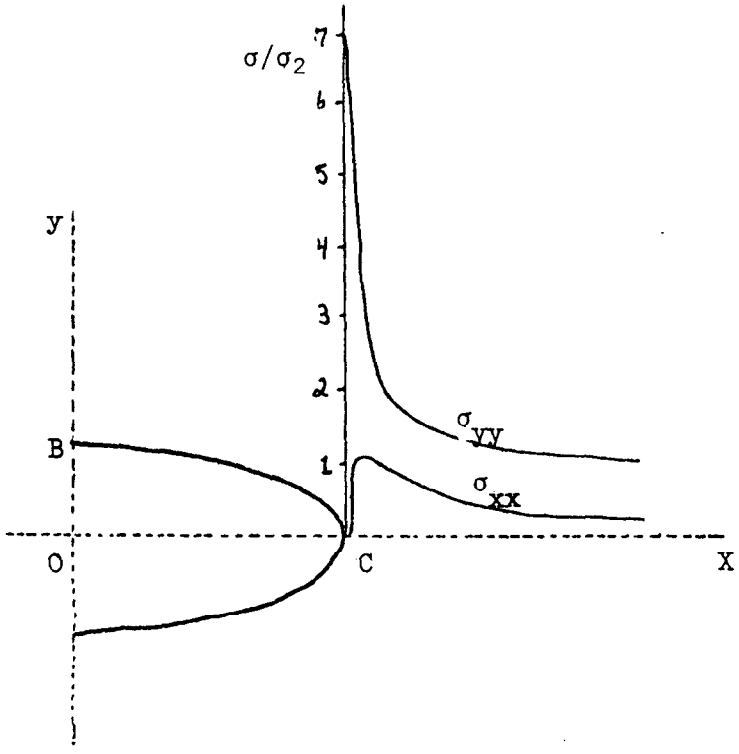

Figure 5, stress concentration away from the end of the major axis of an elliptical hole, C = 3B, loaded as in figure 3a.

Radius of curvature $\rho = B^2/C$

Limiting fracture velocity

Griffith energy balance concept extended to include dynamic processes

Griffith considered the static crack system before and after crack extension. He did not include energy terms for the dynamic processes that take place as the crack front is moving. Mott (1948) deals with this problem by adding a kinetic energy term U_K to the expression for total energy so that equation (2-2) becomes:

$$U_T = -U_L + U_E + U_S + U_K \qquad (4\text{-}1)$$

The kinetic energy term U_K can be evaluated for a linear elastic material by considering the motion of all volume elements within the crack system. The general result is:

$$U_K = 1/2\ \rho v_c^2 \iint_R [(\partial u_x/\partial C)^2 + (\partial u_y/\partial C)^2]\ dx\ dy \qquad (4\text{-}2)$$

where ρ is the material density

v_c is the crack velocity

u_x and u_y are components of displacement

R is the region within which the material experiences a disturbance from the propagating crack.

Consider now the case of a crack system with constant force loading. This loading condition will drive the unstable crack toward some terminal crack velocity which can be evaluated.

The following assumptions must be made to evaluate U_K :

(i) the stress and strains around a moving crack can be adequately defined by the equations of static elasticity theory (quasistatic approximation),

(ii) the region R includes the whole specimen,

(iii) the fracture surface energy γ remains invariant with crack velocity.

With these conditions, Mott argues that the integral in equation (4-2) can be evaluated for constant force loading by considering that (1) the field of the crack must scale with the characteristic length 2C, such that the dimensions x, y, u_x and u_y in the integral may be assumed proportional to C, (2) the displacements also scale with the strain level in the specimen so that the quantities $\partial u/\partial C$, become proportional to σ_L/E. Evaluation of the integral in (4-2) thus gives:

$$U_K = 1/2k\rho v_c^2\ C^2\ \sigma_L^2/E^2 \qquad (4\text{-}3)$$

where k is a numerical constant.

Adequate information is now available to evaluate another important aspect of the fracturing process. This aspect is the limiting velocity of a crack. Thus far, the case of constant force loading, which accelerates the growing crack, has been considered. But as will be shown, crack acceleration does not continue to infinity. Instead the crack velocity v_c approaches a limiting value.

Begin by substituting the values of U_L, U_E and U_S into equation (4-1). The result is:

$$U_T = -\pi C^2 \sigma_L^2/E + 4C\gamma + U_K \qquad (4\text{-}4) \text{ for } C \geq C_o \text{ for plane stress.}$$

where C_o = initial crack length, and C = some crack length $\geq C_o$. Note that when $C = C_o$ the crack is at rest and $U_K = 0$, so that the static equilibrium equation (3-5a) is still satisfied, and $4\gamma = 2\pi\sigma_L^2 C_o/E$. With the above serving as initial conditions it is possible to evaluate the constant U_T and eliminate γ. First substitute the value for U_K from equation (4-3) into equation (4-4). Then since it is assumed that U_T is constant during crack extension, equation (4-4) can be equated with equation (3-4a). For a complete analysis see Erdogan (1968). Solving the result for the crack velocity v_c yields:

$$v_c = (2\pi E/k\rho)^{1/2} (1-C_o/C) \qquad (4\text{-}5)$$

Looking at (4-5), it is seen that v_c approaches the value $(2\pi E/k\rho)^{1/2}$ as C approaches ∞. So it can be written:

$$v_{limiting} = (2\pi E/k\rho)^{1/2} \qquad (4\text{-}6)$$

Now, call on the equality $v_B^2 = E/\rho$, where v_B is the bar velocity for the material. So equation (4-6) becomes:

$$v_{limiting} = (2\pi/k)^{1/2} v_B \qquad (4\text{-}7)$$

A plot of $v_{C/v_{limiting}}$ versus C/C_o (figure 7) shows that v_c asymptotically approaches $v_{limiting}$ where $v_{limiting}$ has the value as defined in (4-7).

Experimentally determined values of $v_{limiting}$ range from 0.47 v_L for certain types of glass to 0.78 v_L for rolled tungsten (see Field 1971 table I), where v_L is the longitudinal wave velocity. Recently values of up to $.91V_t$ in glass have been reported by Snowden (1976). For elastic materials $v_L < v_B < v_D$, where v_D is the dilational stress wave velocity. The variation in the limiting velocity is apparently related to (1) the ability of the material to suppress bufurcation, (2) the extent of dissipative processes, and (3) chemical effects at the crack tip.

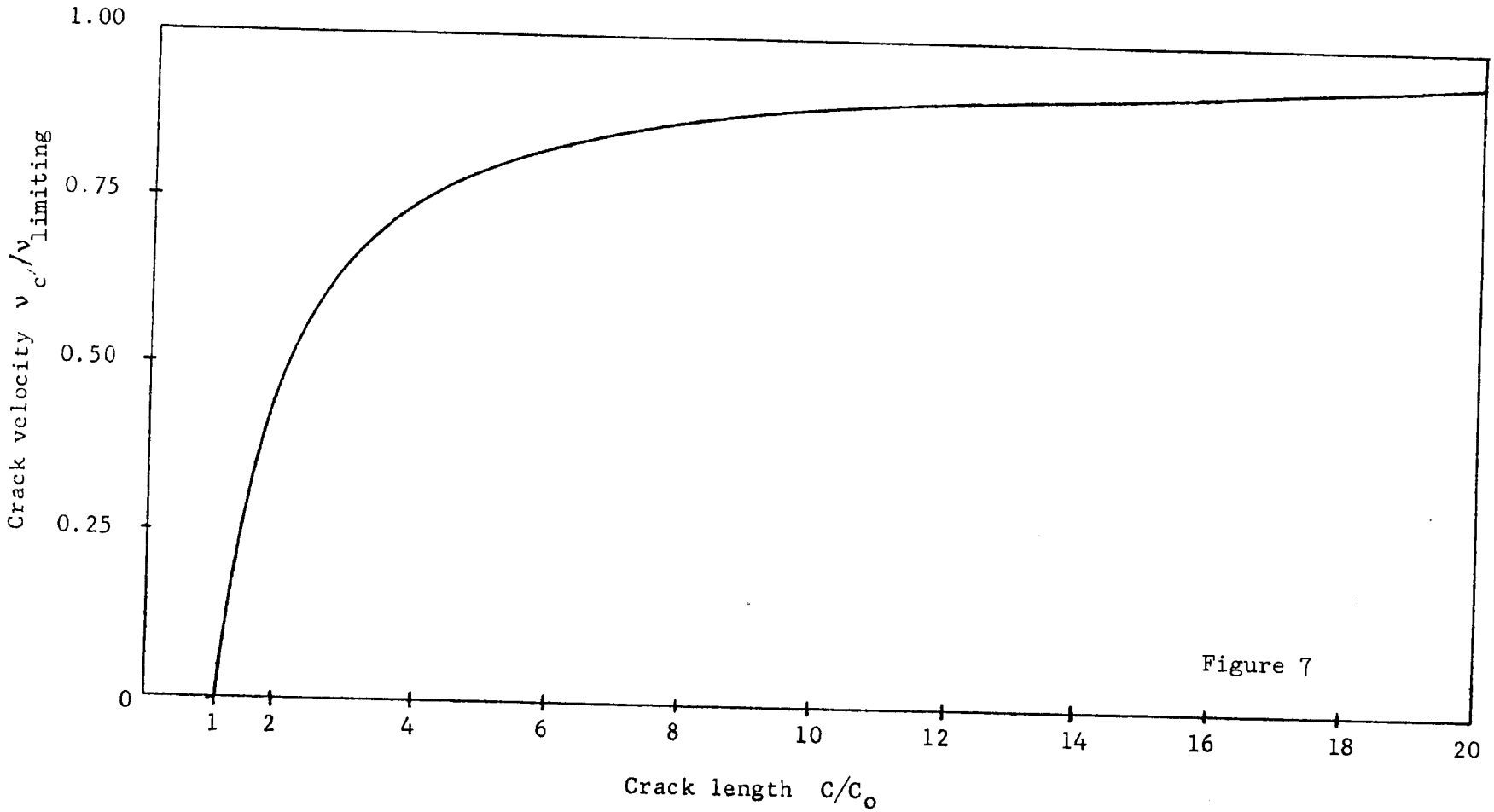
1.00
0.75
0.50
0.25
0
Crack velocity $v_{c'}/v_{limiting}$
1
2
4
6
8
10
12
14
16
18
20
Crack length C/C_o

Figure 7

CHAPTER 4

DIAGNOSTIC MORPHOLOGY OF FRACTURE FEATURES

The previous chapter has shown that the formation of a fracture must not be construed as an instantaneous event. Rather the growth of a complete fracture surface is accomplished as the fracture proceeds through a number of developmental stages. These stages leave a readable record of the progression, from inception to conclusion, of that fracture occurrence (fig. 8, 9). Any fracture is initiated at a discrete origin, and each successive stage is marked by a unique signature attributed to the combined effects of varying fracture velocity, fluctuating dynamic and static stress fields, and the fracturing material's mechanical properties. These signatures are quite simple to decipher, and take the form of large scale or small local undulations of the fracture plane.

Fracture surface characteristics are commonly classified as being either transient or tendential. Unfortunately all the described features in both categories are not present on all fractured rock surfaces. However, some are considerably more common than others.

Transient Fracture Features

Transient fracture features are short-range perturbations of the fracture surface. These surface structures are attributed to undulations of the advancing fracture front produced by fracture propagation velocity changes and local disruptions of the applied stress field. The applied stress field can be altered by:

1. Transverse and longitudinal waves;
2. A material's chemical and physical inhomogeneities; and
3. External alterations of the dominant stress field.

Transient surface features are best studied by observation perpendicular to the fracture face utilizing proper oblique illumination. Transient markings range in size from submicroscopic to a scale so large that they can be seen on a fracture surface from a considerable distance. Transient features observed on fracture faces formed in brittle and semibrittle substances, ranging from glass to polycrystalline material such as rocks, will be described in the following sections. Generally, transient structures are best developed on fracture faces in brittle amorphous substances such as glass, or fine-grained rocks like shale or basalt. A rule of thumb derived from numerous field observations of rock fracture faces is that transient morphology is poorly formed and/or becomes obscure as grain size and rock porosity increase.

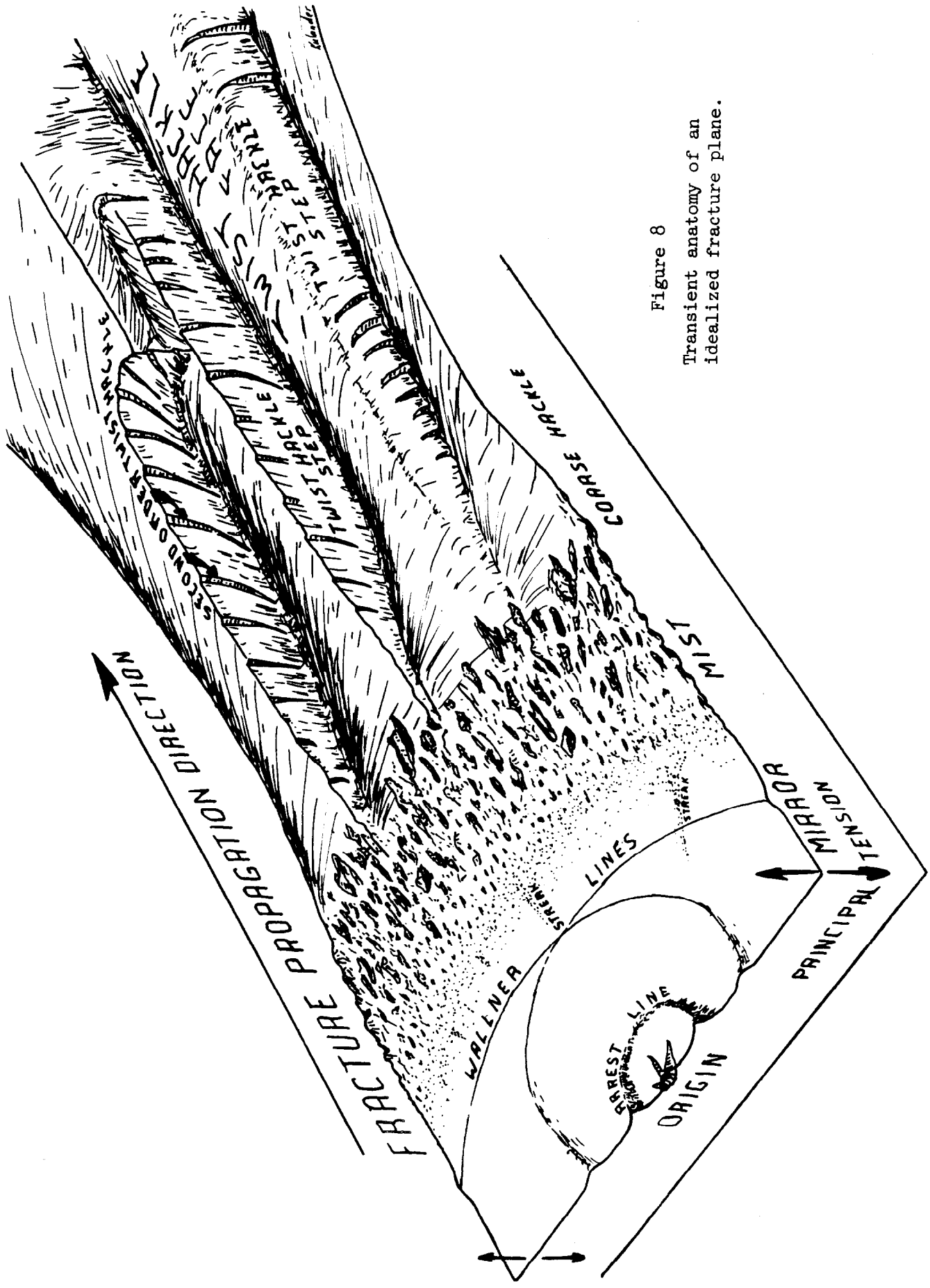

Figure 8
Transient anatomy of an idealized fracture plane.

Figure 9, transient anatomy of a fractured surface transecting a glass rod. The fracture spread from an origin located at the rod's surface (bottom photo). Note the sequential development of the mirror, mist, and coarse hackle regions. Disregard glass shards and chips scattered about the fracture surface. Scanning electron micrograph, 160X magnification. A and B show locations of Figures 13 and 19 respectively.

The fracture origin

The most important feature on a fracture surface is the fracture origin point. This is so because the origin and immediately adjacent regions often prove critical in determining fracture inception mechanics. The origin has been termed the focal point or focal pit by Kies, Sullivan, and Irwin (1950).

Any fracture attributed to a singular failure event has its inception at a discrete origin flaw (fig. 10, 11, 12). However, a single fracture displaying multiple origins is not uncommon in glass and ceramic materials, especially if the stress initiating failure was extremely violent. Frechette (1972) corroborates the observation that multiple origins are not unusual in glass and are even typical when failure is induced by rapidly applied large stresses. Multiple origins are also observed on natural fractures that penetrate rock strata containing numerous internal inhomogeneities. However, it should never be inferred that several origins on a single rock fracture require a large stress to failure value. Most rocks contain any number of flaws that may fail under low tensile stress. As a fracture advances, origins immediately ahead of the fracture front may open resulting in a single fracture or "joint" plane consisting of numerous coalescing fractures. Origins forming fractures

immediately to either side of any given advancing fracture could also relieve tensile stresses at the given fracture's tip, thereby limiting the extent and penetration of that fracture. Overlapping fractures of a given frequency could result, and fractures with a very large surface area attributed to a single origin should be rare.

Fracture origins always occur at a pre-existing flaw. In rocks, these flaws commonly prove to be fossils, concretions, large grains, or clasts, cementation and lithology variations, pores, bedding irregularities, and surface irregularities (fig. 10, 11), etc. Pre-existing fracture tips can also serve as origins. This origin point-flaw association is maintained because any prevailing or applied stress is magnified at flaw edges, thereby facilitating failure. In rocks, especially those of sedimentary origin, the number of flaws available as stress concentration points is enormous. Again this fact is one major reason for the overall low tensile strength of rocks and probable low to moderate rock fracture velocities.

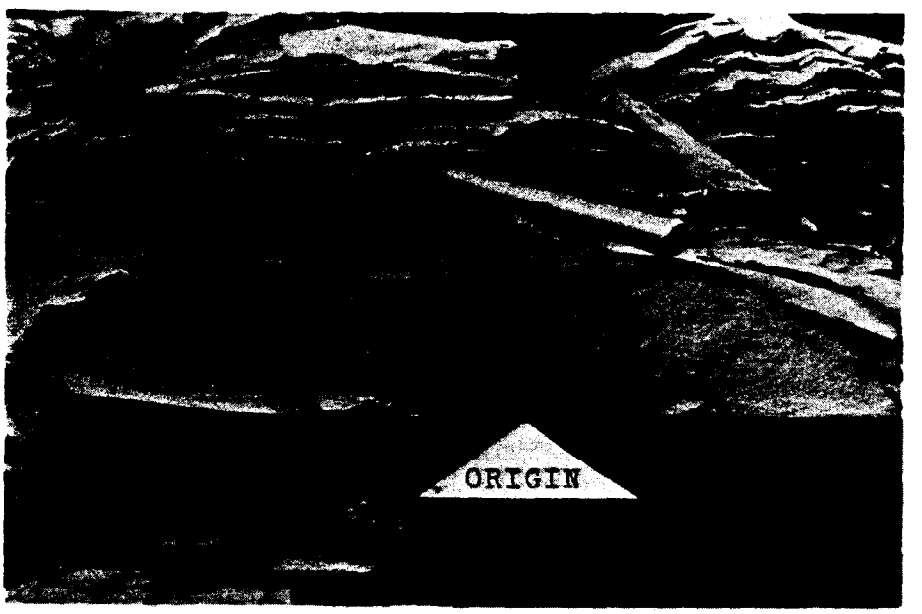

Figure 10, fracture origin at a pyrite nodule near the bottom of a Devonian sandstone stratum in western New York. Note the radiating hackle plumes and symmetrical arrest ridge along the hammer handle. The arrest line is further advanced along the basal stratum plane, indicating the fracture spread faster along the bottom stratum plane and progressively slower towards the vertical and stratum interior. Fracture propagation velocities are directly proportional to the applied tensile stress.

Figure 11, pelecypod that acted as an origin flaw. Cohesion across the fossil face was low or absent causing tensile stresses to peak at the fossil edges. (Fossil acted as an ellipsoidal Griffith crack.) Hackle radiates from the origin curving to meet the core boundary and earlier-formed vertical fracture orthogonally. Note arrest line also curves at boundary to maintain orthogonal relationship to hackle. (Core diameter equals four inches.)

Fracture origins in glass objects are almost always located at the surface which is exposed to abrasion, unless the glass is filled with impurities such as cords, seeds, etc. (Shand, 1967). However, in fractured rocks, origins are commonly located away from bedding or pre-existing fracture planes. The increased frequency of interior origin locations is attributed to the unhomogeneous nature of rocks as compared to glass.

The origin and immediately adjacent area in fine grained rocks or glass can be marked by a dimple (fig. 12). This dimple is produced when the fracture front curves in a very short distance from a plane containing the origin flaw into the plane perpendicular to the principal tension.

In outcrop fracture studies, the location of the origin, in relation to the top or bottom of each individual fractured stratum should be determined for as many individual fractures as possible. This procedure is critical when determining whether principal tension was parallel to layering and was most effective at the top or bottom of a given stratum. From this it can generally be ascertained whether fractures of a given set propagated from top to bottom or from bottom to top across a layer. The significance of the origin location, and its relationship to regional or local stresses is apparent. In horizontal or gently dipping layered rocks, for fractures originating at layer boundaries, the overall fracture propagation direction will become horizontal in a given stratum as the distance from the origin increases.

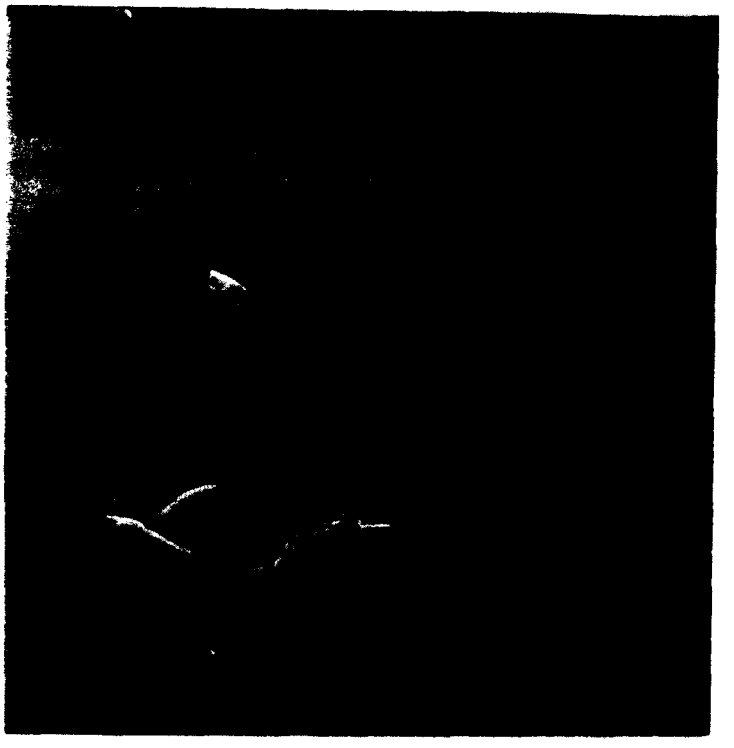

Figure 12, fracture origin at an inclusion (stone) along glass rod surface, previously shown in figure 9. Note the stepped dimple about the origin flaw. Steps are identical to twist hackle steps, discussed in a following section. Scanning electron micrograph, 1600X magnification.

Fracture origins and fracture velocity

The large number of potential origins in rocks, coupled with low tensile elastic strain energy, should lead to fracture velocities well below rock sonic velocities. For example, in controlled tests, Bieniawski (1968) measured terminal fracture velocities in crystalline low porosity norite. Measured velocities were 0.512 that of shear wave velocities in the same substance. A porous sandstone (many potential origins) or a poorly cemented shale should fracture at an even lower terminal velocity.

The combination of high porosity and low permeability, characteristic of many sedimentary rocks, can enhance fracture inception and propagation in another way. Secor (1965) recognizes that a total tensile stress of $\sigma_3 < 0$ is unlikely at depths characteristic of mineral filled fractures. He states that at these depths fractures propagate normal to a resultant or effective tensile stress ($\sigma_3$eff.) where:

$$\sigma_3 \text{ eff} = \sigma_3 - P_f$$

Here, P_f= fluid pressure. This relationship permits a $\sigma_3 < 0$, provided that $\sigma_3 < P_f$. Furthermore, Secor (1969) concludes that fracture growth by σ_3 eff proceeds slowly by intermittent short quick fracture episodes. Each fracture episode is interspersed with a nongrowth period that allows pore fluid to seep into the newly formed fracture segment, thereby allowing σ_3 eff to again reach fracturing stress proportions. Here, pore space is important as both a fluid reservoir and an essentially unlimited source of fracture origins.

The fact that fluctuating rock grain size and porosity may influence rock strength, stored elastic strain energy and related fracture velocities is suggested by investigations into the behavior of ceramic materials (Coble, 1958; Frechette, 1973) and metals (Orowan, 1949; Petch, 1954). Knudson (1959) summarizes previous works and proposes that the strengths (compressive, tensile, bending) of brittle polycrystalline glass-free substances such as ceramics and metals are inversely proportional to porosity (P) and grain size (G). Knudson expresses this strength (S), or stress to failure (σ_f), relationship as:

$$S = \sigma_f = k\, G^{-a} e^{-bP}$$

where K, a, and b are empirical constants and e is the Napierian number (2.71828...). If Knudson's relationship can be applied to rocks at both high and low formational temperatures, it may be expected that rocks of large grain size and/or high porosity could have more and larger potential fracture origins and lower initial fracture and ultimate failure strengths. These low strength values would lead to low fracture propagation velocities.

Frechette (1973) states that Knudson's empirical constants vary widely and that pore shape and average size must be considered. Also, Frechette indicates that a distinction must be made between closed and open pores. A large or sharp-edged pore is more likely to serve as a fracture origin. Evans and Tappan (1972) have also emphasized the role of flaws as stress concentrators and have indicated that flaw shape may directly influence stress to failure.

The origin flaw and shape factor is shown by Griffith (1920). He states that stress concentration at a crack tip is:

$$\sigma_c = \sigma_L [1 + 2\sqrt{L/r}]$$

where σ_c = crack tip stress, L = crack length, r = crack tip radius of curvature, and $\sigma_L \cong$ prevailing tensile stress. From Griffith's formula we see that stress concentration is inversely proportional to the radius of curvature at the crack tip, and directly proportional to crack length.

Frechette (1973), in the manner presented in chapter three, relates stress to failure with effective surface energy and elastic properties in a ceramic body subject to fracture. He has calculated the tensile stress to fracture (σ_f) for a crack propagating from an origin flaw as:

$$\sigma_f = K\, (2E\, \gamma i/C)^{1/2}$$

where γi = effective surface energy for fracture initiation, E = Young's modulus, C = surface flaw depth and K = constant depending on test configuration, flaw geometry and interaction between flaws. Frechette also states that where all surface flaws are small enough to allow the application of a large applied stress, viscous flow at a microscopic scale (σ_Y) may occur to the point where it cannot be ignored. This microplastic flow acts to concentrate stress at grain boundaries instead of surface flaws. When microplastic flow constitutes a critical proportion of the total strain, stress to failure (σ_f) is again (as in Knudson's relationship) indirectly proportional to grain size $(G)^{-1}$ instead of surface flaw depth (C) as shown by:

$$\sigma_f = K^{1} [\sigma_Y + K^{11} (2E\ \gamma i/G)^{1/2}]$$

Again K^{I} and K^{II} are empirical constants. In a metamorphic situation where microplastic flow contributes to overall strain, internal stresses cannot be neglected, and the uneven distribution of stresses attributed to varying elastic modulii must be considered.

All calculated stresses are not necessarily those required for fracture propagation and failure. Bieniawski (1967, part I) and Hoek and Bieniawski (1965) have shown that the stress required to initiate fracture in rocks is less than that needed to cause strength failure and rupture (σ_f). The difference between these stress values can be quite large in rocks subjected to compressive stress.

Brace (1964, 1971) also investigated the effect of grain boundaries on rock strength. He states that rock grain boundaries possess a relatively low tensile strength and that this strength can be further lowered by mineral cleavage. Brace states that rock compressive strength (related to hardness) is inversely proportional to grain diameter. Furthermore, Brace (1972) and Secor (1965) conclude that rock fracture at shallow low pressure conditions may occur at depth in regions of high pore pressure. Brace emphasizes that fracture origin flaws (cavities) may exist to 50 - 100 km.

Pugh (1967) observes that there is a relationship between cleavage, grain boundaries and crack propagation. He states that grain boundaries in polycrystalline oxides and metals possessing cleavage can act to stop cracks propagated under tension. Fracture blockage occurs at grains with their cleavage directions oriented parallel to the applied tension. Furthermore, Pugh observes that the effectiveness of this particular crack stopping action is increased if the grain size is small, for tip stress of cracks traversing small grains may not be high enough to cause fracture in neighboring grains wrongly oriented for easy cleavage. For example, fracture propagation in limestone and marble may be affected by cleavage orientation. Again strength and related fracture velocity is inversely proportional to grain diameter.

It is apparent that the size of the surface or internal flaw is important in determining whether or not a particular flaw will be the locus of a fracture origin. When microplastic flow contributes to rock strain, grain size can be the critical factor in fracture origin location. If a flaw or a particular grain is very large, and/or porosity is high, the stress necessary to initiate failure need not be high.

The mirror region

Any fracture spreading from its origin point, and subject to ever-increasing stresses at its crack tip, will accelerate to some critical and perhaps maximum spreading velocity characteristic of that material. Generally, the fracture surface immediately about the origin, especially in brittle amorphous or fine grained polycrystalline material, is smooth and essentially flat. This smooth flat region, formed while the fracture was spreading at a generally accelerating rate, is termed the fracture mirror surface (figures 9, 13). The essentially featureless anatomy of the mirror surface is attributed to the fact that fracture velocity and tip stress have not reached values necessary to break a large number of bonds oblique to the advancing fracture front. Therefore, the fracture maintains continuity along its entire front.

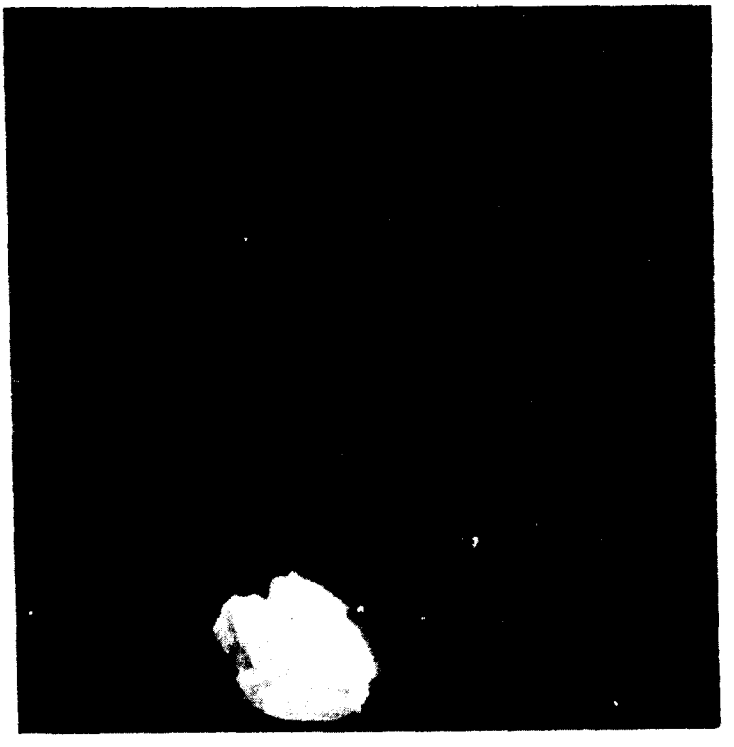

Figure 13, section of the fracture mirror surface depicted in figure 9. Scanning electron micrograph, 8000X.

The radius of the mirror region can range from microscopic dimensions to a size limited only by fracture extent. Generally fractures produced by large stresses have a small mirror surface. The stunted mirror is attributed to the

high crack tip stress imparted by the large stress to failure value and higher stored elastic strain values. In addition, under conditions of constant applied stress, crack tip stress increases as the square root of the crack length. At some critical velocity the fracture will terminate the mirror by breaking into hackle and frequently bifurcating into a number of fracture radiants by a process called forking.

During the fracturing of any substance capable of producing a mirror, critical values of crack tip stress and propagation velocity are reached at the mirror boundary (Shand, 1954). These critical factors give rise to a new transient fracture anatomy commonly referred to as the mist region. This mirror-mist boundary may be quite sharp megascopically or under low magnification in brittle amorphous or fine grained substances.

A useful relationship has been found to exist between the mirror radius, measured from origin to mirror-mist boundary, at some standard magnification, and the stress to failure. Shand (1959) determined from tests on glass rods that breaking stress could be determined from the radius of the fracture mirror if the rods were free of large residual stresses, and mirror size was small compared to rod diameter. Terao (1953) found that the breaking stress of glass varies inversely with the square root of the mirror radius. The breaking stress (σ_f) relationship to mirror radius (R) can be approximated by:

$$\sigma_f = K (1/R)^{1/2}$$

where K is a constant that depends on material properties. A qualitative appreciation of this relationship can be gained by breaking several glass rods after scribing each with origin flaws varying in depth (see appendix II). The smaller origin flaw will require a higher breaking stress. The larger breaking stress will lead to rapid fracture acceleration and high crack tip stress that results in early hackle inception and smaller mirror radius.

The fact that easily discernible mirror regions are not formed on rocks is attributed to their polycrystalline nature, large grain size, high porosity, and in some cases, mineral cleavage. Mirrors in glass are well-formed because the homogeneity of the body extends to the atomic level. Therefore the prevailing stress field is not disrupted at large material inhomogeneities and the mirror remains smooth. In contrast, mirrors on fine grained ceramic materials (figure 14) are only evident at the boundary marking the advent of hackle. In some ceramic materials composed of large crystals, the crystal size marks the lower level of material homogeneity and no mirror is formed (Shand, 1959). Some extremely fine grained rocks can possess a mirror region. It is conceivable that rock fractures with surfaces containing no undulations larger than the rock grain size (except perhaps twist hackle, Wallner lines, and arrest lines) may have propagated at less than the critical velocity (approximately 0.5 of transverse wave velocity, V_t) and may represent a form of mirror region.

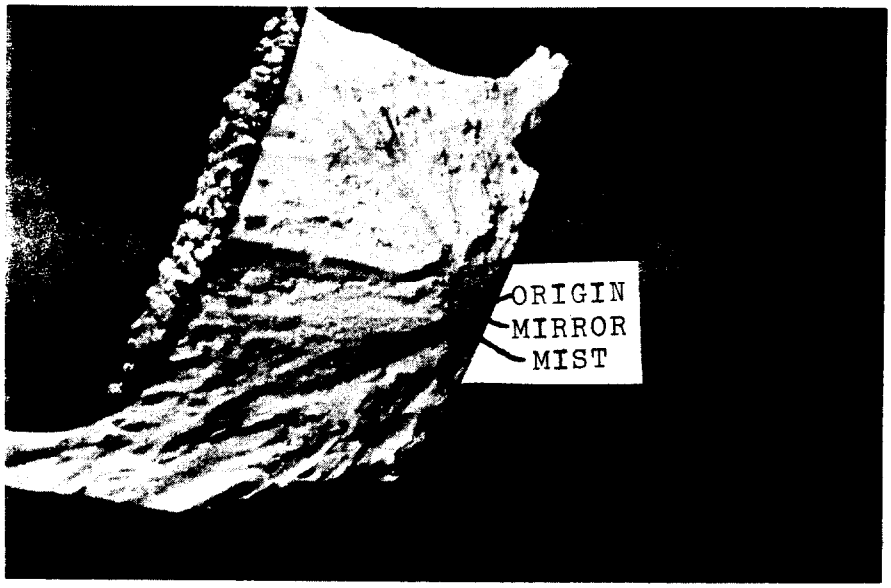

Figure 14, fracture mirror on fractured surface of a ceramic insulator fragment. Note also the origin dimple, mist, and radiating coarse twist hackle.

Poncelet (1965) states that all experimental evidence to 1965, leads to the conclusion that fractures in isotropic brittle materials produce mirrors that are perpendicular to the prevailing maximum tensile stress. He also concludes that a limiting fracture velocity (approximately 0.5 V_t) is reached with the advent of the first velocity hackle. However, by use of the electron microscope Poncelet found velocity hackle in the mirror region that was too small to be resolved by visible light. It has subsequently been demonstrated that Poncelet's limiting velocity is not the maximum fracture velocity. It is, however, the velocity critical to the formation of velocity hackle in the mist region and subsequent termination of the fracture mirror.

Wallner lines

Wallner lines (Wallner 1939, Frechette 1972) or ripple marks (Poncelet, 1958) in glass are most easily observed within, but not restricted to, the mirror region. They are subtle, rounded, low-relief features that arise from the coupling of sonic wave displacement stress with the principal stress at the fracture front (figure 15). The sonic waves responsible for the Wallner lines are generated when the fracture front passes and accomodates itself to a previously existing flaw. The disrupted stress field about the flaw causes the fracture front to dip slightly, and elastic waves, propagated by a stress oblique to the prevailing stress, spread from the flaw. These high velocity waves originate behind the slower moving fracture front and overtake the crack tip. Wallner lines form at the instant of interception by wave coupling and the fracture plane undulates in an attempt to remain perpendicular to the resultant tension.

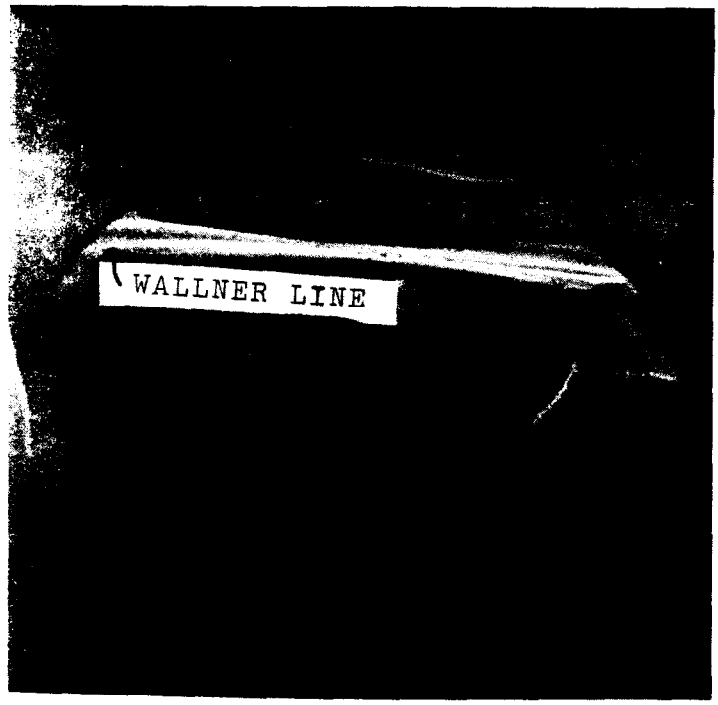

Figure 15, Wallner lines on fractured surface of a glass rod. Wallner lines visible on the curved hook region are concave toward the fracture origin at rod surface (bottom photo). Scanning electron micrograph, 20X magnification.

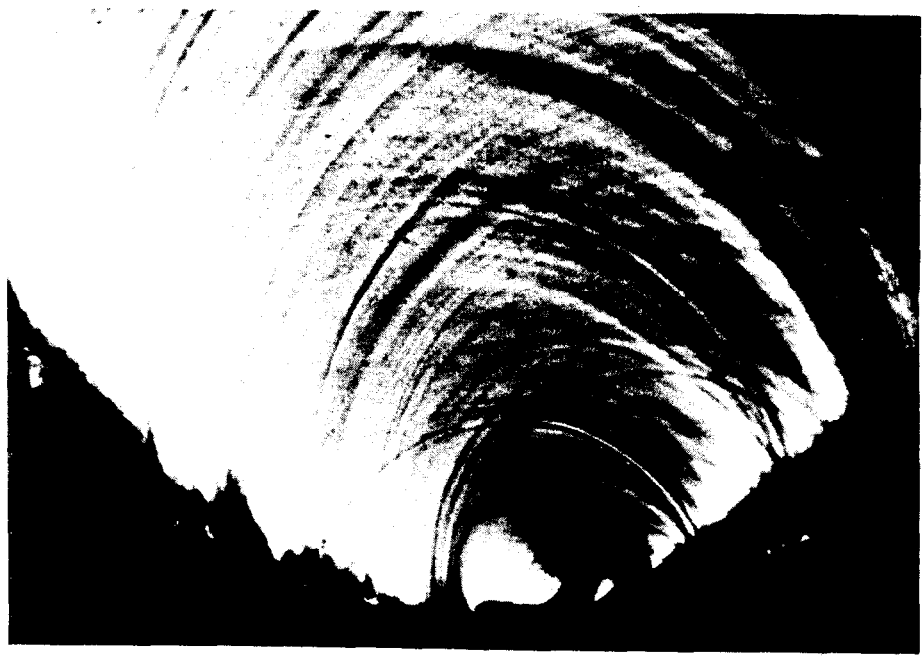

Figure 16, intersecting Wallner lines on mirror surface, concave toward the fracture origin, located at the glass rod boundary (bottom photo). Optical micrograph, 40X magnification.

Wallner lines, when visible, can serve as a useful fractographic tool because they are concave towards the fracture origin and convex in the direction of fracture propagation (figure 16). This useful relationship is based on the fact that sonic waves causing the Wallner lines originate on the already-formed fracture surface. These sonic waves therefore must overtake the fracture tip. Subsequently a given sonic wave does not intersect the fracture tip simultaneously all along its front. Consequently the Wallner line is an exaggeration of the fracture front and is not a true picture of that advancing fracture at a given instant. It follows that Wallner lines are most exaggerated nearest the generation point of the transverse wave. As with disannealed glass, intersecting Wallner lines (figure 16), attributed to this exaggeration, can provide valuable information on the propagation velocities of a fracture front (Poncelet, 1958).

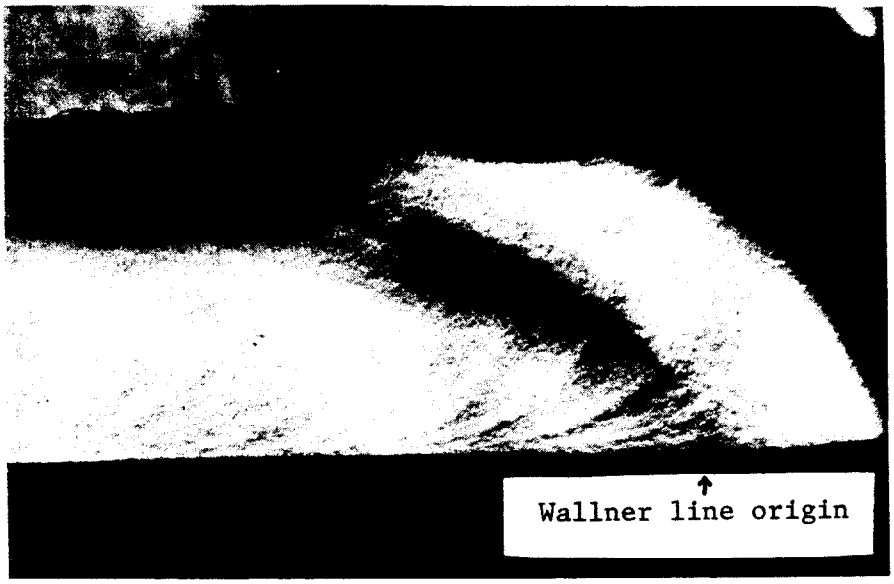

Figure 17, broad low-amplitude Wallner line in ceramic insulator, initiated within zone of thickened insulator cross section. Closely spaced undulations crossing Wallner line are attributed to the extrusion process during fabrication of the insulator and are unrelated to fracture propagation direction. Rocks also possess anisotropies that must be considered during fractographic examination. The fracture originated off-photo at the bottom interior insulator surface and advanced left to right. Asymmetrical stresses propagating the fracture peaked at the insulator interior surface causing the fracture to lead along this boundary.

Wallner lines are compatible with all other fracture surface features. However, they do not generally form on extremely slow moving fractures because the sonic waves outdistance the sluggish fracture front before it can travel any great distance. Rapidly propagating fractures in glass do not

show subtle Wallner lines because of the rough fracture surface. Wallner lines, unless of large wavelength and amplitude, are generally not apparent on rocks because their subtle nature is easily disrupted by coarse transient features and the polycrystalline granular texture of the rock itself. However, Wallner line amplitudes are directly proportional to the size of the flaw (including boundary shape configurations) responsible for the sonic waves (figure 17). This fact enables discernible Wallner lines to form even in coarse rocks if conditions permit (figure 18).

The interaction of sonic waves generated by intentionally introduced cyclic vibrations (10^6 to 10^7 cps) produced Wallner lines that can be used to measure the fracture propagation velocity in glass (Kerkhof, 1956, Schardin, 1959). Figure 57 shows ultrasonic-induced Wallner lines on a fractured glass surface. The Wallner lines resulting from controlled and constant ultrasonic frequencies are spaced further apart at increased fracture velocities. The relationship of Wallner line spacing to sonic frequencies and fracture velocity illustrates the fracture modifying effect of elastic waves and supports Wallner line formation theory.

Paired Wallner lines formed on a fracture surface in disannealed glass possess a unique relationship to the spatially related velocity and twist hackle. These fracture surfaces offer an opportunity to interpret fracture propagation history utilizing fracture surface (transient) structures under a known relative stress situation. The resulting transient strecture geometry is attributed to the in situ stress distribution locked in the glass during cooling. The inner median plane in disannealed glass is under high two-dimensional tension while the outer surfaces are in two-dimensional compression. This stress distribution and concomitant stored strain energy necessitate two neutral planes between the single maximum tension surface and the two outer compression surfaces. An initiated fracture propagates faster along the median plane of high tensile stress, and in so doing leaves behind a band of velocity hackle. This chaotic hackle alternates with mist (see pages 32 - 34), formed when the effort of producing the coarse velocity hackle has slowed the fracture. Lateral fracture progress into the zone of compression on both sides of the median plane is inhibited until the neutral surfaces move outward. The fracture slows in response to a decreased crack tip stress and two mirrors are formed. As the fracture penetrates into the zone of relieved compression it generally breaks into twist hackle (to be discussed). The twist hackle is orthogonal to the Wallner lines that are now almost parallel to the glass surface which was originally under compression. The Wallner lines in this case are generated at the intersection of the two mirror surfaces with the central velocity hackle zone.

Figure 18, broad Wallner line on blast-induced sandstone fracture surface, western New York. Hackle plumes radiate from the fracture origin at the tip of a pre-existing fracture. Coarse twist hackle originates at the Wallner line. Note secondary twist hackle on primary hackle steps. Twenty-five cm. hammer handle points to Wallner line. Arrow indicates secondary hackle.

Velocity hackle - mist region

As fracture velocity and crack tip stress increase, the previously described mirror becomes frosted in appearance (figures 9, 19). This frosted zone, attributed to countless minute velocity hackle undulations in the fracture plane, is called the mist region. The dulled and gray mist region has also been termed the mat surface by Preston (1939). Fracture mist is discussed separately from the mirror because the intervening velocity hackle boundary, at any location along the fracture front, marks the spot where crack velocity and tip stress reached some critical level. Schardin (1959, tables 1, 2) has shown that, in glass, this critical velocity, that can be maximum velocity under given test parameters, is dependent upon chemical composition and is equal to approximately one half the speed of the transverse wave propagation rate in a given material. Schardin states that highest critical (maximum) velocities (2155 meters/sec) were observed in 100% SiO_2 glass. Lowest critical velocities (750 meters/sec.) were measured in glass containing 40.5% PbO. At these critical fracture velocities and increased crack tip stresses, the continuity of the fracture front is not maintained, and all along the front, sections of the fracture tip deviate above and below the mean propagation plane. These deviating fracture sections must rejoin to complete material separations, and thereby form minute undulations that disrupt light reflections and produce the foggy appearance of the mist region

(figures 9, 19). The term critical velocity, indicating that velocity at which forking (see page 53), velocity hackle and mist first occur is preferred over maximum velocity. This distinction is based on the fact that fracture velocities exceeding 0.9 transverse wave velocity in a given material have been attained with controlled tests (Snowden, 1976).

Figure 19, velocity hackle within mist region in close proximity to mist-coarse hackle boundary on fracture surface shown in figure 9. Fracture propagation direction was from lower left to upper right. Scanning electron micrograph, 8000X magnification.

The fracture mist is considered to be a zone of very fine velocity hackle. Poncelet (1958) states that within this mist zone fracture propagation velocity rises, while the angles between sloping hackle surfaces and the main fracture plane become larger in the direction of fracture growth. Concomitant with increased hackle angle is an increased hackle size.

Schardin (1959) has illustrated that fracture velocities do increase through the mirror region as the stress at the fracture tip increases. This velocity and stress increase enhances the possibility that bonds oblique to the fracture front will begin to break. Poncelet (1965) supports this thesis and further concludes that all bonds along the fracture front, at any given instant,

need not break simultaneously and that consequently some bonds may remain intact. The fracture surface will pass by the unbroken section which increases the stress on the lagging bonds. The added stress forces the unbroken section to separate with an accelerated velocity. This situation, if it occurs in the mirror region, may lead to fine velocity hackle streaks which are discernible on the mirror surface (figure 8). If the crack tip stress is permitted to rise slowly, the streaks are generally long and distinctly visible. However, if the stress and related fracture velocity rises precipitously, an increasing number of bonds oblique to the advancing front may part. This situation produces a greatly increased number of minute deviating fractures that are oblique to the mean fracture propagation plane. Poncelet implies that in this case a large number of streaks merge rapidly into a mist surface of fine velocity hackle producing a sharp mirror-mist boundary.

Frechette (1972) concludes that the mist region is not completely understood and suggests that mist may be caused by sonic waves generated along an accelerating fracture front by parting bonds. The sonic waves interact with themselves and the prevailing stress field producing a myriad of small-scale local deviations from the average fracture plane. Frechette (1972) and Poncelet (1965) stress the importance to the formation of velocity hackle of interfering sonic vibrations generated as an accelerating crack tip deviates from the mean fracture propagation plane.

As the crack tip stress increases, the velocity hackle surfaces become increasingly oblique to the mean fracture plane. Consequently the fracture tip stress is reduced by the square of the cosine of the obliquity of the velocity hackle surface to the applied tension direction. The reduction of crack tip stress coupled with the effect of the increased surface area and related surface energy produced by velocity hackle can result in a reduction of fracture propagation velocity. Therefore a fracture might "regress" from mist to mirror just as it progressed from mirror to mist (Preston, 1926). However, under the influence of an increasing and complex stress field, and increasing fracture velocities, the mist region is generally terminated by the inception of coarse velocity and twist hackle and fracture forking (bifurcation) depicted in figure 20.

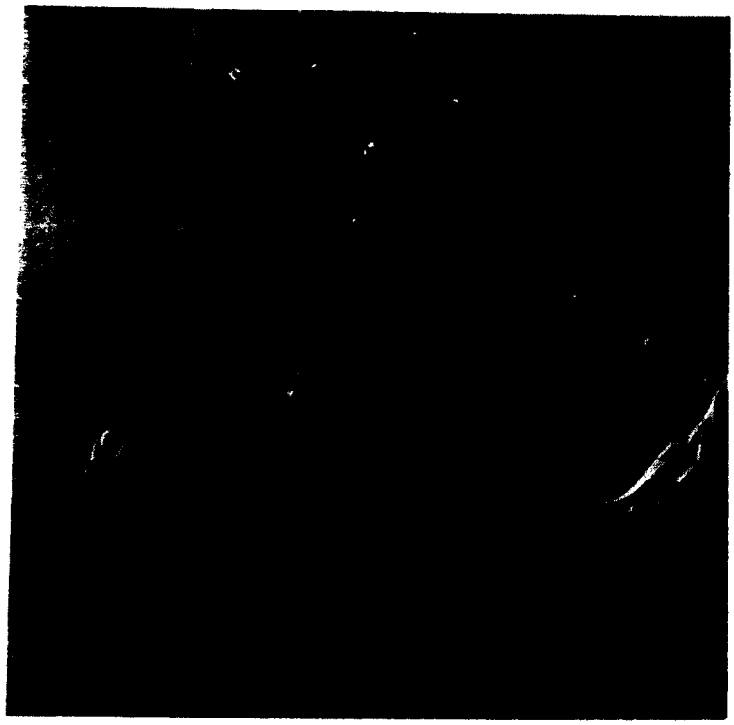

Figure 20, coarse velocity and twist hackle in close proximity to mist-coarse hackle boundary on fracture surface shown in figure 9, Fracture propagation direction was from bottom to top. Scanning electron micrograph, 400X magnification.

Twist hackle

Twist hackle (Frechette, 1972) refers to a transient feature discussed by various individuals under the general term hackle, or hackly fractures (Preston, 1926; Murgatroyd, 1942/ Gash, 1971). Identical features have been described as striations (Poncelet, 1958, 1965; Preston, 1939), and river lines (Pugh, 1967). Geologists have referred to twist hackle of slightly different form produced by varying degrees of twist "severity" and twist hackle steps as feather fracture, border planes and cross fractures (Woodworth, 1896), plumose structure, F-joints, and C-joints (Hodgson, 1961), and fringe faces and steps (Bankwitz, Peter, 1965, 1966).

Twist hackle forms when a propagating fracture abruptly enters a region of different stress orientation. The fracture breaks (twists) into a series of en echelon individual lance like twist hackle faces, each perpendicular to a resultant tension.

Twist hackle is unrelated to crack tip stress intensity and spreading velocity. Only twist "velocity" is important. In other words, if the twist acts over a large region no twist hackle will form; the fracture front will turn as a unit to become perpendicular to the prevailing stress. The lack of a direct relationship of twist hackle to fracture velocity and stress effects enables it to form anywhere on a fracture surface and concomitantly with any transient feature. For example, twist hackle is often formed about a fracture origin within the mirror region (figure 12). Twist hackle, being generally a coarse fracture feature is very common on all rock types (figures 21, 22).

Figure 21, twist hackle faces and steps on systematic fracture surface in Mississippian shale, West Virginia. General fracture propagation direction was horizontal and from right to left at photo top. Fracture spread vertically downward at inception of twist hackle (see arrows). Five foot shale section is shown.

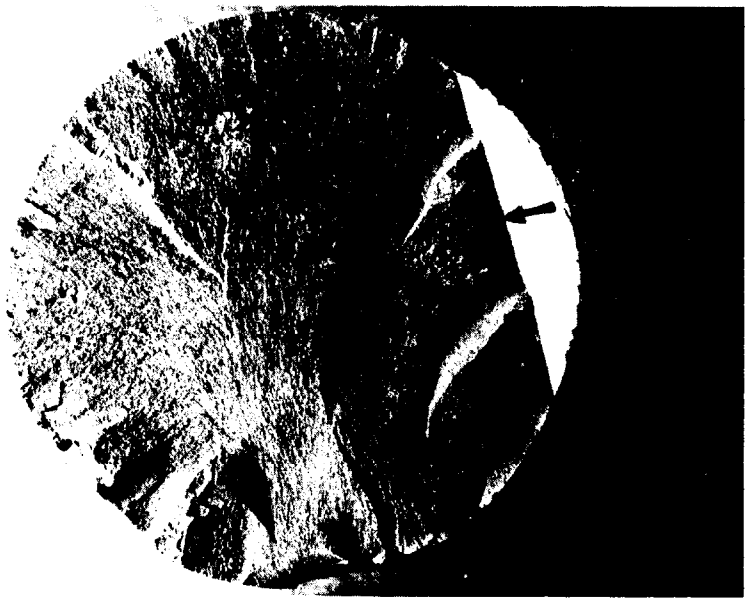

Figure 22, extended fracture origin along circumferential core boundary. Hackle plumes and coarse twist hackle radiate from the origin to meet the core boundary orthogonally. Note twist hackle forming near fracture boundaries. The fracture spread across the core, leading in the core center. The core center spreading direction was parallel to the strike direction of the pre-existing fracture that is nearly perpendicular to the plane of the photograph (see arrow).

Twist hackle is produced in response to fracture progression into a region where the principal tension and a locally superposed tension produce a resultant tension that is oblique to the advancing fracture front (figure 23). The entire fracture front cannot respond by an instantaneous rotation to allow the fracture plane to become perpendicular to the new resultant principal tension. Therefore at the crack tip, the fracture front breaks into en-echelon elongate hackle face "tongues" (figure 23). Each hackle face is inclined to the original fracture plane and turns to become perpendicular to the local resultant principal tension. The net result is an appearance much like the blades of a half-opened Venetian blind. These lath-shaped hackle faces continue to advance, maintaining their en echelon and parallel relationships to each other. If the hackles continue to advance in this fashion and hackle steps did not form, the fracture would not completely separate the material. An excellent example of incomplete hackle steps holding a partially fractured material together is given by core samples that belatedly fall apart during handling. Generally, the hackle faces will eventually curve laterally into one another behind the advanced hackle faces to complete the fracture, thereby forming the hackle steps (figures 8, 24). The joining of the hackle faces through step development permits the dissipation of stored elastic strain and produces the sawtooth profile characteristic of twist hackle. This sawtooth hackle pattern can be mimicked by preferred breakage along cleavage planes. Therefore, transient features on fracture faces traversing minerals possessing cleavage must be viewed with this fact in mind.

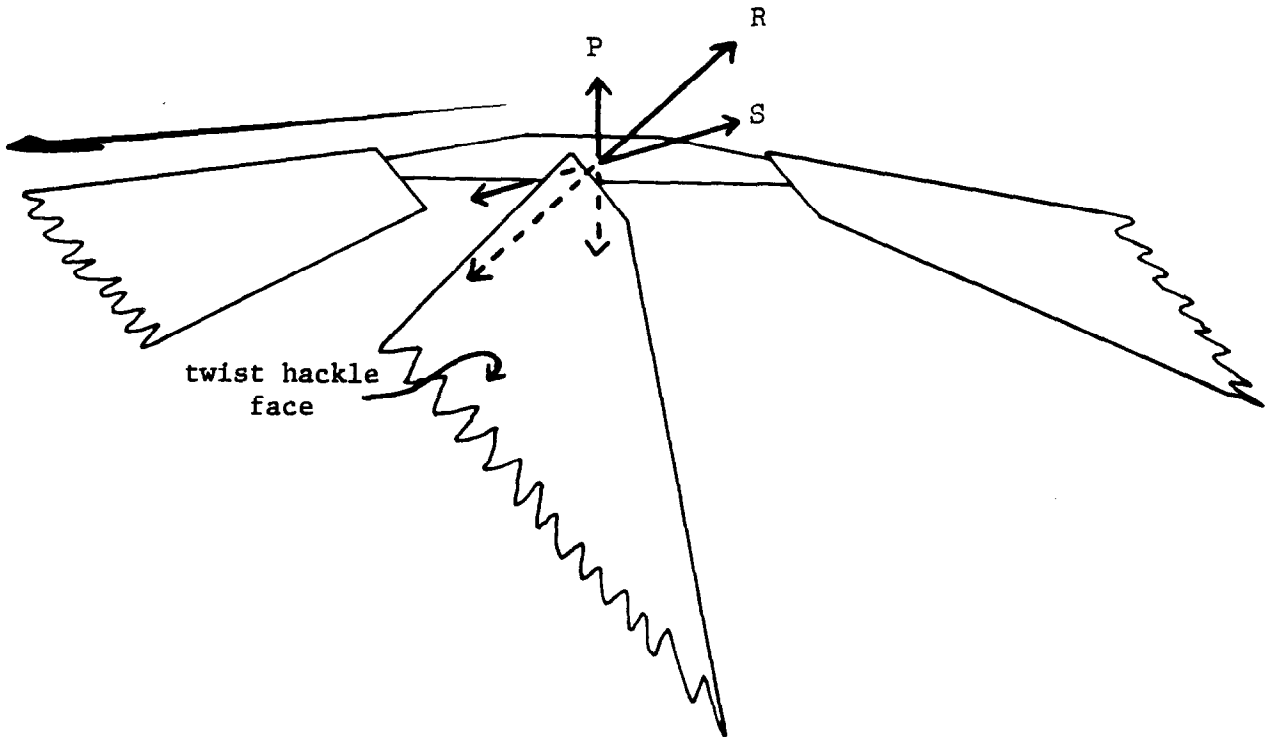

Figure 23, schematic illustration depicting the formation of twist hackle by rotation of the principal stress. The fracture propagation direction is out of the page. P = principal stress before initiation of twist hackle, S = superimposed local stress, R = resultant principal tension direction responsible for twist hackle and perpendicular to twist hackle faces.

The lateral spreading of the advanced en echelon fracture tongues (and subsequent complete separation) cuts long slender needles from the fracture surface (figure 24). Portions of these needles, commonly called Woodsworth feathers (Preston, 1926), can remain attached to one of the two fracture surfaces depending upon which laterally spreading step connects the adjacent hackle face first. If laterally spreading hackle steps join two immediately adjacent tongues, a complete separation of the needles is facilitated. A not uncommon geological counterpart to Woodsworth feathers in glass are thin pencil-like or tabular rock fragments produced by twist hackle face-step joins in highly fractured rock.

As the hackle step spreads it does so in a stress field that is usually oblique to the hackle step fracture front. This forces the hackle step itself to break into twist hackle. The faces of this secondary (second order) twist hackle are perpendicular to the long axis of the needle and result in a feather-like appearance (Freminville, 1914). Second order twist hackle is well-formed in the sandstone shown in figure 24.

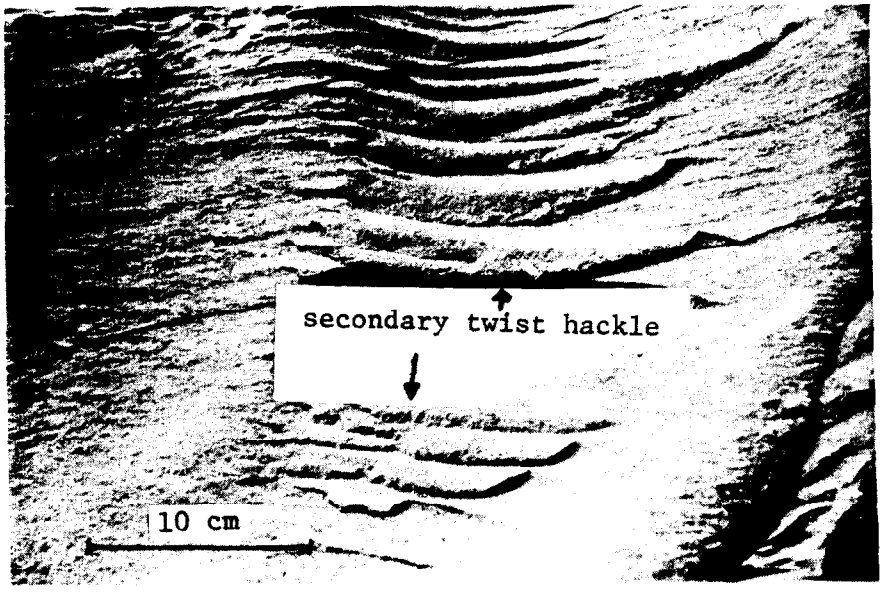

Figure 24, close-up of well-developed twist hackle on the fracture face depicted in figure 18. Note secondary twist hackle developed on the primary twist hackle steps. Fracture propagation direction was from left to right.

Poncelet (1965) perceives the formation of twist hackle to be related to an uneven advance of the fracture front previous to the "twist." He views the fracture front as merely a line separating broken from unbroken bonds. Occasionally, as with streaks, a group of bonds does not break at the same time as other bonds in response to the applied stress. However, on either side

of the unbroken bonds, the fracture progesses with no hesitation. If the principal tension direction ahead of the fracture changes, each of these advanced fracture segments orients itself orthogonally to the altered stress. These segments continue advancing along en echelon parallel planes. This sequence of events implies that advancing fracture tongues form prior to their advance into an altered stress zone. The final twist hackle profile will, however, be the same.

Some investigators conclude that hackle marks occur geologically on fracture surfaces interpreted as shear joints. The shear joint classification is usually based on the orientation of a given fracture set in relation to surrounding structures attributed to compression. Roberts (1961) states that the development of feathers or plumose structures (hackle) is restricted to shear joint surfaces. He states that plumes are seldom viewed on fractures produced by a tectonically induced tension. His shear joints are located symmetrically about the a c planes of folds. Gash (1971) suggests that hackle marks are indicative of shear macrofracture. Macrofracture is allegedly accomplished by the coalescence of microfractures. These microfractures are held to be generated by a stress pulse initiated at the instant of initial failure. Murgatroyd (1942) propounds that hackle marks in glass are formed by a large, perhaps impact-induced, shearing stress. Parker (1942), in a field study of fractures in the Allegheny plateau of New York, states that plumes are best formed on joints of compressional origin oriented oblique to the a c plane of nearby folds. He states that feather structures are rare on rough curved fractures parallel to the b - c planes of folds which are attributed to tension.

The authors do not agree that hackle marks or hackle plumes are best formed on alleged shear fractures. They have found hackle of varying relief in the form of plumes and larger fringe hackle faces and steps on fractures of all sizes and geometrical orientations. Well-defined plumes and coarse twist hackle are common on fractures produced by dynamite blasts, also hackle is common on fractures attributed to unloading (figures 25, 26). These can only be tension fractures. On a large scale, hackle plumes and twist hackle faces and steps are commonly observed on regional systematic fractures in the Allegheny Plateau of West Virginia. These are not "shear" fractures in any sense of the word, even though the fractures are almost everywhere oblique to regional structure. It has been shown that the regional fractures predate folding (Dean and Kulander, 1977; Dean, Kulander, Williams, in press). The authors feel that fractures possessing hackle form only in response to a tensile stress, and that this effective tensile stress always acts at right angles to the fracture surface.

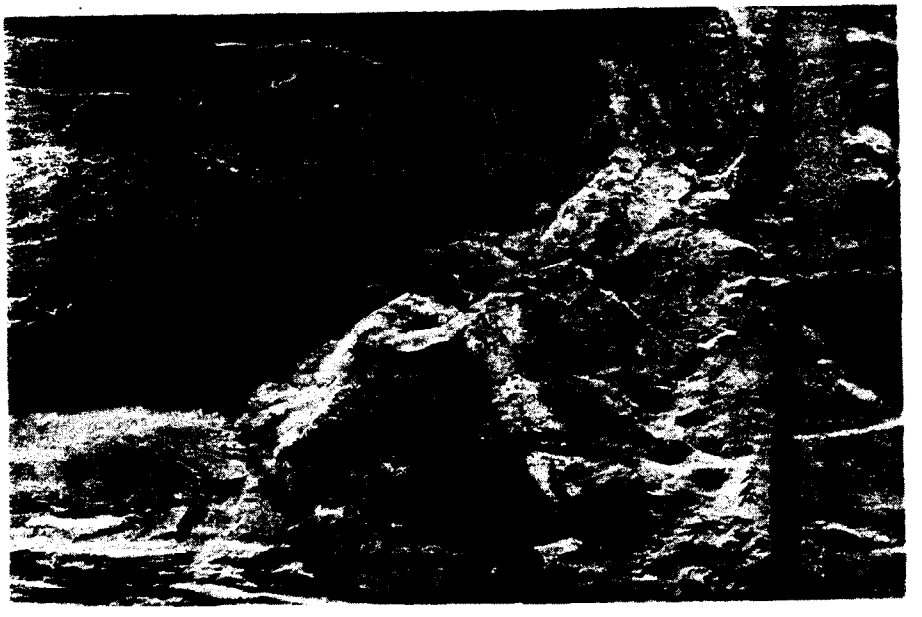

Figure 25, hackle plumes developed on the surface of a blast-induced fracture in Mississippian limestone, West Virginia. The fracture originated at the point of explosion within the vertical drill hole immediately off the upper right corner of the photo. Note the penny for scale (at arrow).

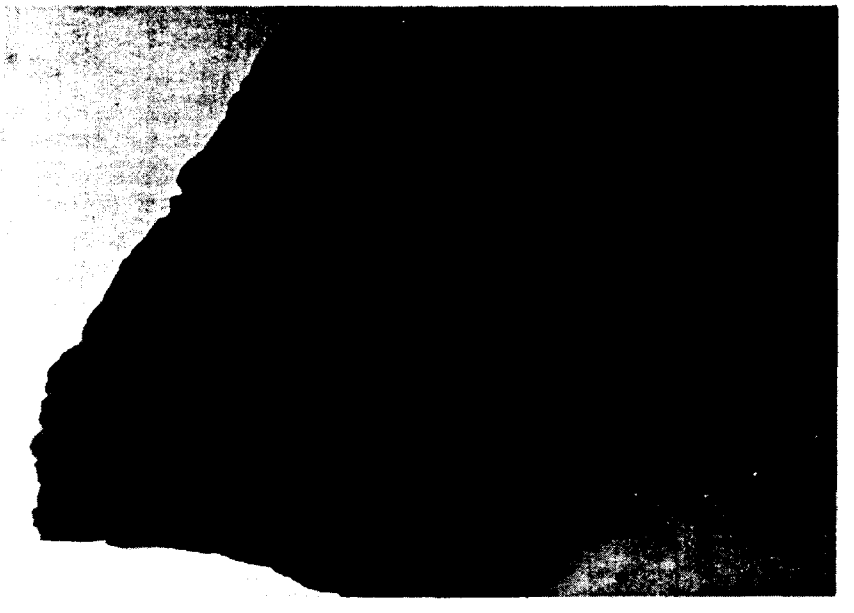

Figure 26, bedding plane release fracture in middle Devonian black shale from a limestone quarry floor, western New York. Hackle plumes radiate from a cephalopod that acted as the fracture origin. Cephalopod origin is eight cm. in diameter through its shortest section.

Twist hackle may disappear as quickly as it originated when hackle step relief diminishes to zero in response to a stress field that again becomes normal to the mean fracture propagation plane (figure 24). Several hackle steps may also merge, or join, typically at an angle approaching ninety degrees, to form a hackle step of greater relief (figures 8, 27). Joined and unjoined hackle steps generally diverge in the fracture propagation direction, and under a new stress configuration may fork into several hackle steps. The forked step is distinguished from the joined step because, after splitting, the steps diverge from one another. In addition the forked steps, at inception, generally enclose an angle of less than ninety degrees.

Frechette (1972) summarizes the view of many investigators that the twist hackle pattern on a fracture surface resembles a natural drainage system. The joining hackle resemble tributaries flowing together to form a river of increased discharge (step height). The rivers join and diverge downstream in the fracture propagation direction and at some point may split or fork to form deltas.

Figure 27, twist hackle steps on mirror fracture surface in glass bar merging at angles approaching ninety degrees to form river pattern. Fracture propagation direction was from top to bottom. Scanning electron micrograph, 1400X magnification.

Twist hackle and fine hackle plumes (chevron and herringbone markings) are quite common in fractured rocks and are responsible for much of the plumose structure familiar to geologists. It can be a useful structural tool to the trained observer (figure 28). At the same time twist hackle may be misleading if misinterpreted. For example, twist hackle on a gross scale, and the main fracture plane from which it diverged, might be misconstrued as two different fracture sets of differing trend, when in reality they formed during the same fracture event (figure 29). Any method of determining fracture sets statistically or graphically such as that given recently by Currie and Reik (1977) must also distinguish fracture events.

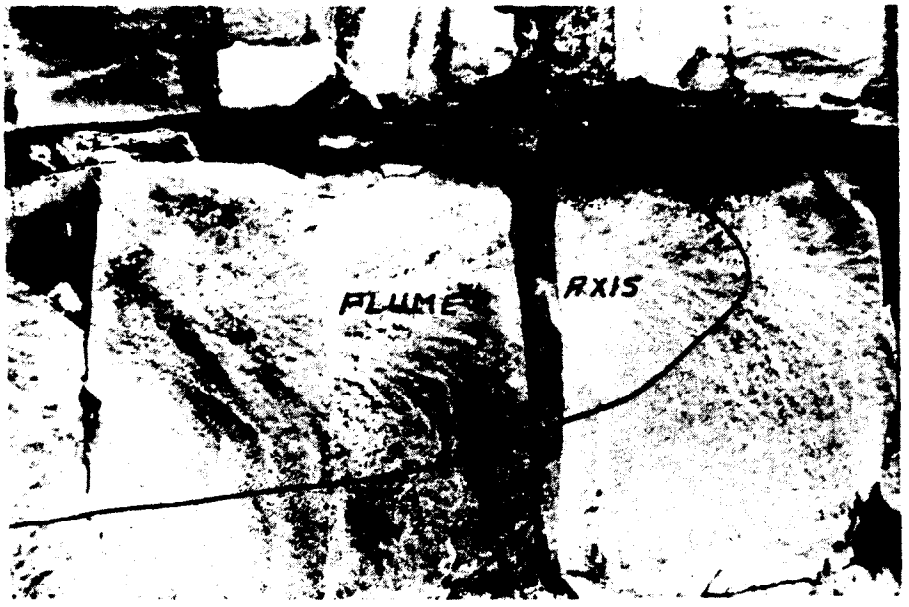

Figure 28, well-developed hackle plume on a systematic fracture face in Devonian siltstone stratum, Pennsylvania. Line indicating fracture front at time past indicates the fracture led toward the stratum top in response to peak tensile stresses perpendicular to the fracture surface in that location. Lens cover is parallel to another fracture set that cuts the plume, and thereby formed later than the systematic fracture (see figure 37).

Generally the formation of twist hackle leads to a reduction of fracture propagation velocity. Two factors are primarily responsible for this decelerating effect. First, the inclined and en echelon fracture faces no longer form an energy economical flat plane and the resulting increased fracture surface elevates surface tension which retards fracture propagation. Secondly, the unconnected twist hackle faces and steps absorb energy and do not permit a complete separation of the fractured material.

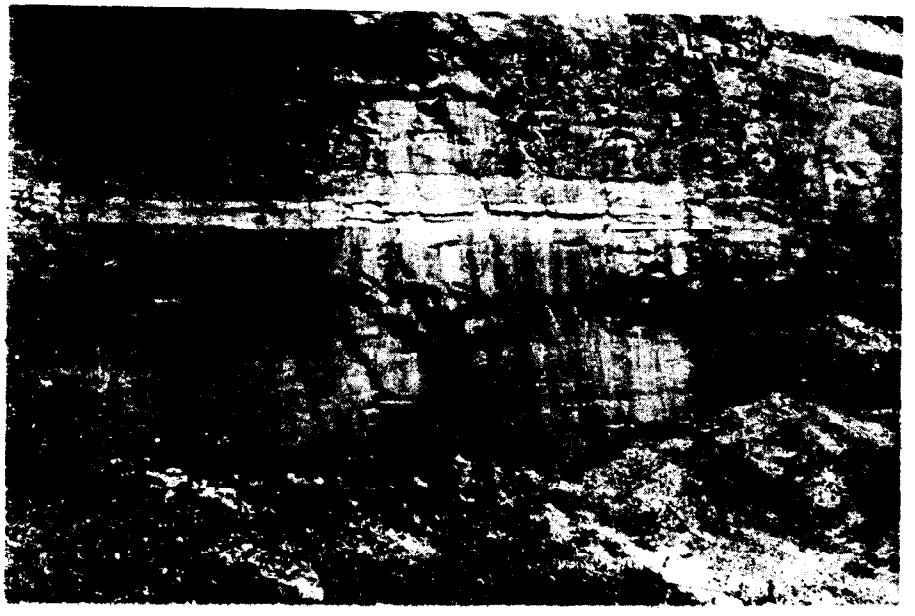

Figure 29, well-developed twist hackle faces and steps formed within maximum curvature zone where the lower exposed section of the systematic fracture undergoes a change in trend. The trend of the upper fracture face section remains unchanged. The two systematic trends and twist hackle faces in the trend change zone are products of the same fracture event. Fracture propagation direction is from left to right and down along twist hackle faces to ground level. Arrows indicate propagation directions.

Inclusion hackle and gull wings

Inclusion hackle (Kulander, Dean, Barton, 1977) is distinguished by the fact that it is not caused strictly by fracture velocity or by a superposed stress direction. Inclusion hackle, which is probably the most common constituant of hackle plumes in polycrystalline rocks, is generated in the following manner. When a fracture front advances into the vicinity of an inclusion (pore space, vug, weakly cemented zone, fossil, grain of different composition or size, etc.) the fracture propagation velocity decreases and the fracture plane is locally warped by the interference of local stress gradients associated with the inclusion. The local stress gradients are attributed to stored stresses in the vicinity of the inclusion or principal stress relaxation about and within the inclusion. When the elastic moduli of the inclusion are high, the inclusion will break as it is intersected by the fracture plane. If the inclusion elasticity is low, the inclusion may not break until the fracture is long past. Contrary to a solid inclusion, a bubble or pore surface must be tangent to any principal stress.

The planar warping, occurring as the main fracture plane passes around an inclusion, often results in a bifurcation of the fracture to different levels by the time it reaches the far side of the inclusion (side opposite that first

encountered by the fracture). As a consequence of this divergence, the fracture is not interconnected. Therefore, after passing the inclusion, the fracture should be advancing on two closely spaced sub-parallel levels. However, the fracture does not continue advancing indefinitely on two different but closely spaced levels and soon rejoins to advance as a single front. In order to complete the break, the trailing fracture plane will step (hook up or down) into the other. This step forms a tail. (Preston, 1939) on the far side of the inclusion that points in the direction of fracture propagation. The tail can be quite narrow or fairly broad. Figure 30 shows inclusion hackle on a core fracture face. This tail has been referred to in glass as a wake (Frechette, 1972). This wake or inclusion hackle step diminishes in relief and disappears away from the inclusion. The authors and V.D. Frechette (oral communication) feel that hackle plume morphology on rocks could be primarily the result of closely spaced inclusion hackle and small scale closely spaced twist hackle faces and steps.

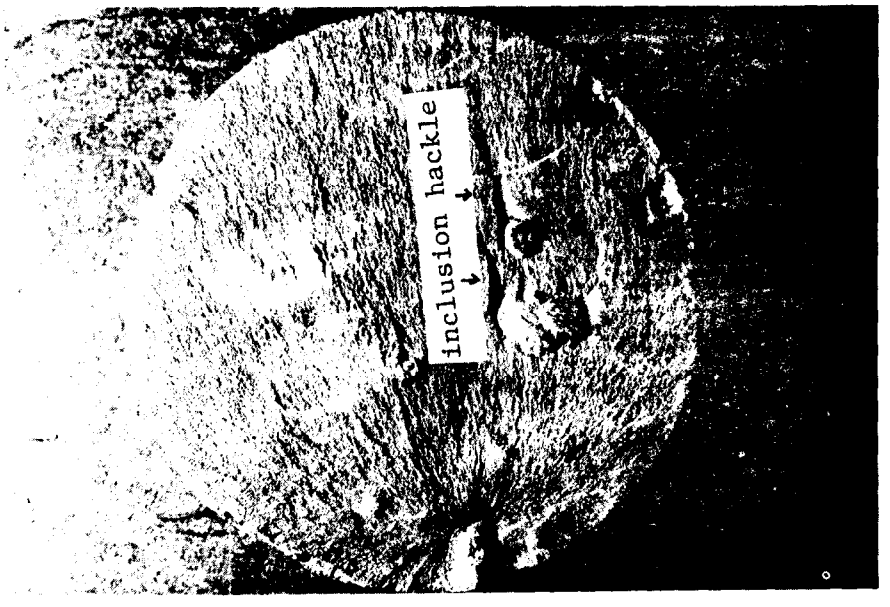

Figure 30 , pyrite nodule near circumferential core boundary that served as an origin flaw. Hackle radiates straight across the fracture face through core center and curves to meet the core boundary orthogonally. Note inclusion hackle generated at pyrite nodule boundaries that face away from the origin ("lee side" of nodules).

Another unique set of transient features related to inclusions and inclusion hackle are called gull wings (Frechette, 1972) or ripple pairs (Poncelet, 1958, 1965). The term gull wings is appropriate because these paired markings on either side of the inclusion hackle tail resemble a gull in flight (figure 31). However, each wing tilts or strikes in an opposite direction at its origin point along the inclusion hackle tail. The gull wings are generated when hackle tail formation causes a redistribution of stress that is transferred by sonic waves to the crack tip. The coupling of the sonic wave stress and crack tip stress, as with Wallner lines, produces a resultant that causes a brief undulation in the fracture plane which is responsible for the wing-shaped line. Broad gull wing-like ripple pairs can be formed as the advancing crack slopes gradually under the influence of a resultant stress attributed to large pores or bubbles. Sonic waves are transmitted from the locally warped fracture about the inclusion that interact with the fracture front producing broad paired ripples.

Gull wings generally exhibit a low rounded relief, and for this reason are not commonly observed in polycrystalline rocks. They are abundant, however, in fractured obsidian that contains inclusions or bubbles. Broad gull wing-shaped ripple pairs are also undoubtedly present in very fine grained crystalline sedimentary and igneous rocks.

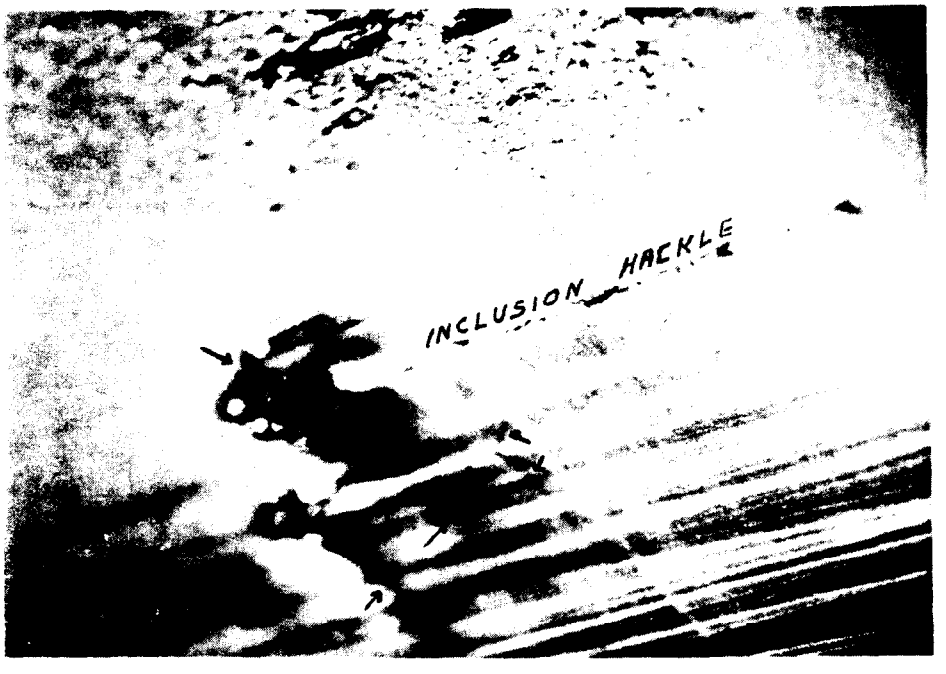

Figure 31, inclusion hackle and gull wings (arrow) formed on fracture surface in refractory glass. Fracture propagated from left to right. Optical micrograph, 20X magnification.

Arrest lines

Arrest lines or rib marks (Preston, 1926; Murgatroyd, 1942) are attributed to temporary fracture hesitation resulting from a momentarily decreased stress field and/or a sudden change in principal tension direction (figures 32, 33). These actions produce a sharp change in fracture propagation direction. Arrest or rib marks can be caused, in some cases, by a cyclic stress resultant, oblique to the major fracture plane, and alternating between tension and compression. These features have been called conchoidal structures (Hodgson, 1961), annular structures (Bankwitz, 1965, 1966), and rib marks (Dennis, 1971) in geological literature.

Figure 32, arrest lines, and twist hackle on fracture face in folded Devonian shale, Maryland. The fracture originated towards the upper bedding surface in this shale sequence and propagated down. Note cigar for scale parallel to twist hackle and propagation direction.

Arrest lines are significant because they record an almost instantaneous picture of the fracture tip configuration at a particular time during fracture propagation. Arrest lines are convex in the direction of fracture spreading for all but very slow fracture velocities in the range of 10^{-3} meters per second (Frechette, 1972). The profile of an arrest line resembles a cusped wave. Therefore, these features are more readily visible than Wallner lines which generally possess less relief and are rounded in cross section.

Non-circular, parabolic, arrest lines may indicate a differential stress configuration at the fracture front before arrest. The most advanced arrest line section possessing the smallest radius of curvature marks the area of

maximum tension active at the time of fracture passage. The trailing arrest line segments, especially if more closely spaced, mark the fracture plane area of reduced tension (figures 34, 35). This relationship is accentuated by twist hackle that forms perpendicular to arrest lines. This purely qualitative analysis is valid only if the fracture arrest is instantaneous, and the arrest line does not possess a constant radius of curvature (i.e. is circular, figure 36). Murgatroyd (1942) states that a series of closely spaced arrest lines indicates a fracture moving at an extremely slow velocity of less than one centimeter per second. Slow propagation has been inferred for petal-centerline coring induced fractures (chapter 8). These fracture faces possess closely spaced arrest lines (figure 36, Kulander, Dean, Barton, 1977).

Hackle marks are formed perpendicular to arrest lines. The geometry of this relationship is consistent with the observations that 1) hackle marks are parallel to and arrest lines are perpendicular to the fracture propagation direction, and 2) hackle marks diverge in the direction of fracture propagation to accomodate a fracture front of increasing length and varying curvature. Twist hackle and arrest lines commonly occur together at all scales in many rock types, contrary to some previous reports that these transient features, individually or together, are geologically rare (Gash, 1971; Nickelsen, 1967). Arrest lines are common on core fractures and also in outcrop. They can form on an individual stratum less than an inch thick or form with a radius of curvature of hundreds of feet on massive sandstone or igneous cliffs

Figure 33, non-circular arrest lines on a fracture face in folded Devonian shale, West Virginia. Parabolic arrest line form indicates a differential stress condition at time of fracture with the greatest tension being perpendicular to any given arrest line at its most advanced point. Note the small band of twist hackle beneath the parabolic arrest lines (at arrow).

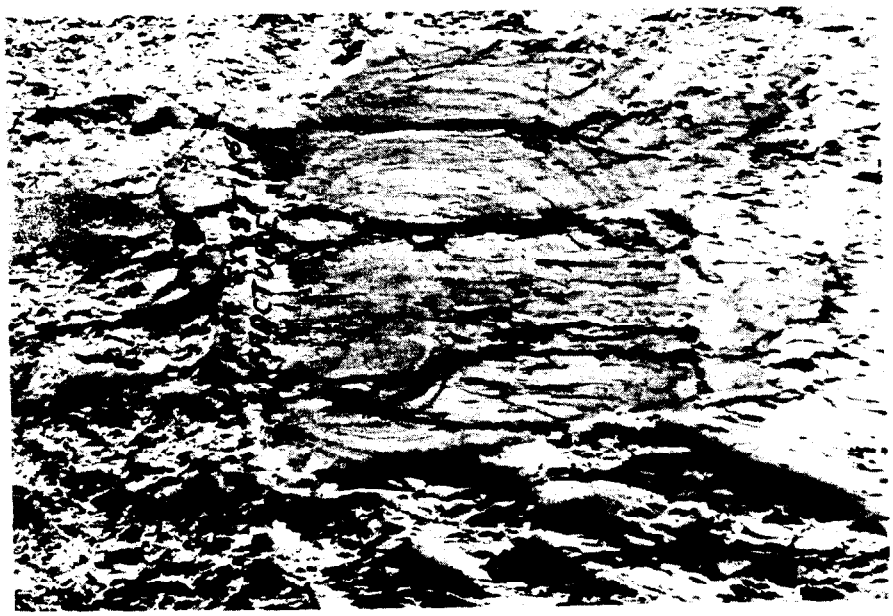

Figure 34, arrest lines changing from circular to non-circular away from the fracture origin. Arrest lines at arrow attempt to swing parallel to pre-existing fracture trending oblique to the plane of the photograph.

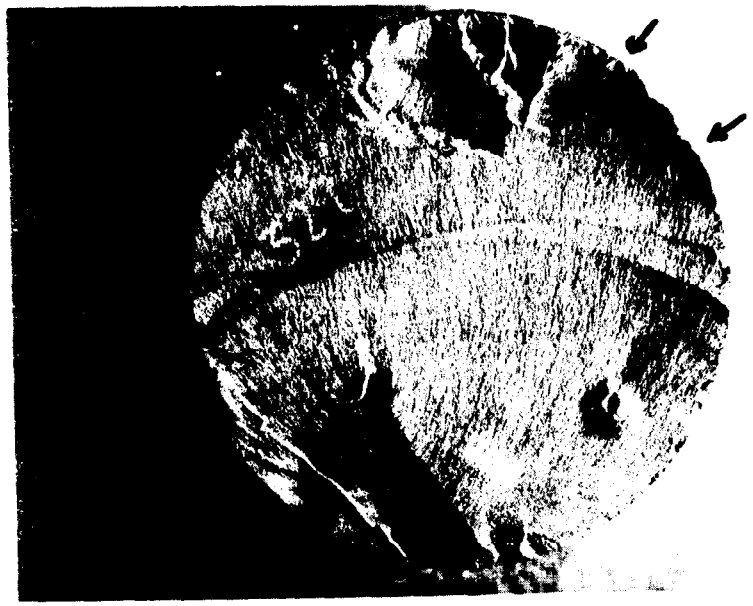

Figure 35, arrest lines on disc fracture, concave towards the fracture origin. Arrest lines curve abruptly in an attempt to become tangent to the pre-existing core boundary. A large fossil fragment served as the origin flaw and the fracture hooks (curves abruptly) into the opposite core margin at arrows.

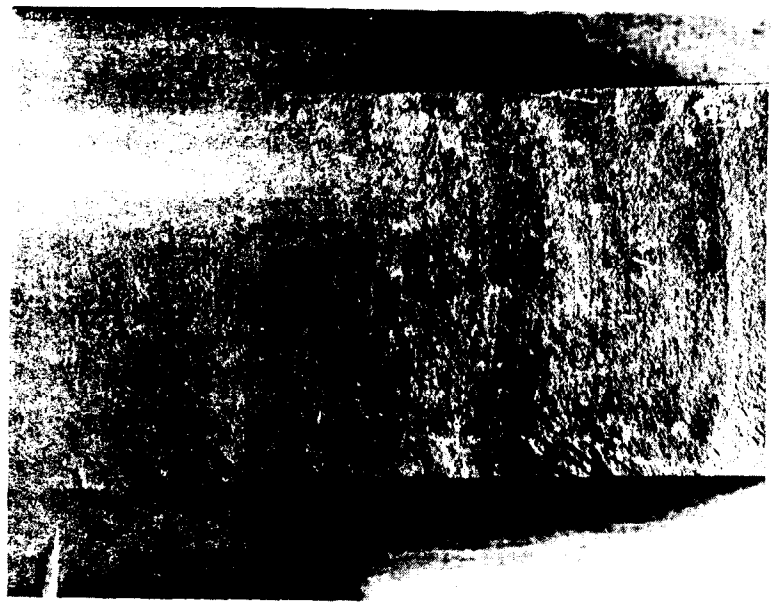

Figure 36, symmetrical circular arrest lines convex downcore, and orthogonal twist hackle diverging downcore on a centerline fracture in a Devonian shale core from Kentucky. Note that the arrest lines and twist hackle do not attempt to become tangent and orthogonal respectively to the core boundary, indicating that the fracture occurred immediately before the section was drilled.

Hackle plume geometry and fracturing stress distribution

Hackle plume geometry is comprised of inclusion and twist hackle faces and steps. Plume geometry records the fracture propagation direction, relative fracturing stress distributions and relative fracture propagation velocities. In the ensuing discussion it is assumed that the fracturing material is mechanically homogeneous. It is also assumed that both arrest lines and lines constructed perpendicular to plume components represent fracture hesitation at all points along the fracture front.

The overall hackle plume pattern can be used to construct past fracture fronts along any surface profile if lines are constructed perpendicular everywhere to hackle plume components. This constructed line can be viewed as the fracture front at a particular time during the history of the fracture development. Arrest lines are also perpendicular to plume hackles. Parallel hackle plume components, and straight plume components radiating from a common origin, indicate a uniform velocity along the corresponding straight or circular fracture front. In contrast, curvilinear plume components indicate a greater fracture propagation velocity at the leading section of the related elliptical or irregular fracture front at the point of its greatest curvature.

Several representative plume geometries (figure 37 a-f) are described and interpreted in following paragraphs.

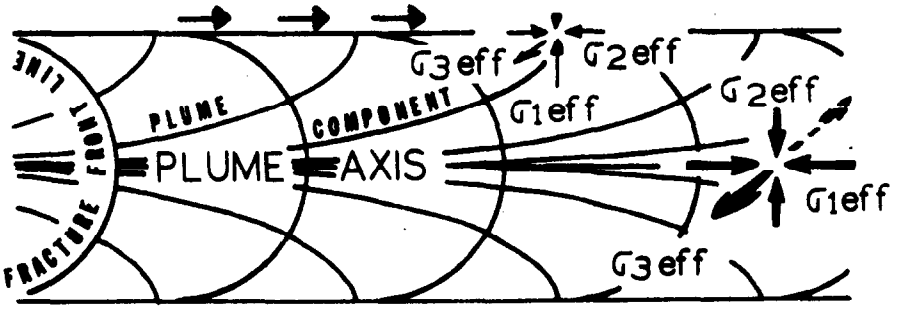
G3eff
G2eff
G2eff
G1eff
PLUME
COMPONENT
PLUME AXIS
G1eff
G3eff
FRACTURE FRONT

a

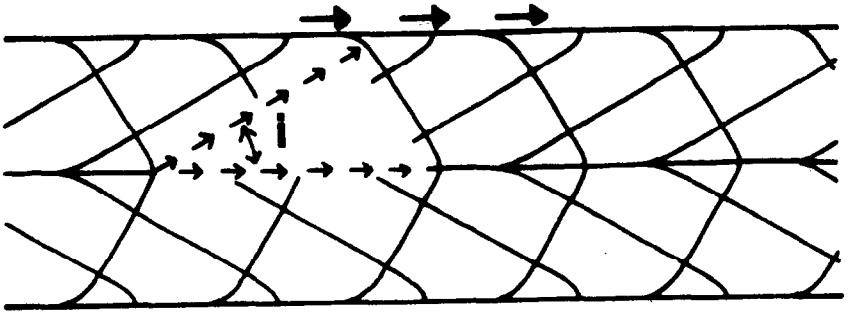

b

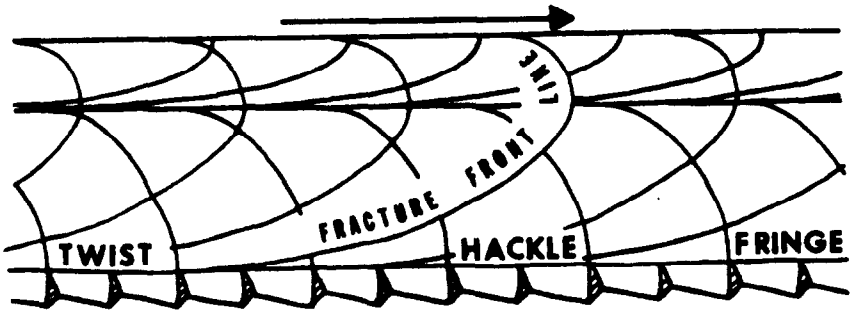
FRACTURE FRONT
TWIST
HACKLE
FRINGE

c

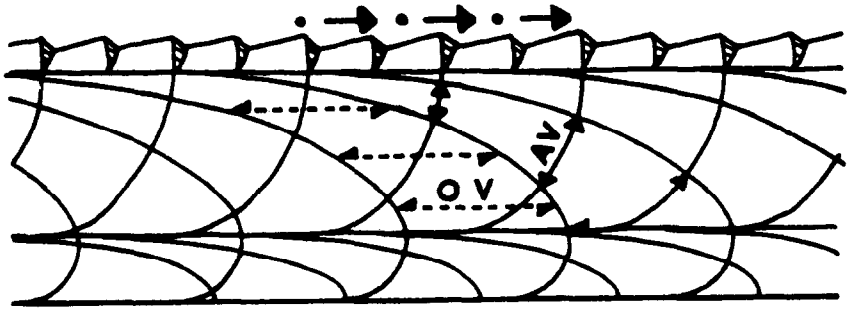
ΔV
OV

d

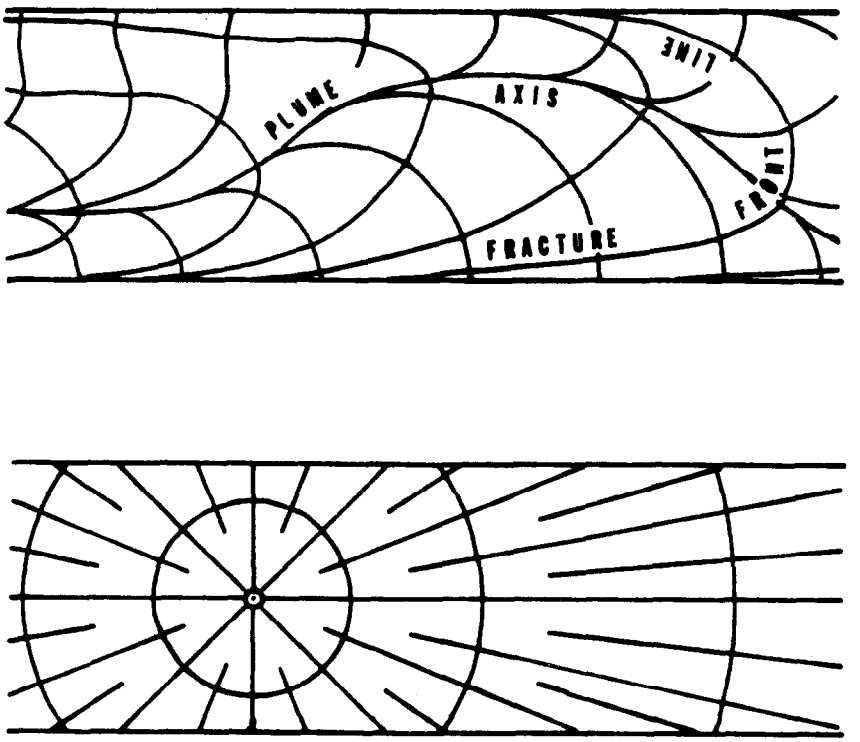

Figure 37 a through f, hypothetical fracture surfaces illustrating the use of hackle plume geometry to approximate past fracture fronts, fracturing stress distributions, and relative fracture propagation velocities. Arrows over stratum top indicate overall fracture propagation directions. Arrow pattern indicates intrastratum location of maximum fracturing stress and highest actual fracturing velocities.

Figure 37a - The horizontal plume axis bisects the stratum. Plume components are curved and symmetrical about the axis. Adjacent plume components are not parallel to each other and diverge toward stratum boundaries in the fracture propagation direction. In this case, constructed lines depicting the fracture front at any past time are circular arcs, each with the same radius of curvature. Adjacent fracture front lines are not parallel to each other and diverge toward the plume axis.

The varying hackle component lengths, bounded by, and perpendicular at intersection with, adjacent past fracture fronts, are directly proportional to the average fracture velocity along these plume component lengths (AV, Figure 37d). Here, a constant time is represented by the distance between two adjacent fracture fronts. It follows that the actual fracture velocity increases to a maximum along the plume axis. Increased actual velocity toward the plume axis is shown by greater hackle component lengths in this direction. Note, the overall rate of fracture propagation, parallel to the linear plume axis, is constant between adjacent fracture front lines throughout the stratum (OV, Figure 37d). Constant velocity is necessary to maintain an equal radius of curvature at intersection points on successive fracture fronts in the overall fracture propagation direction.

Figure 37a demonstrates how any hackle plume axis or plume component can show the principal effective stress directions. The greatest and intermediate principal effective stresses ($\sigma_1$eff; $\sigma_2$eff) are assumed to be compressive. The least effective principal stress ($\sigma_3$eff) is tensile. This stress situation is not uncommon at depth where pore pressure plays an important role in the fracture process (Secor, 1965, 1969). Effective stresses must be attributed to another mechanism in rocks of extremely low porosity or where pore pressures were low at the time of fracture.

The described stress configuration that leads to subsequent fracture propagation can be appreciated by perceiving a fracture originating at a penny-shaped (circular) flaw. The plane containing the flaw also contains $\sigma_1$eff and $\sigma_2$eff. The least principal effective stress ($\sigma_3$eff) is perpendicular to this plane and fracture tip. The fracture, once initiated, will advance at the highest velocity parallel to $\sigma_1$eff. This is because the tensile component at the crack tip contributed to $\sigma_3$eff by compressive $\sigma_1$eff is greater than that contributed by compressive $\sigma_2$eff. It follows that the plume axis and any plume component, forming perpendicular to the fracture front, will parallel $\sigma_1$eff. In contrast, $\sigma_2$eff is perpendicular to plume axis and plume components (tangent to fracture front) at the crack tip. This relationship applies anywhere on the fracture surface and regardless of whether the hackle is primary or secondary. Again, both $\sigma_1$eff and $\sigma_2$eff act in the plane containing the fracture front. $\sigma_3$eff remains perpendicular to the crack tip plane all along its length. It follows that $\sigma_3$eff is perpendicular to hackle plume axis and components. The fact that dynamic fracturing stresses constantly change throughout a fracturing rock is shown by the 90 degree rotation of $\sigma_1$eff from plume axis to stratum boundaries.

Figure 37b - The horizontal plume axis bisects the stratum. Plume components are straight over much of their length, parallel to each other, and arranged symmetrically about the axis. Any constructed line depicting the fracture front at some time past can be divided into two straight line segments symmetrical about the plume axis. These straight line fracture front segments are parallel to each other (as are plume components) indicating uniform fracture velocity along the linear fracture fronts. During the time represented by the distance between two parallel fracture fronts, the fracture advanced an equal amount parallel to plume components all along the front.

However, along the plume axis, the fracture advanced a greater distance. Again, this suggests higher fracture velocity along the axis in response to greater effective fracturing stresses.

A direct relationship exists between the acute intersection angle (i) bounded by plume axis - straight plume components and the effective tensile fracturing stress difference from plume axis to straight line fracture fronts. A smaller angle i indicates a lower effective fracturing stress difference. It follows that a straight fracture front, perpendicular to stratum boundaries, would indicate uniform fracture velocity and fracturing stress throughout the stratum. In this case no unique plume axis would exist.

Figure 37c - The plume axis lies in the upper stratum section. Plume components are curved and are not arranged in a symmetrical pattern about the plume axis. Adjacent plume components are not parallel and diverge at different rates on opposite sides of the plume axis. Constructed lines depicting past fracture fronts are parabolic and not symmetrical above and below the plume axis.

The effective stress to fracture and corresponding fracturing velocities were greatest in the upper stratum section and least at the stratum bottom. Actual fracture propagation velocities are proportional to plume component lengths contained between adjacent fracture front lines. Again the overall fracture propagation rate (OV) parallel to the plume axis is constant between adjacent fracture front lines throughout the stratum.

The fracture origin (off illustration to left) would also lie in the upper stratum section assuming the availability of an appropriate origin flaw. Without such an origin location, the fracture could have initiated in the lower stratum section at a very weak flaw under lower effective fracturing stress. However, the leading fracture section (plume axis) would sense the up-stratum maximum fracturing stresses and migrate towards that area. A similar fracture origin argument can be applied to all given examples except 37f.

Figure 37d - The explanation for 37d is identical to that given for Figure 37c. The notable difference is that plume axis location and plume asymmetry indicate the greatest effective fracturing stresses acted in the lower stratum section. Consequently the resulting fracture led in the lower stratum level.

Marked twist hackle with high relief on hackle steps can be expected in fracturing situations depicted in Figure 37c and 37d. Twist hackle would form in the bottom and top stratum sections respectively. Here, fracture velocities are lowest in response to low effective fracturing stresses. Any resultant fracturing stress direction, caused by a superposed stress, would vary markedly from the direction of the principal effective fracturing stress in areas where this effective principal fracturing stress is low. It can be expected under these conditions that twist hackle faces, perpendicular to the resultant stress, will form at an increasing angle to the main fracture face, and related hackle step relief will become more pronounced toward stratum boundaries. This mechanism may explain the twist hackle fringe commonly observed on a fractured rock stratum.

Figure 37e - The plume axis and corresponding leading portion of the fracture front migrates left to right from lower to upper to lower stratum levels. Plume components and past fracture fronts vary in orientation and can converge or diverge away from the plume axis. The sinuous migration path formed as the plume axis turned to remain parallel to a changing greatest principal effective stress ($\sigma_1$eff) direction while the fracture plane remained perpendicular to the least principal effective tensile stress ($\sigma_3$eff). It follows that the intermediate principal stress direction ($\sigma_2$eff) was perpendicular to the plume and plume components at the crack tip and lay within the fracture plane.

Figure 37f - The fracture origin location (not shown in preceding examples) at stratum center was determined solely by the location of the weakest flaw. Plume components are straight lines and radiate from the fracture origin. Constructed fracture front lines are concentric circles about a common center (fracture origin). All portions of adjacent fracture front lines are equidistant, and plume components between adjacent fracture front lines are equal in length. It follows that the fracture propagation velocity was equal in all directions and no leading fracture front section exists. Therefore, there is no unique plume axis. In this case, the fact that the fracture front, away from the origin, is most advanced at the fracture center has no significance. The least effective principal tensile stress ($\sigma_3$eff), perpendicular to fracture plane and crack tip, was equal all along the fracture front and $\sigma_1$eff equalled $\sigma_2$eff. The fact that plume components do not curve to meet stratum boundaries orthogonally shows that these boundaries had no effect on fracturing stresses. During fracture, presently existing stratum boundaries could not have acted as free surfaces.

Summary. Hackle plumes are a powerful tool for qualitative interpretation of past fracturing velocity and corresponding stress distributions. Several general rules are summarized that apply to rock fracture investigations.

1. Fracture origin locations are controlled by a combination of flaw weakness and stress distribution. Generally fracture origins are located where effective fracturing stresses were greatest.

2. Hackle plume axes in fractured rock mark the region of highest stress concentration and resulting fracture velocities.

3. Hackle plume components generally diverge away from plume axes in the direction of fracture propagation. If effective tensile stresses, acting perpendicular to a fracture front, were uniform in the overall propagation direction throughout a fracturing rock stratum, a statistically valid number of plume opening directions would show fifty percent opening in each fracturing direction. If effective tensile stresses were not equal in the overall propagation directions, a tensile stress gradient would exist through a fracturing stratum. In this case a majority of plume opening directions would be in the direction of the increasing effective tensile stresses. Propagating plume axes would extend further in the direction of the increasing tensile stress.

4. The most pronounced twist hackle may exist at stratum levels subjected to the lowest fracturing stresses. Here, generally fracturing velocities were lowest. Twist hackle steps increase in relief toward stratum boundaries. In this direction principal effective stresses decrease, superposed stresses have greater effect, and the resultant stress (perpendicular to twist hackle face) may deviate more from principal stresses. Also imposed stress at stratum boundaries may form twist hackle.

5. Straight hackle plume components and corresponding straight line fracture fronts indicate uniform fracture propagation velocity at these locations. Uniform fracture velocity is also indicated by circular fracture fronts with a common origin and hackle plumes radiating from that origin.

6. Hackle plume geometry gives the orientation of principal effective stresses. The least principal effective stress ($\sigma_3$eff) is tensile and perpendicular to a plane containing the fracture front. The greatest principal effective stress ($\sigma_1$eff) can be compressive and is parallel to the plume axis or plume components (parallel to local direction of fracture advance) at the fracture front. The intermediate principal effective stress ($\sigma_2$eff) can be compressive and is perpendicular to the plume axis or plume components (perpendicular to local direction of fracture advance) at the fracture front. The greatest and intermediate stresses lie within the fracture plane at the crack tip.

7. A map view indication of fracture propagation direction and intrastratum plume location can be given by arrows placed adjacent to a fracture or fracture set symbol (Figure 37a through f). A solid arrow indicates a fracture or fracture set leading predominently in upper stratum levels. A dashed arrow indicates a fracture or fracture set leading predominently at midstratum levels. A dash-dot arrow indicates a fracture or fracture set leading predominently in lower stratum levels. This, or some similar scheme, is useful in depicting map results of regional or local fracture investigations.

Tendential Fracture Features

Tendential fracture features are attributed to long-range changes in the stress field. This situation is in contrast to the local, often sonic wave induced, short range stress perturbations responsible for transient features. Tendential features are recorded as undulations in the fracture profile or trace. This trace can be visualized as the line formed by the intersection of the fracture plane and a free surface. Obviously the fracture trace on the surface gives no indication of the angular relationship between the fracture plane and surface.

Tendential features generally proved to be of slightly less value than transient markings in the prototype core investigation, and were used mainly as an aid in determining the formational sequence of fracture sets. However, the proper interpretation of tendential features is an invaluable tool when studying fractures in outcrop.

Hooking

Hooking is a localized tendential effect that can be initiated in several different ways. A fracture plane may curve due to interaction with the neutral surface of a flexed object (Poncelet, 1965). If a fracture originates at the outer arc surface and advances inward, the neutral surface cannot move ahead of the fracture into the compression zone toward the inner arc of the flexed object until the neutral surface is lengthened by a dilational wave that is reflected from the ends of the flexed beam. The fracture, upon contact with the neutral surface, swings approximately ninety degrees to run parallel to that surface. This indicates local tension perpendicular to the neutral surface and rod axis. After compressional stresses are relieved by the passage of the dilational wave, the fracture turns ninety degrees and again runs perpendicular to the rod axis to complete the separation. Figure 38 depicts a qualitative illustration of the hooking-neutral surface relationship. In this case, the larger the origin flaw the lower the stress to failure and subsequent fracture velocity. Low fracture velocities allow the neutral surface to move out of the way. Stress to failure and fracture accelerations became higher and origin flaw smaller from rod a to c. A propagating fracture may also hook locally in an attempt to meet a free surface orthogonally. Such fracture behavior is not surprising since a principal stress can only act parallel or perpendicular to a free surface.

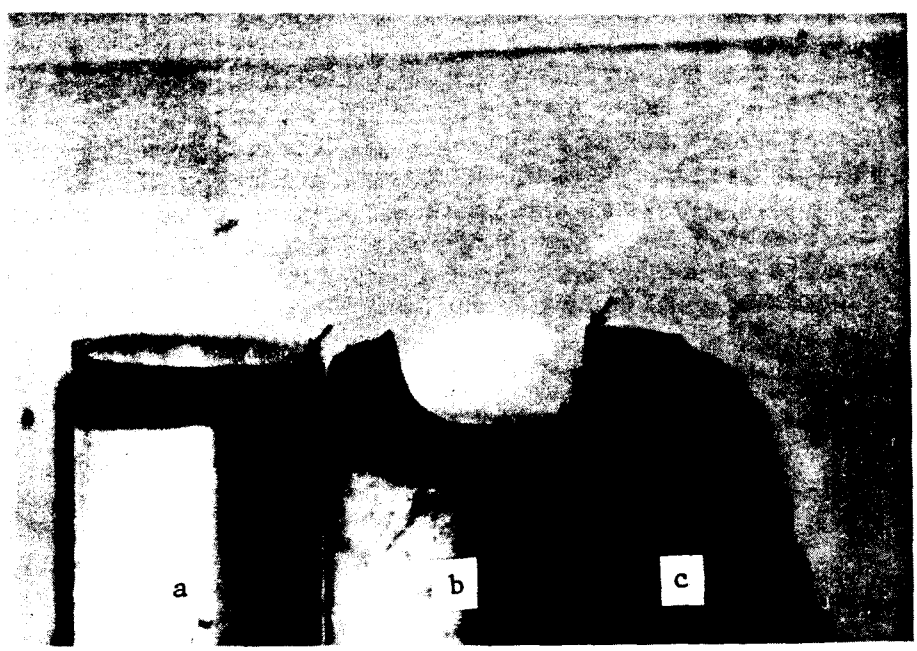

Figure 38, tendential view of fractures through three glass rods. Rods 'a' through 'c' possessed progressively smaller origin flaws and required progressively higher stresses to failure. Fracture velocity subsequently increased from rods 'a' through 'c'. Rod 'a' possesses no appreciable hook and a mirror region that extends entirely across the fracture. Hooking is initiated closer to the origin from rod 'a' through 'c'. The fracture origin point on each rod is indicated by the arrow. Optical micrograph, 7X magnification.

Schardin (1959) describes another fracture possibility at the neutral surface. He visualizes a high stress concentration at the propagating fracture tip that is responsible for elastic energy. The elastic energy maintains fracture propagation and may enable the fracture to penetrate beyond the neutral zone into the compression region. The traveling fracture may thus be accompanied by its own kinetic energy that provides fracture tension.

Hooking proved to be helpful in certain cases for determining fracture sequence in core sections (chapter 8). The hooking relationship can also prove useful in outcrop fracture studies. Later formed fractures may curve sharply and hook into earlier formed fractures. Oftentimes a given fracture of a single set will hook at both adjacent ends into parallel or orthogonal fractures indicating the fracture origin to be in the central portion of the fracture. In this case the fracture spread laterally in both directions from this origin point. This example again illustrates the futility of relying on fracture spreading directions alone for meaningful structural data. Figure 39 shows a hooking fracture that has been stylolitized. The tendential hook is a strong indication that the fractures occurred first and later lateral compressive stress created stylolite seams on these faces.

Figure 39, tendential view of hooking by fractures that have been subsequently stylolitized. Stylolite teeth are asymmetrical and trend in the same direction on both straight and hooking fracture sections. Arrows indicate fracture propagation direction. Stylolitized fractures indicate a principal tension and subsequent principal compression. The two stress events acted in nearly parallel orientation.

Forking

The term forking is applied to the process of fracture bifurcation into two or more diverging fracture planes. The point of bifurcation has been termed the radiant by Preston (1926). Forking is imminent when a fracture reaches a critical or terminal velocity concomitant with an ever-increasing crack tip stress. Again, the critical or terminal fracture propagation velocity for a given material at the onset of fracture forking need not be the maximum velocity. Under different test conditions designed to restrict velocity hackle and suppress forking, fracture velocities approximating sonic wave velocities can be attained (Snowden, 1976). The critical velocity in glass and various rock types is reported to be approximately one-half the transverse wave velocity (Frechette, 1972; Schardin, 1959; Bieniawski, 1967, 1968).

A qualitative appreciation of the above statements can be gained by the following simple test. Scribe the surface of several glass laths (microscope slides) parallel to their intermediate axis directions with scratches of varying length and depth. Place a strip of transparent tape on the glass face opposite the scratched surface. Flex the microscope slides about the intermediate axis with the scratched surface under tension and the tape on the compressive surface (please wear gloves). The tests highlight the conclusion that the increased stress to failure that is needed for the small scratches produces an increased number of bifurcations and a decreased initial zone from origin to radiant. The fracture surfaces can be folded back along the tape permitting perusal of the transient features. The geometry of observed transient features will prove a fracture spreading in two directions from a singular origin at the superimposed scratch. All bifurcations produced are the result of a single fracture event and are caused by simple tension (figure 40). Also refer to Appendix II.

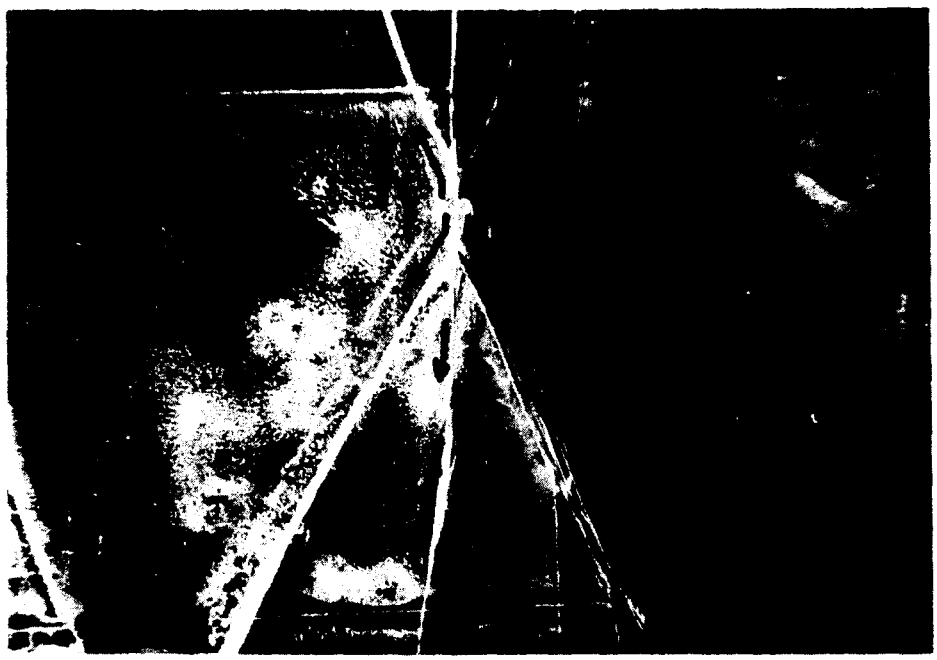

Figure 40, forking produced by bending a glass microscope slide. The fracture progressed from the origin, leading on the upper surface (toward viewer) that was under tension. Fracture propagation directions are indicated by arrows. Optical micrograph, 4X magnification.

The fact that some rocks contain a high density of serious flaws (deep scratches and anisotropy planes) may help explain the lack of fracture forking in certain strata. These intra-stratum flaws impart a weak tensile stress to rocks, thereby lowering stored elastic strain energy before failure, thus impeding fracture velocity. Please be aware that results of tension fracture experiments utilizing glass rods and laths must be viewed qualitatively. In rocks, the stress for fracture initiation and stress needed for actual failure do not coincide, indicating tension fracture processes differ in rocks and glass. Also the absence of grain boundaries, internal flaws and high elastic modulii promotes rapid crack propagation in glass.

Schardin (1959) concludes that crack bifurcation in a glass plate has no effect on the critical fracture velocity, even immediately adjacent to the radiant where the diverging cracks are in close proximity. This implies an excess of elastic energy within the fracturing material at the radiant. Consequently the fracture velocity need not decrease even though the amount of new crack surface created per unit of time is increased.

Fracture forking or bifurcation has been produced and studied experimentally in rocks. Bieniawski (1967, part II) found that when the critical and terminal rock crack propagation velocity was reached under certain test configurations, fracture bifurcation occurs. Bieniawski concludes that fracture forking marks the termination of stable crack propagation and the onset of unstable crack propagation. The distinction here is that up to the inception of forking the elastic energy released by crack extention is not sufficient to maintain fracture growth, and crack propagation can be controlled by the applied load. However, at the onset of forking elastic energy is sufficient to maintain fracture propagation even though the forking process acts to dissipate excess elastic energy. During unstable crack propagation Bieniawski found that fracture propagation is not controlled by the applied load, and individual rock grains are shattered by the forking process. Finally, according to Bieniawski, stable and unstable fractures propagate at slow and fast velocities respectively. Irwin (1960) also implies that the transition from stable to unstable crack propagation, during the brittle fracture of metals, occurs when the energy released per unit of crack surface attains a critical value.

The fact that forking and extensive individual grain damage in grains and nodules adjacent to the fracture surface has not been observed in systematic Allegheny plateau fractures (figure 41a) is further evidence that propagation velocities of natural fractures were below the critical forking velocity. Also, if Bieniawski's observations for controlled tests can be extrapolated to natural systems, fracture growth at less than critical velocities could be stopped by lowering the applied stress. For example, figure 41b shows a dessication fracture in dried paint with a well-developed hackle plume. Arrest lines indicate that fracture propagation proceeded in spasmodic advances marked by periodic hesitation. When shrinkage induced tensile stresses fell below a critical value fracture progress ceased. Here, stable crack propagation was controlled by the applied load. Figures 41c and d show mineralized natural fractures in Devonian siltstone. Hackle plumes and a terminal arrest line are similar in geometry to those on the paint fracture, thereby implying stable crack propagation. However, on the rock fracture, formed under appreciable confining pressure, the effective tensile stress might be attributed to pore pressure or some other mechanism.

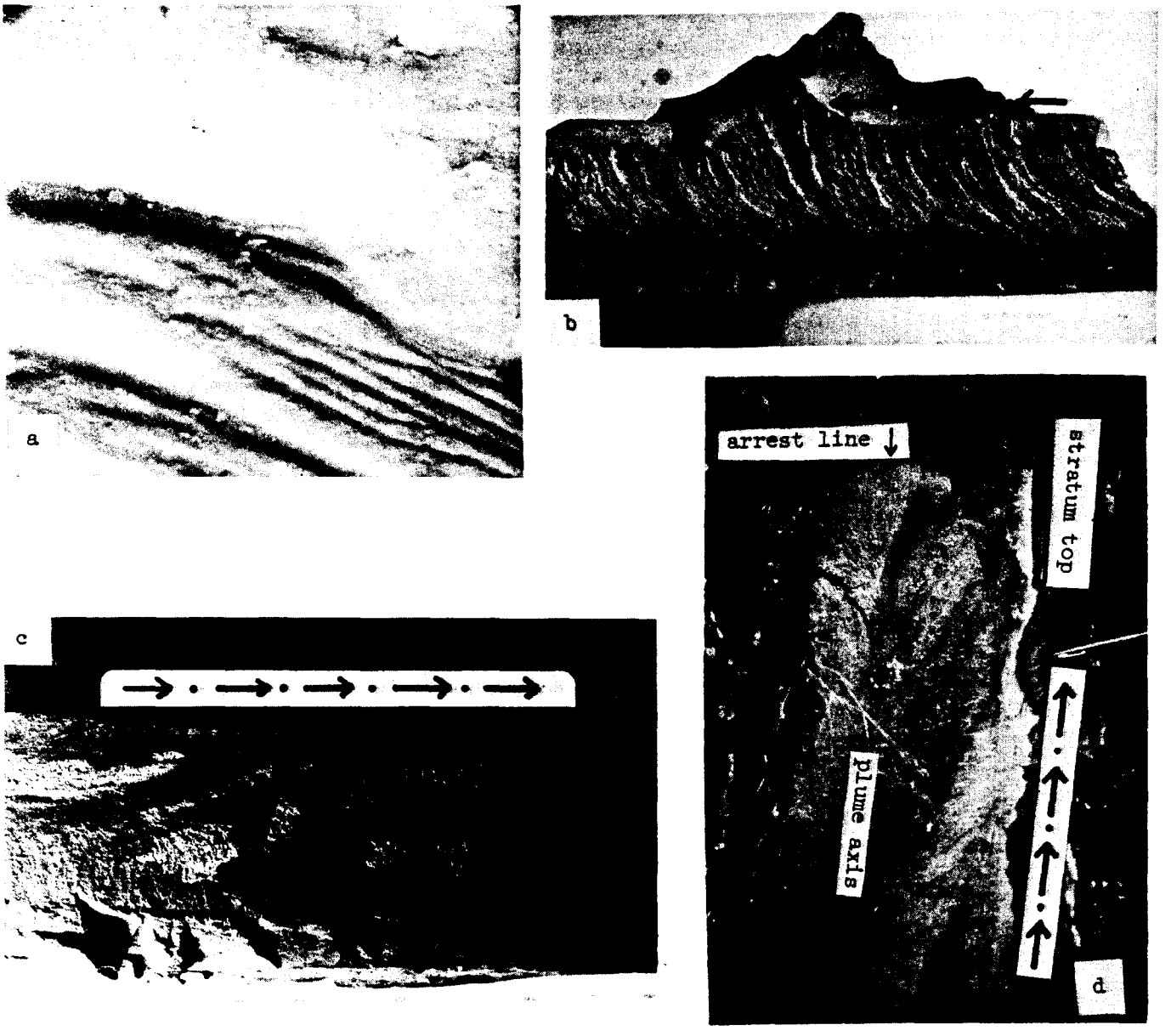

Figure 41a, systematic fracture surface cutting a quartz pebble, Mississippian sandstone, West Virginia. The main fracture face is not extensively damaged and no coarse velocity is observed. Scanning electron micrograph, 2400X. b, dessication fracture in dried paint. Note well developed hackle plume and arrest lines. c and d, mineralized natural fractures in middle Devonian siltstone. Note well developed hackle plumes, twist hackle fringe, and arrest line on overturned stratum. Arrows at stratum and paint layer tops show overall fracture propagation direction, location of greatest intralayer fracturing stress, and highest actual propagation velocity (see figure 37). Paint fracture courtesy of Mike Evans and George Clarkson, West Virginia University.

Figure 42, systematic fracture face in Mississippian limestone, West Virginia. Note smooth fracture surfaces on chert nodules. The propagating fracture cut through chert nodules and limestone matrix with no variation in direction. Fracture forking and coarse velocity hackle is not evident on freshly exposed chert nodule fracture faces.

If fractures do reach a propagation velocity critical to forking in certain rocks, forking should be a tendential feature observed in outcrop. Preston (1935) describes an interesting relationship in thin glass laths and bottles between the greatest (σ_1) and least (σ_3) principal stresses and the forking angle, that may have geological application (figure 43). The intermediate principal stress is assumed to be negligible, and the forking angle is that angle bounded by the two outermost fractures of a radiant. σ_1 and σ_3 lie in the plane of the glass objects. One of these stresses must be tension and is assumed to be positive. All stresses are measured at or near the fracture origin point.

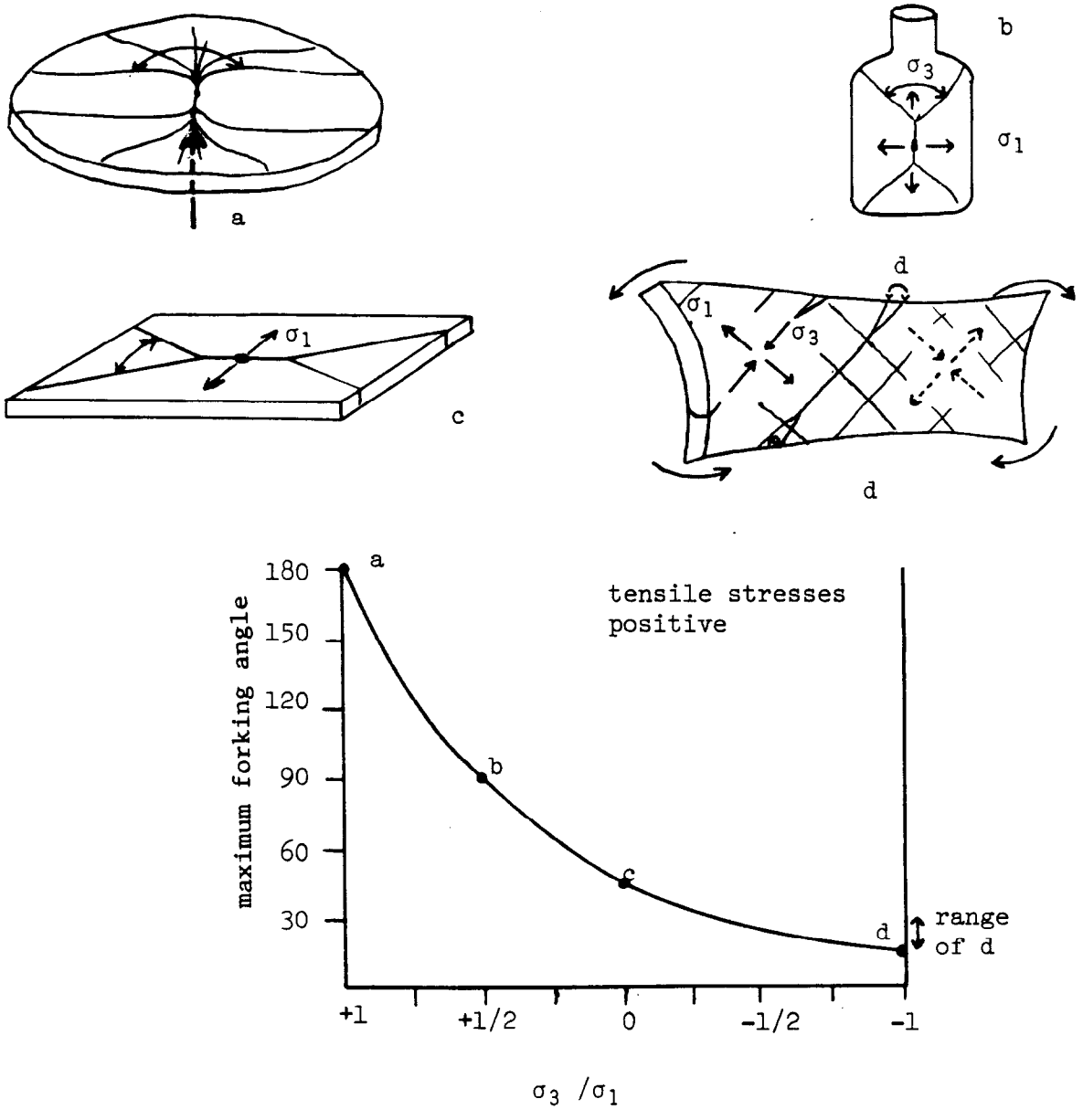

Figure 43, relationship of forking angle for fractures in thin glass laths and bottles to the ratio of the least (σ_3) and greatest (σ_1) principal stress. a, central pressure ($\sigma_3 = \sigma_1$); b, internal pressure test ($\sigma_3 = 1/2\ \sigma_1$); c, cross bending of laths ($\sigma_3 = 0$); d, torsion test ($\sigma_3 = \sigma_1$). Modified from Preston (1935).

Preston attributes the range of torsion induced forking angles in glass laths to stresses produced by a combination of torsion and bending. If a glass rod or tube is twisted the forking angle is generally closer to 15°. With proper precautions, all of the forking experiments can be verified with material available in any laboratory. The cross bending experiment has already been described.

Preston's observations and the possible occurrence of forking phenomena in outcrop make it imperative that geologists studying fractures do not overlook this tendential feature, especially if critical fracture velocities have been reached. A single fracture event subject to forking, as in cross bending, might be incorrectly interpreted as three or more separate fracture sets. Two of these sets could be erroneously construed to be oblique or "shear" joints. Locally, in certain tectonic settings, rocks subject to torsion might also lead to a compression-induced "shear" joint misinterpretation. Here the cross cutting relationship is formed because each fracture set originated and spread on opposite sides of the lithotectonic unit as in the case of the glass lath. This is easily verified by observing the transient features on the fracture faces (figure 44).

The 180° fork produced by central pressure may not be dependent upon a critical fracture velocity. Once the primary origin fracture has spread a short distance, tensile stresses perpendicular to it are released somewhat. The tensile stress perpendicular to this is now larger and the crack will veer 90° in one or two directions to be perpendicular to the new greater principal tension. This produces the 180° forking angle. The higher the applied tensile stress and stored strain energy, the greater the number of radiants between the 180° bounding fractures. The possibility that fracture velocity may not be critical to central pressure forking is shown by clay sheets subjected to doming (Cloos, 1955, 1968). Fracture velocities in plastic clay are not high, yet a similar 180° forking pattern can be produced. However, few, if any, radiants are formed. It is intriguing to note that the same fracture pattern is observed within strata over any number of salt domes. The fracture pattern on clay and salt dome cover strata can actually resemble rectangular rather than radial fracturing.

Finally, <u>if</u> fracture velocities in rocks did reach a critical value for forking, the principal stresses applied to Preston's glass laths could correspond with effective stresses (Secor, 1965) at geological depths. Again, the authors feel that natural rock fractures have not propagated at critical forking velocities.

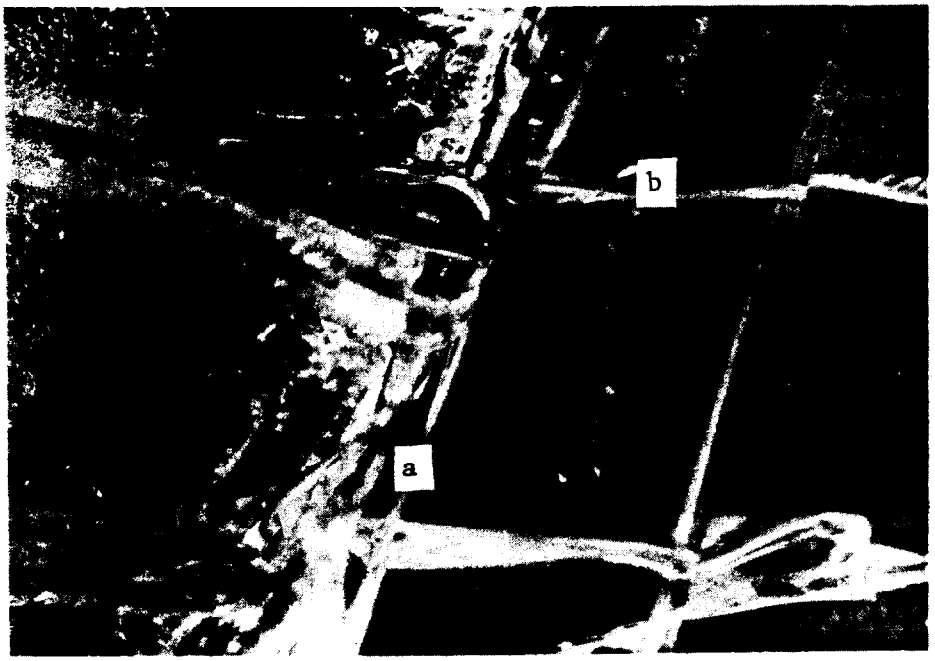

Figure 44, apparently intersecting fractures in glass lath subjected to torsion. Fracture set 'b' formed last with 'b' set fracture fronts leading on the underside of the lath and spreading vertically to the lath surface facing the viewer. This spreading history is evidenced by the twist hackles on fractures of this set that are initiated where the fracture hooks towards the upper surface. These hackles show the fracture spread vertically upward within the hook. Fractures in set 'a' formed before set 'b' and led in the upper lath surface hooking toward the bottom. Note slight offsets of 'b' fractures at intersection points (arrows).

Fracture intersection relationships

The sequence of fracture formation can, in many instances, be deduced at fracture intersection points. The most straightforward intersection relationship is formed when a later formed fracture abuts against, and is terminated by, an earlier formed fracture. One fracture abuts another because the tensile stress at the crack tip cannot be extended across a free surface (figure 45). This particular phenomenon, familiar to all geologists, is often utilized to help determine fracture sets and relative fracture ages in outcrop. The abutting relationship is also very useful in core fracture analysis.

In some instances the abutting relationship fails and the fractures of different trends are observed that appear to cut across each other in violation of fracture propagation mechanics. Apparent crosscutting of two fractures can be achieved by at least four different means.

1. If the first formed fracture has been recemented by secondary mineralization, the tensile stress at the tip of an intersecting later fracture can be maintained. The secondary minerals may be subsequently dissolved but the crosscutting relationship remains (figure 46).

2. The intersected fractures need not be recemented if a torsion stress in a given stratum is responsible for two fracture sets propagating from the top down and from the bottom up (figures 47, 48).

3. If a shallow fracture, not penetrating the entire thickness of a given stratum is intersected by a later formed fracture that penetrates the entire stratum thickness, this fracture may crosscut the earlier formed one. The later formed fracture passes under the shallow earlier fracture and then spreads upward on the other side to intersect the earlier formed fracture from the other direction. This propagation pattern is verified if the face of the intersecting fracture is made visible and hackle patterns (plumose markings) are evident (figure 49).

4. If a point load is applied to a weakened glass (surface lightly scoured with fine sandpaper), three fractures can be produced that seem to crosscut each other. The crosscutting relationship generally, but not necessarily, forms an orthogonal pattern and occasionally more than three fractures may be produced. There is no reason to believe that this situation could not exist in a thin sandstone unit overlying a shale subject to localized differential compaction. A number of these cross-cutting relationships could be produced in the sandstone (figures 50, 51).

The formation of new shear planes in a material formerly cut by brittle fractures can produce an abutting fracture relationship that is the reverse of that normally expected. Later shear movement along one of two intersecting pre-existing brittle fractures can result in an even more confusing abutting relationship as shown in figure 52.

Figure 53 shows two hypothetical systematic and nonsystematic fracture sets that can be attributed to different events. The systematic - nonsystematic fractures, the former paralleling and the latter perpendicular to the slickenside directions, are local and formed early in folding. Slickensides are on a bedding surface and formed by a flexural slip mechanism. The pervasive systematic and nonsystematic fracture sets oblique to the fold axis (perpendicular to slickensides) are regional and older than the fold-related fractures as shown by the intersection relations.

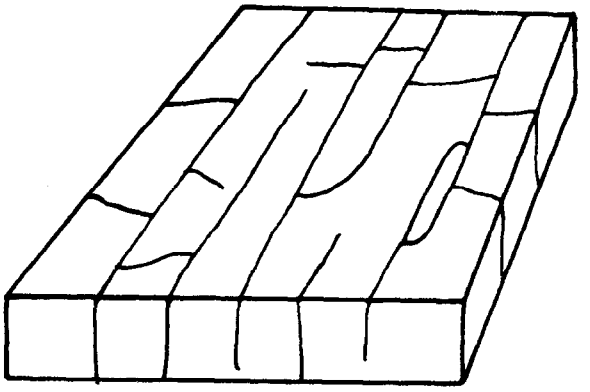

Figure 45, general tendential pattern of systematic and non-systematic fractures

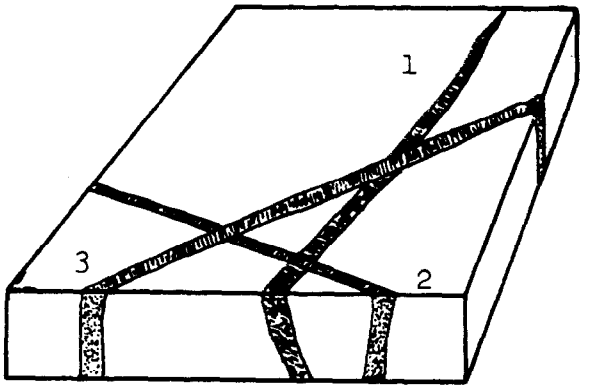

Figure 46, mineralized fractures and cross-cutting relationships

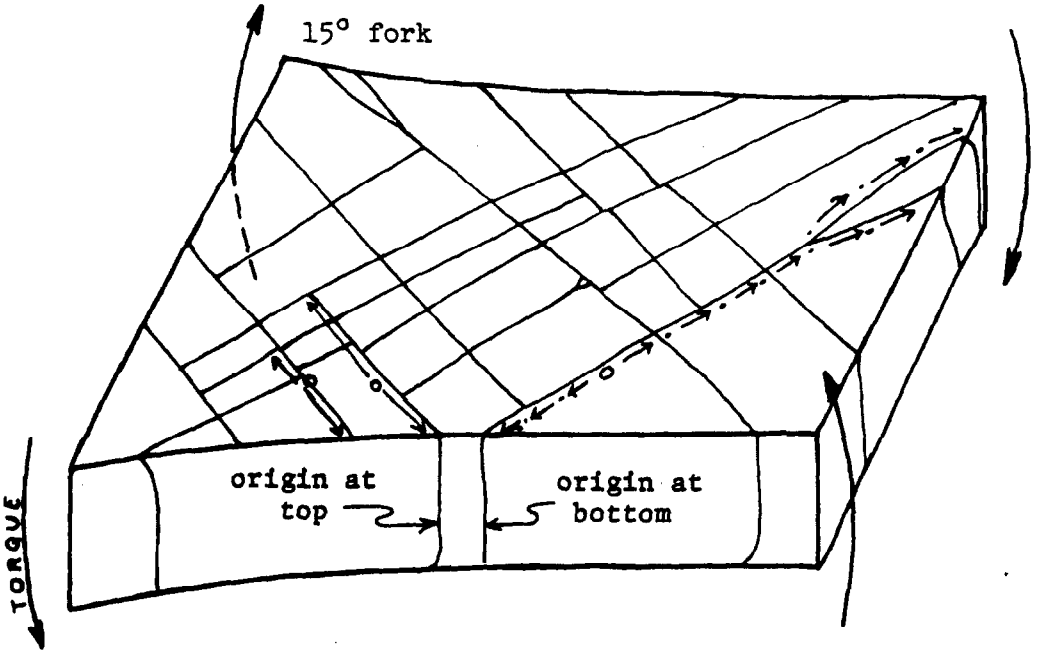

Figure 47, general tendential pattern of torsion fractures

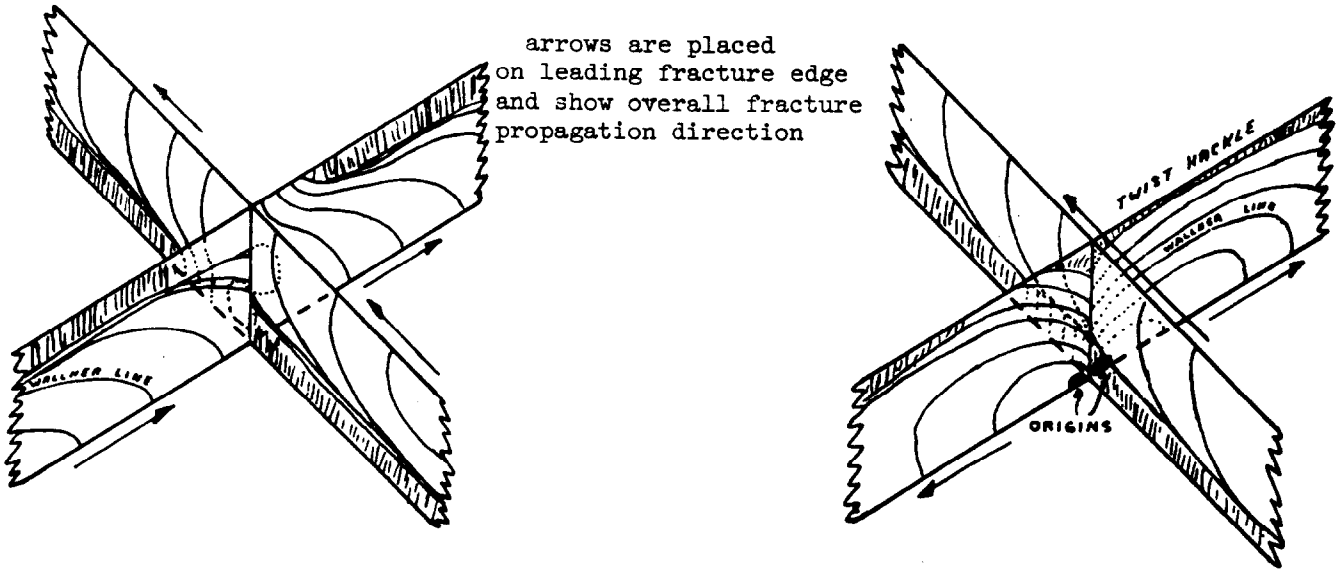

Figure 48, two possible mechanisms for torsion fracture intersections. Arrows indicate fracture propagation direction and are placed on fracture's leading edge. Twist hackle is formed on the fracture's trailing edge.

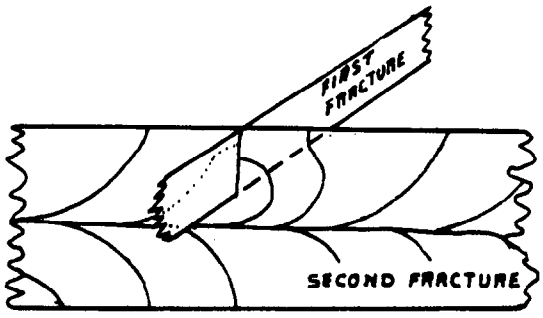

Figure 49, shallow fracture, not penetrating an entire stratum, intersected by later formed fracture that penetrates the entire stratum thickness.

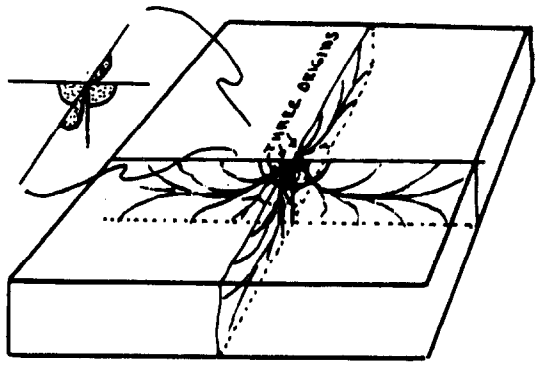

Figure 50, three individual fractures produced by point load applied at bottom.

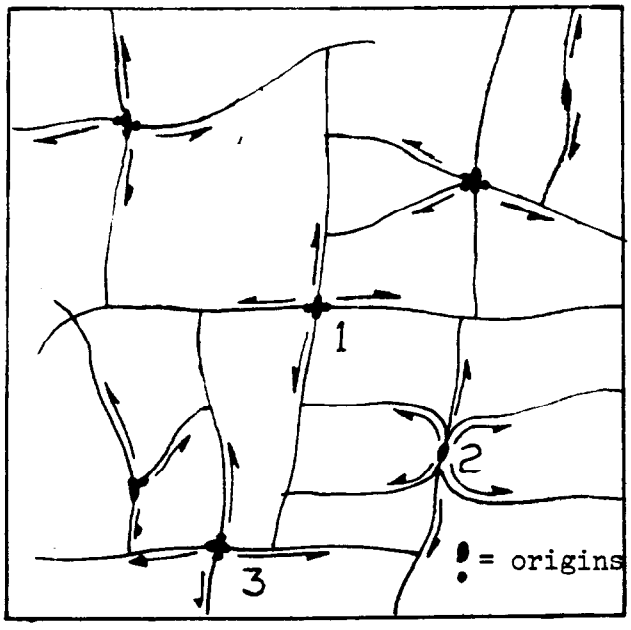

Figure 51 : generalized tendential pattern of point load fractures, single major origin secondary origins about major origin.

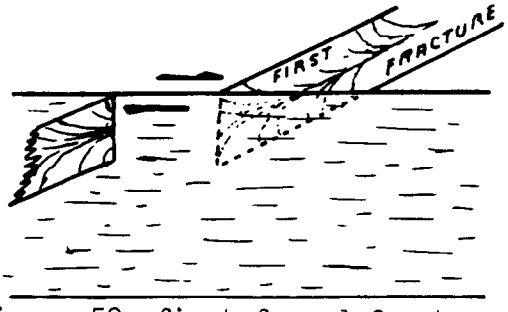

Figure 52: first-formed fracture offset by shear movement along later fracture .

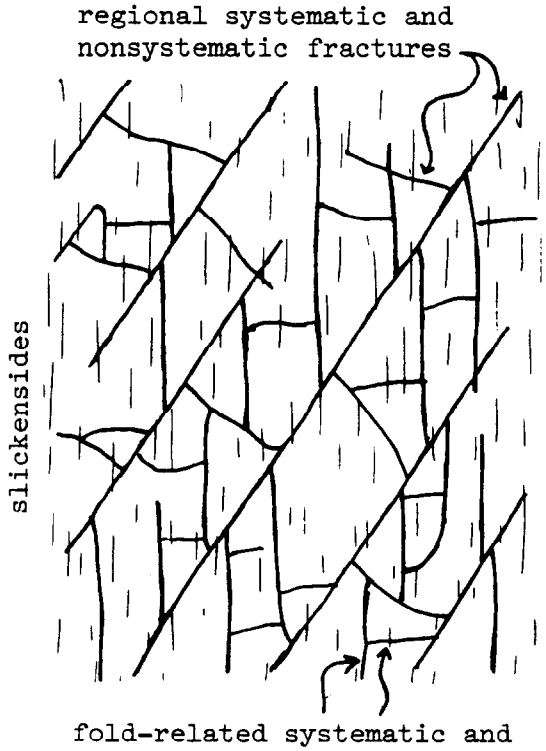

Figure 53

CHAPTER 5

A QUANTITATIVE APPLICATION OF FRACTOGRAPHIC FEATURES

Use of Wallner lines to determine fracture velocity

As discussed in a previous section, Wallner lines are the locus of coupling of the propagating crack front with elastic shear waves generated from points of crack interaction with extraneous defects. The generation of a Wallner line is shown schematically in figure 54 after Field (1971).

The solid circular lines are the crack front at successive times after its origin at O (assuming no boundary effects and that at any time t, the velocity is the same everywhere along the front). The advancing crack front intersects a defect at S. This disturbance initiates an elastic shear wave which propagates from S, at the shear wave velocity for the material. The shear wave catches up with, and couples with, the crack front successively at a, b, and c, thereby forming Wallner line S abc. The dotted circular arcs centered at S mark successive positions of the shear wave front. It is possible to produce "higher order" Wallner lines by reflection of the shear wave when it reaches the specimen boundary (see line S'C, figure 55b). The intensity of the reflected wave is usually less than that of the incident wave, and so the amplitude of higher order Wallner lines is correspondingly less than the primary lines.

When Wallner lines are present on the mirror surface, there are at least three methods for determining, post mortem, the velocity of the crack front. Each method requires a knowledge of the elastic shear wave velocity (V_s) for the material, an assumption about the shape of the crack front, and the position of the origin and defects as outlined below:

Method I (Congleton and Petch, 1967) This method allows the determination of an average crack velocity. It requires one Wallner line and the location of the origin O and defect S. The assumption is a circular crack front.

Method II (based on Poncelet, 1965) This method allows for the determination of an instantaneous crack velocity. It requires two intersecting Wallner lines and the location of defects S and S'. No assumption of crack front shape need be made.

Method III (Congleton and Petch, 1967) This method allows the determination of an average fracture velocity. It requires one primary Wallner line and its second order line, and the location of defect S. No assumption of crack front shape need be made.

Method 1 -- The constructions necessary for this method are shown in figure 55a. SS' is the Wallner line and the dotted lines mark successive positions of the circular crack front. The average crack velocity from E to F can be determined as follows. At time t_1 the crack front is simultaneously at positions E and E'. At some later time t_2 points F and F' would lie on the crack front. Now, E' and F' are on the same Wallner line and are also points on the shear wave front spreading from S. So the average crack velocity over the distance EF is given by:

$$V_{E \rightarrow F} = (EF/SF'-SE') \; V_S \qquad (1)$$

Method 2 -- Note that while this argument is developed here for a straight crack front it is general to any crack front shape. The constructions necessary for this method are shown in figure 56. Here the propagation direction is from bottom to top. S and S' are defects and ST and S'T' are the Wallner lines. Dashed lines F_2F_2 and F_1F_1 mark the position of the crack front at times t_2 and t_1 respectively. Lines OR and OR' are tangent to Wallner lines S'T' and ST at the point of intersection O. Lines SO and S'O mark the path of the elastic shear waves generated at S and S' that intersect the fracture front simultaneously at point O. The angle between OR' and OR is ω ; ψ is the angle between OR' and OP'; and ϕ is the angle between OP and OR. The line OO' is parallel to the direction of crack propagation. At time t_1 the crack front is at points R and R' along tangent lines OR and OR'. At the same time the shear stress waves generated at S and S' are at points P' and P on lines OS and OS' respectively. From time t_1 to t_2 the crack front travels a distance O'O and the shear waves travel a distance P'O and PO. So the ratio of the crack velocity V_F to the shear wave velocity V_S is:

$$\frac{V_F}{V_S} = \frac{O'O}{PO} = \frac{\cos\alpha}{\cos\phi} = \frac{O'O}{P'O} = \frac{\cos\beta}{\cos\psi} \qquad (2)$$

By trigonometry (appendix 1) these simple relations can be manipulated into a form which involves only the angles ω , ϕ and ψ , so that:

$$V_F = V_S \sin\omega \,/(\cos^2\psi - 2\cos\phi \cos\psi \cos\omega + \cos^2\phi)^{1/2} \qquad (3)$$

This result can be applied to the intersecting Wallner lines on the mirror of an experimentally produced glass fracture, figure 57, photo from Schardin 1959. The heavy arcuate bands result from the modulation of the growing crack front by ultrasonic waves introduced perpendicular to the face by a piezoelectric transducer. These bands, then, are themselves artificially induced Wallner lines. The numbers are the fracture velocities (m/sec) calculated from the spacing of the bands and the known frequency of the waves. So the calculated answer from equation 3 can be checked with the velocities marked on the photo. Figure 58 shows two traced intersecting Wallner lines from figure 57. Points S and S' are not in the photograph so the Wallner lines have been extrapolated (dashed lines) to their approximate position on the edge of the specimen. With the construction lines added all the information needed to calculate the velocity at point O is available. Where $\omega = 125°$, $\emptyset = 16°$, $\psi = 25°$ and V_S (for window glass) = 3039 m/sec; the calculated V_F is 1503 m/sec compared to 1440 m/sec, as determined by the ultrasonic method. One might use method 1 to calculate the average crack velocity in the region of O.

Method 3 -- The constructions necessary for this method are shown in figure 55b. SS' is a primary Wallner line and S'C is a secondary line produced by a coupling of the elastic shear wave front reflected at S' with the advancing crack front. B and B' are points on the shear wave front at time t_1. At t_2, the crack front has advanced to point C.

The average crack velocity from B to C is then:

$$V_{B \rightarrow C} = (BC/B'S'+S'C)\ V_S \qquad (4)$$

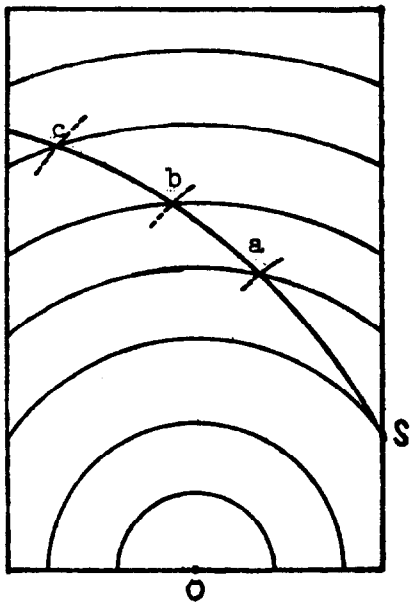

Figure 54, schematic representation of Wallner line formation. Crack originates at O and interacts with defect at S.

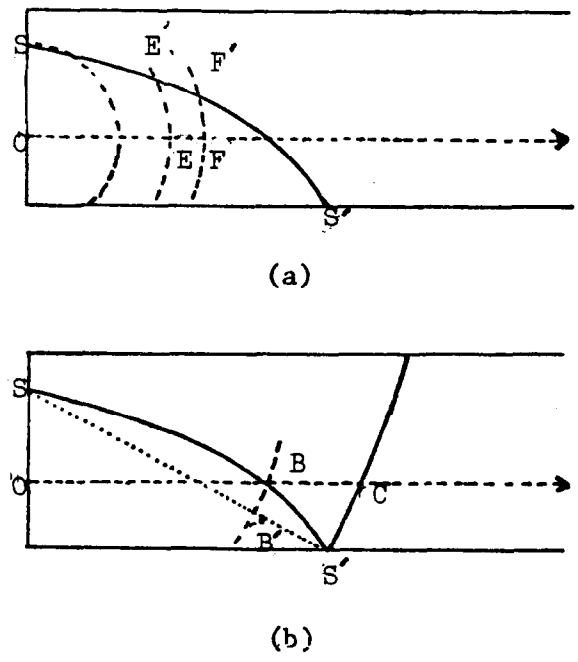

Figure 55, schematic representation of primary and secondary Wallner lines on a fracture surface. From Field, 1971.

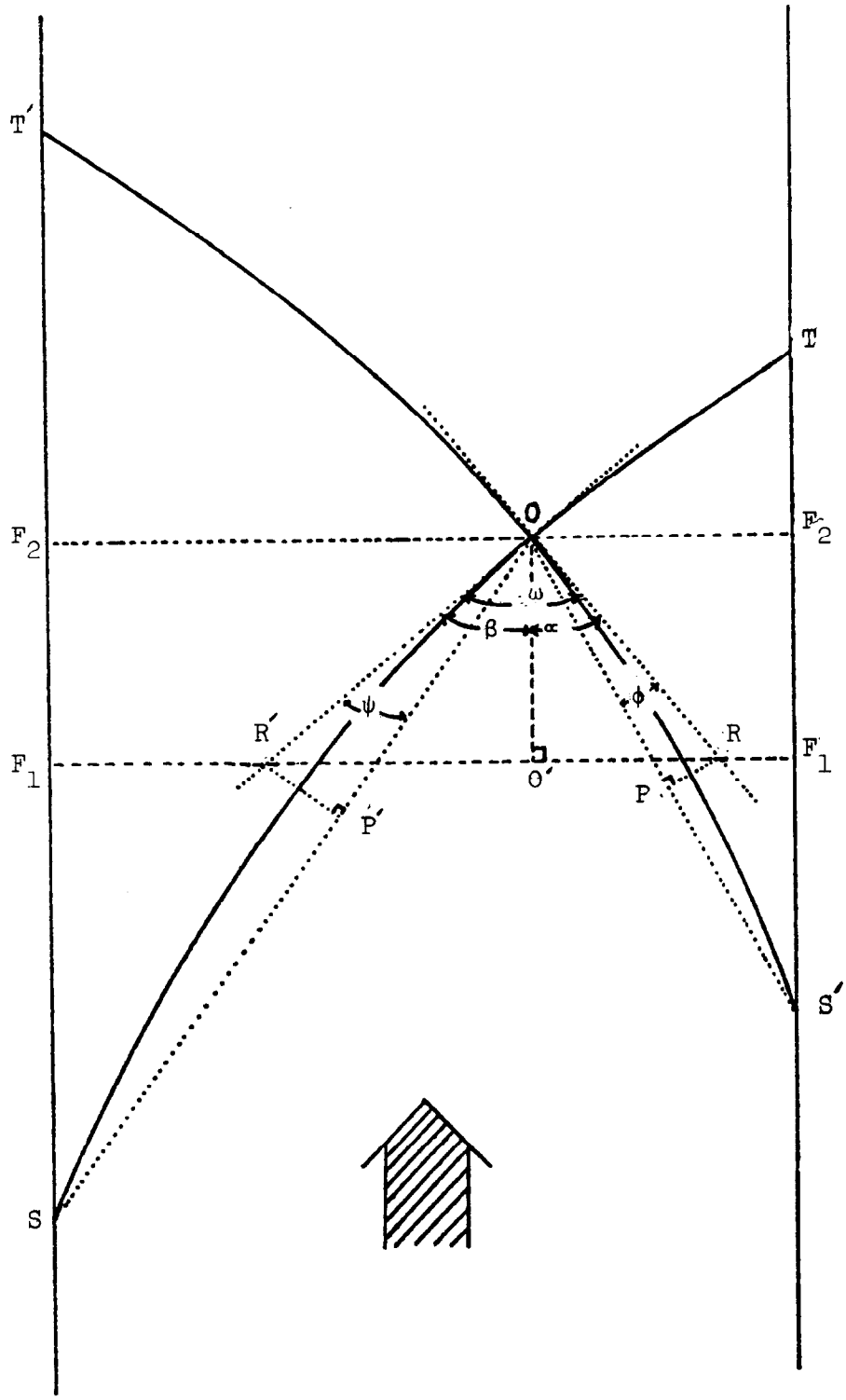

Figure 56, intersection of Wallner lines on a fracture surface. Construction lines dotted and dashed.

Figure 57, ultrasonic-induced and conventional flaw-induced Wallner lines on a fractured glass surface. From Schardin, 1959, figure 6, in Fracture, edited by B. L. Averbach et al., M.I.T. Press, p. 297-330, Copyright 1959 by the Massachusetts Institute of Technology.

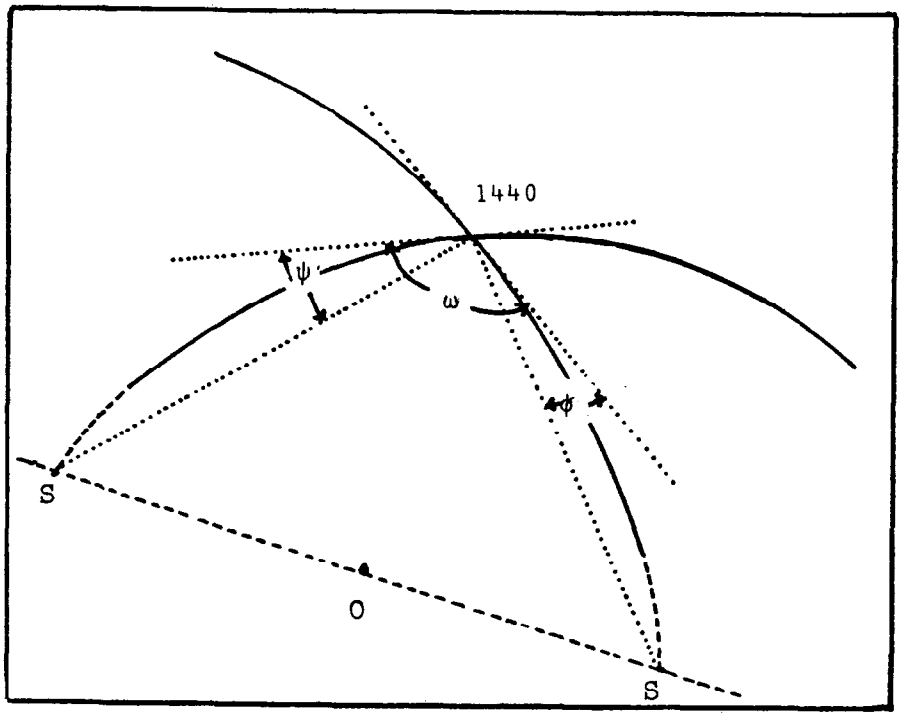

Figure 58, traced from photo, figure 57. Construction lines dotted. Extrapolation lines dashed. $\psi = 25°$, $\phi = 16°$, $\omega = 125°$.

CHAPTER 6

FIELD INVESTIGATION OF FRACTURES

The investigation of bedrock fractures must be conducted in a thorough and methodical fashion based on the sound interpretation of structural chronology and the sequence of fracture events. Older and time honored interpretations of rock fractures such as shear and tension joints, based on the orientation of these features with regard to local or regional structures, must be suspect because of work by many investigators showing a greater antiquity for many fractures than the folded structures in which they are found (Dean, Kulander, 1977; Nickelsen and Hough, 1967; Nickelsen, 1976).

The detail of any outcrop fracture study depends on the projected desired results. For a reconnaissance investigation, various specific procedures listed on the fracture data sheet (figure 59) and outlined below, may prove to be too time consuming. In this case the methodology can be modified. However, the investigator should be cognizant of the principles upon which the detailed procedure is based. Such knowledge will insure that a maximum amount of valid information will be derived from any field survey record.

Scope of the investigation

Regardless of the scope or scale of the fracture study it is necessary to first establish the nature of the regional fracture background. Deviations in orientation, frequency or other parameters from this background indicate zones of possible regional tectonic significance or local structural anomalies. Correlations between regional fracture deviations and new fracture sets and surface geology should be carefully investigated by establishing fracture stations near and within all lineament components. This procedure should be followed regardless of whether the deviations or lineaments are defined by faults, zones of change in fold style or trend, or are merely linear features visible from various remote sensor sources. Attention should also be focused on lineaments apparent in geophysical data since these may be reflections of deep-seated structures that could have influenced the surface fracture pattern (Dean, Kulander, Williams, in press; Gay, 1972; Kulander, Dean, 1976). In areas where fracture changes are apparent or are suspect, the number of stations is increased to determine whether or not the fracture anomaly is real or illusory.

Field traverses

It is generally not possible to position station localities in a grid pattern because of the irregularities in outcrop occurrence or difficult accessibility. Large-scale aerial photographs and topographic maps are essential in planning the field traverses because of their utility in locating areas where bedrock is likely to be exposed. They are especially useful in locating quarries, excavations, and surface and deep mines where large expanses

FIELD FRACTURE DATA SHEET

Note: anisotropy includes fractures

Location and major station no. (letter subscripts for substations if necessary) (key to sketch or Polaroid picture)

Formation or formations

Exposure description (i.e. natural or man-made, quarry face, stream cut, road cut, etc.)

Description of outcrop (i.e. one or two sentences stating estimated age of outcrop, orientation of outcrop to hill slope, possibility of release joints. proximity of outcrop to regional or local structures).

Structural complexity (i.e. horizontal bedding, folds, faults, etc.)

sub-station no.	lithology	bedding attitude	bedding thickness	anisotropy inc. fracture sets	attitude of anisotropy	penetration	extent	mesoscopic structures associated with anisotropy					
								slicken-sided slip lines	mineraliz-ation	transected pebbles or clasts	offset features	drag phenomena	other

Fractographic Features (for particular anisotropy)

Transient - (for particular anisotropy)
Include complete description including sketches.
For example, fracture leading on top of stratum,
origin at top - parabolic arrest lines -
lack of velocity hackle - etc.

Tendential - (for particular anisotropy)

Chronology of anisotropy development relative to local or regional planar anisotropies (i.e. cleavage, regional fractures, thrust faults. flexural slip bedding, slickensides, etc.)	Chronology of anisotropy development relative to other structures (i.e. local folds or faults).

Figure 59

of bedrock may be visible. In some cases enlargements from copy negatives of large-scale aerial photographs reveal the bedrock fracture pattern.

Station notation

The fracture station is assigned a number which may represent an outcrop or exposure of any size. If the station shows structural complexity, has several different lithologies or several different fracture sets formed at various places in the outcrop, then each of these different locations within the outcrop or station area becomes an observation station. The The various observation stations should be given a substation designation which is merely the major station number followed by a letter. The relationships of all substations to the complete outcrop should be clearly recorded by means of a detailed sketch or Polaroid camera picture, complete with all necessary appended structural orientation information.

Rock unit

The name of the formation in which a fracture station has been established should be determined as precisely as possible. If this cannot be determined in the field then the name of the formation in question should be taken from the best available geologic information. Determination of the formation name and age is important because fractures may vary geographically within lithologies of the same age. Fracture trends may also vary stratigraphically in different age rocks even though the formations have the same lithology.

Description of outcrop

The type of exposure should be noted with regard to whether it is natural or man-made, and the specific cause for the outcrop, such as quarrying face, stream cut, road cut, etc. should be described. Particular care must be taken for fracture studies in man-made cuts because of the development of a large variety of fractures caused by excavation and blasting. Close inspection of fracture attitudes, frequencies and surface markings generally reveals the origin of the anisotropy. If the exposure is man-made, the time lapse since exposure should be estimated. The orientation of the outcrop relative to the hillslope should be noted because of the tendency for exposures to show well-developed release fractures parallel or subparallel to the topographic trend. However, not all fractures trending parallel or subparallel to the topography must be discounted as release joints. An incipient fracture or other anisotropy may have been tectonic and acted as a plane of weakness during uplift and unloading (Price, 1966). The anisotropy may also have controlled erosion and subsequent topographic grain. If exceptionally well-developed planar fracture faces are parallel to the hillside or exposure face, and have the same trend as regional fractures mapped elsewhere throughout the area, then these fractures are unlikely to be caused strictly by stress release due to erosion. Other

criteria may aid in the discernment of release fractures. Release fractures may 1) increase in frequency toward the exposure face; 2) show surfaces that slope toward the valley and are curviplanar with an origin generally located on the interior fracture face.

The proximity of the outcrop to local or regional structures and the location of the outcrop within a given structure should also be noted if this can be determined (Stearns, 1964, 1968). This procedure is important in determining the geometric and genetic relationship of all fractures to different local and regional tectonic events (figures 60, 61).

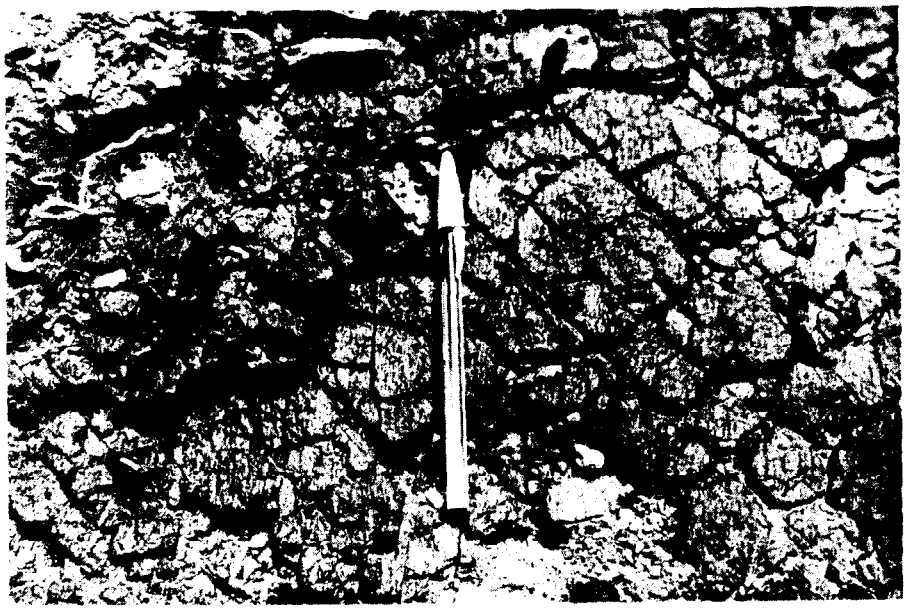

Figure 60, tendential view of regional and local systematic - nonsystematic fracture sets. The regional systematic fracture set parallel to arrow and abutting orthogonal regional non-systematic fracture set predate folding. A second local systematic fracture set, parallel to bedding slickenlines and pen, and related orthogonal nonsystematic fracture set, formed after the regional fractures. The local systematic fractures are a strain event related to the folding process. The abutting relationship in this case can be used to derive fracture chronology. Local fold axes are perpendicular to the pen, and local dips are less than 10 degrees.

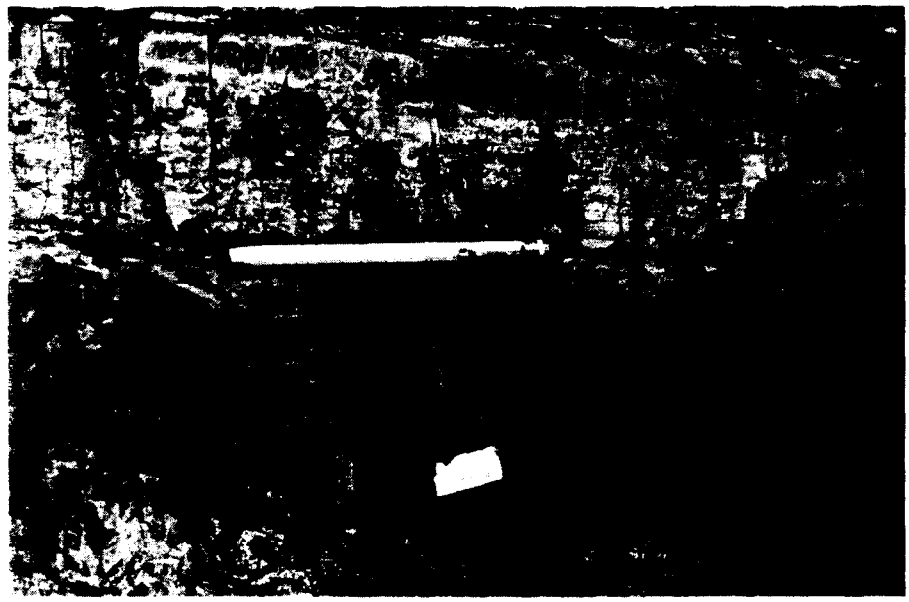

Figure 61, transient view of regional and local systematic fractures in coal. The regional systematic fracture set parallels the rectangular paper fragment. The local systematic fractures parallel the pen. The pen is situated on a thin shale layer that contains slickenlines trending parallel to the pen and local systematic fractures. Abutting relationships not evident in the photo show that the regional systematic fractures predated the local fractures.

Structural complexity

Before fracture readings are taken, the bedrock structures and chronology of structural development must be established in order to determine if the fractures present predated or postdated folding or faulting, or occurred in response to the stresses associated with folding or faulting (figures 62, 63, 64). If the rocks are folded, the type of folding must be determined. All evidence of bedding slip or rock flowage should be recorded as well as any evidence of stress directions that may have been active before, during or after fracturing (deformed fossils, ooids, etc.). All faults, slip directions, and discernible displacements, such as pre-fold fractures offset by bedding slip, are noted. As previously mentioned, all structures and their chronology of development should be shown on a sketch or Polaroid picture.

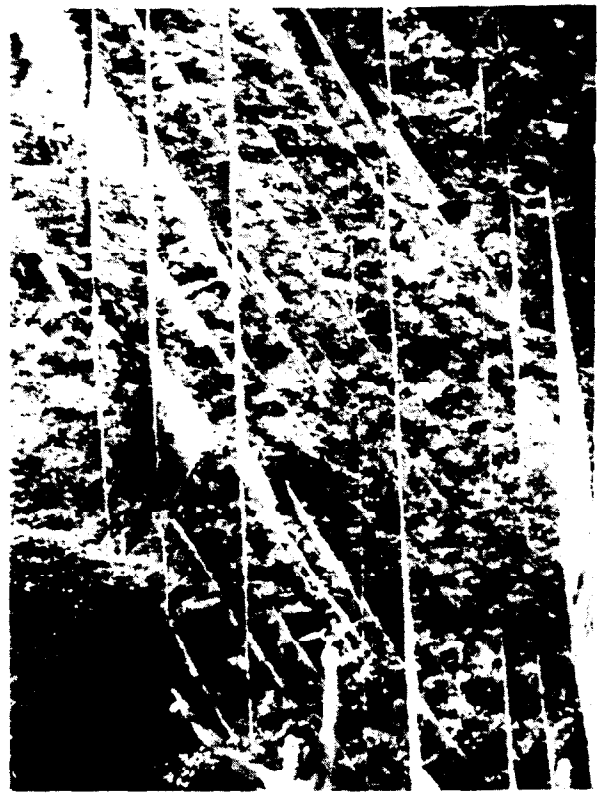

Figure 62, vertical systematic fracture set oblique to strata dipping towards the right. Fractures are not offset by flexural slip at bedding surfaces. Lack of offset indicates fractures post date or formed late in the folding process.

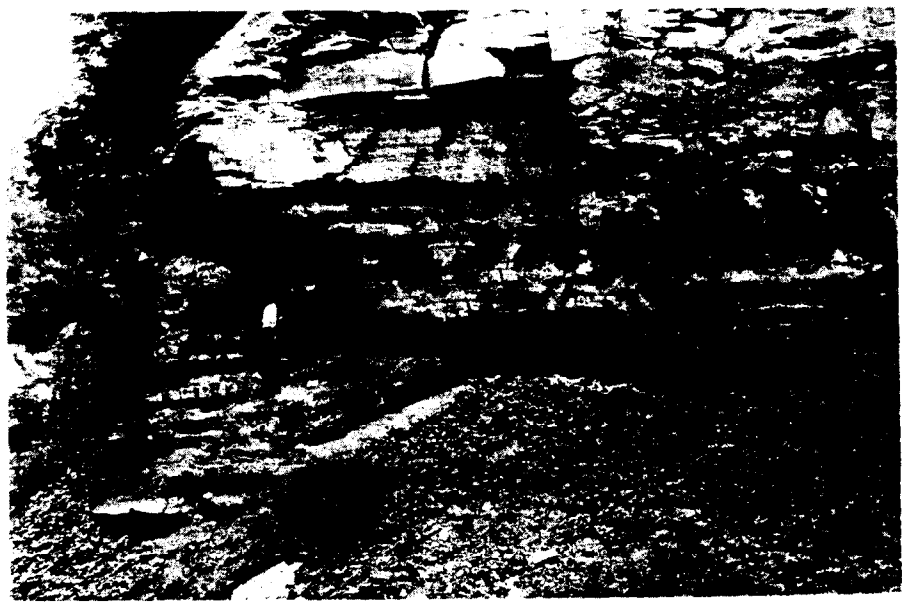

Figure 63, coal seam offset by thrust faults. Regional systematic-nonsystematic fractures in footwall predate faulting and rotate from the vertical to maintain an orthogonal relationship to bedding towards the fault. Nonvertical systematic-nonsystematic fracture trends in the drag zone assume an attitude parallel to the regional coal fracture trend when bedding is rotated back to horizontal by stereographic projection.

Figure 64, pre-folding stylolitized systematic fractures opened by flexural slip folding. Open fractures become closed and pass into stylolite seams at and below each stratum's neutral surface within the zone of compression. Fractures predate folding. Note clipboard (arrow) inserted in open fracture section.

Lithology and bedding attitude

Rock type is of fundamental significance in any fracture study. Fractures do not maintain the same orientations, frequencies and degree of development in different lithologies whether on a regional scale (figures 65, 66, 67, 68) or on the scale of the local outcrop (figure 69). If several different lithologies are present at an outcrop, then each lithology with its set or sets of anisotropies (this includes fracture sets) is recorded as a separate substation. The strike and dip of bedding is noted for the rock type of each substation.

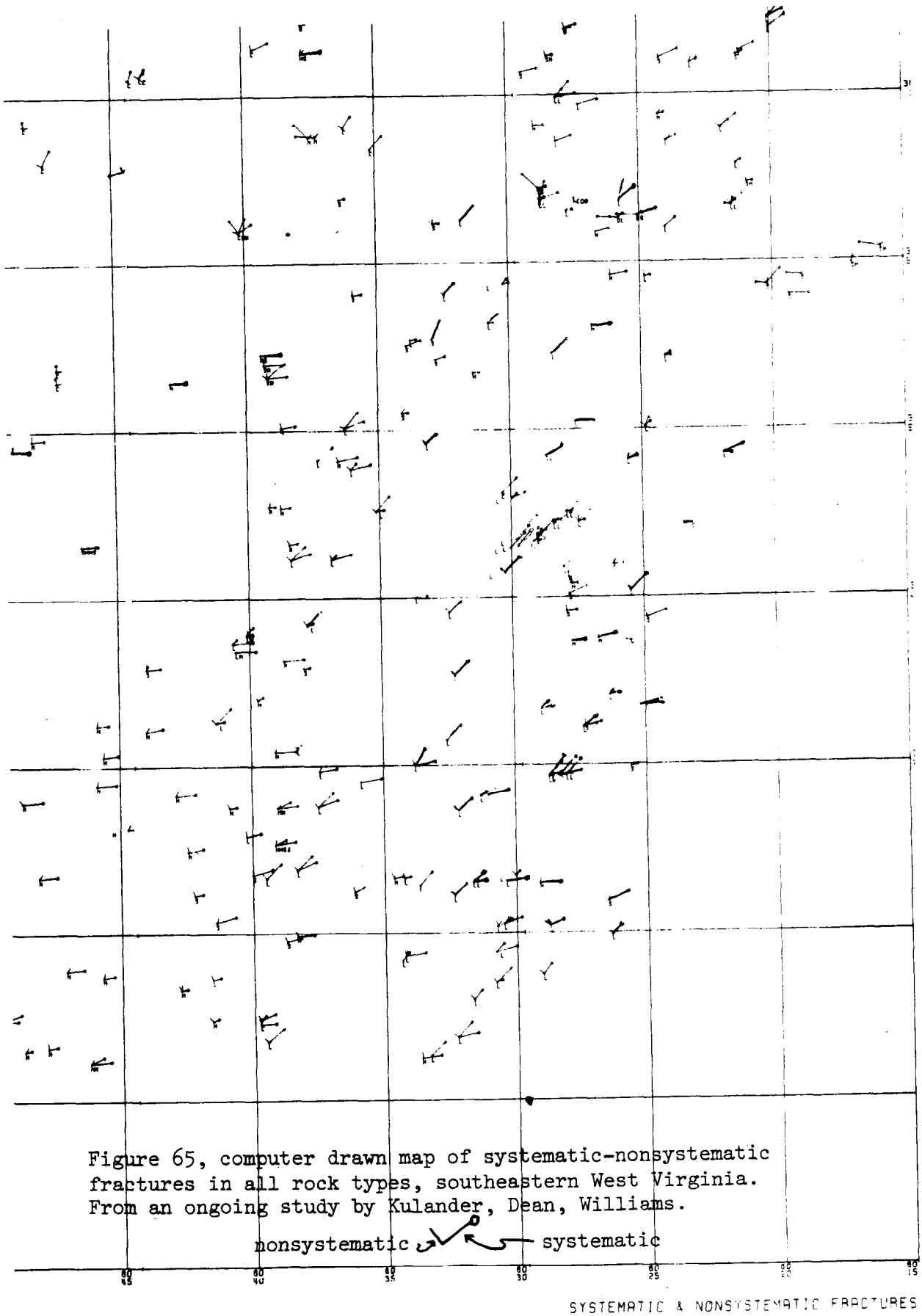

Figure 65, computer drawn map of systematic-nonsystematic fractures in all rock types, southeastern West Virginia. From an ongoing study by Kulander, Dean, Williams.

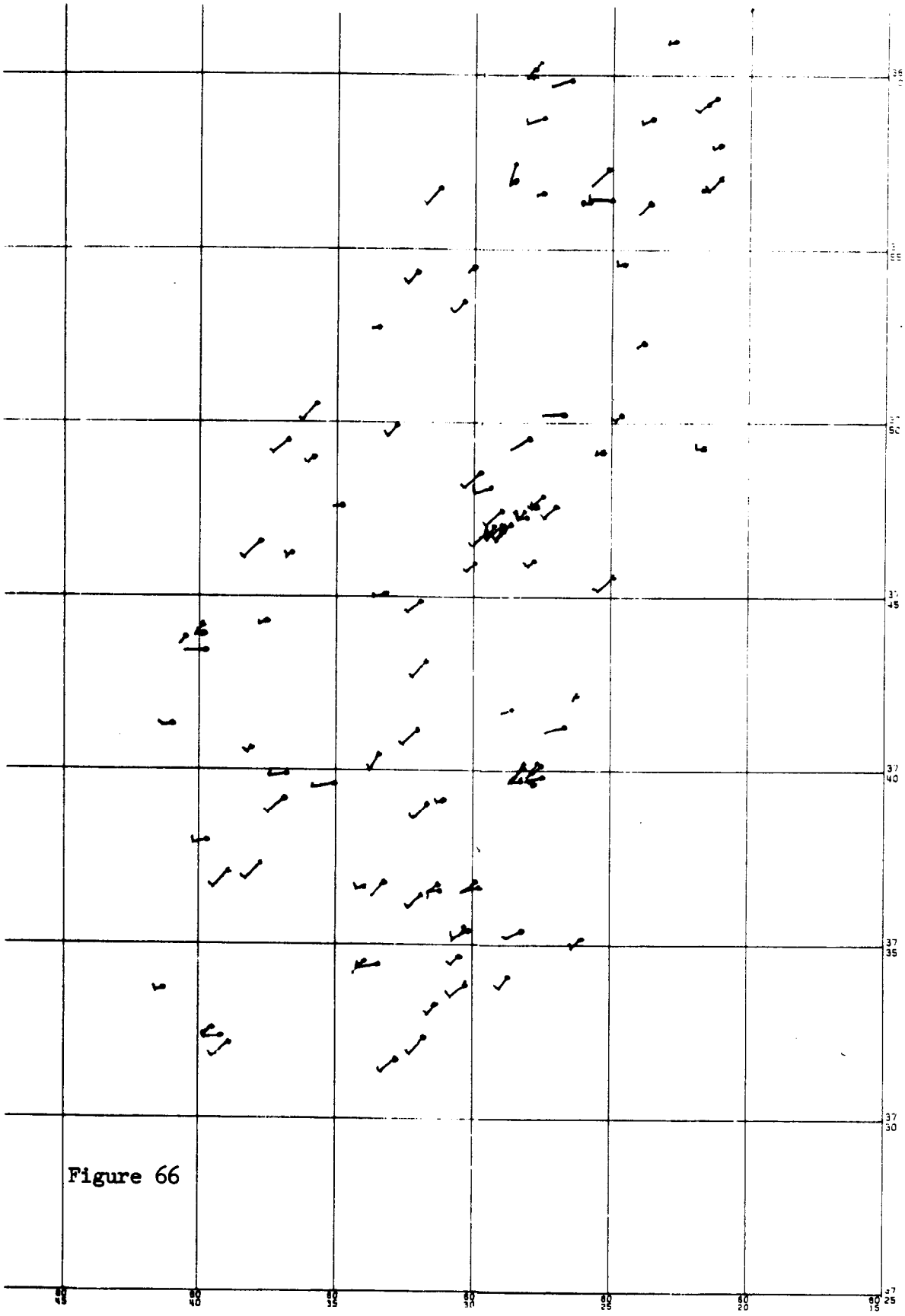

Figure 66

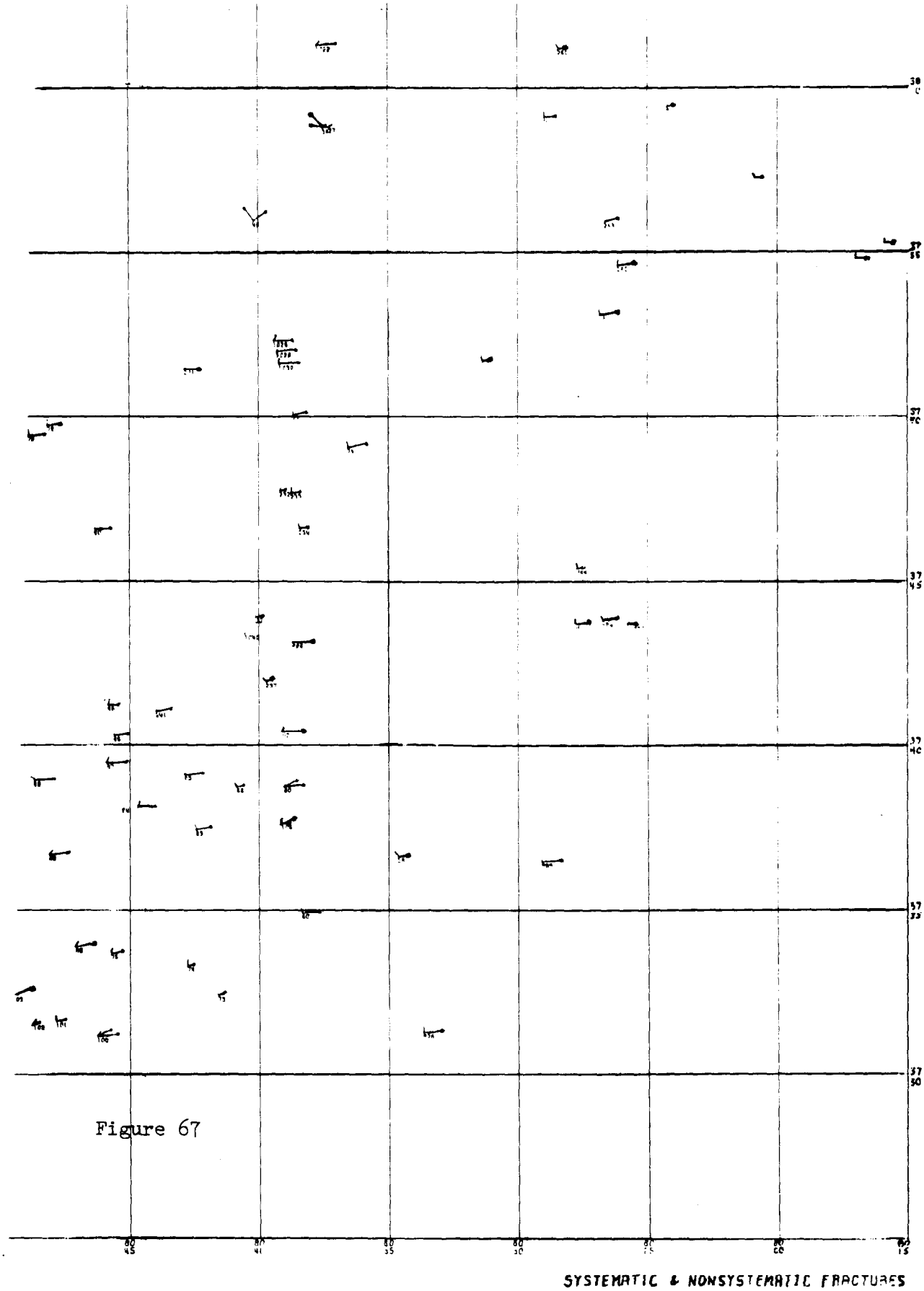

Figure 67

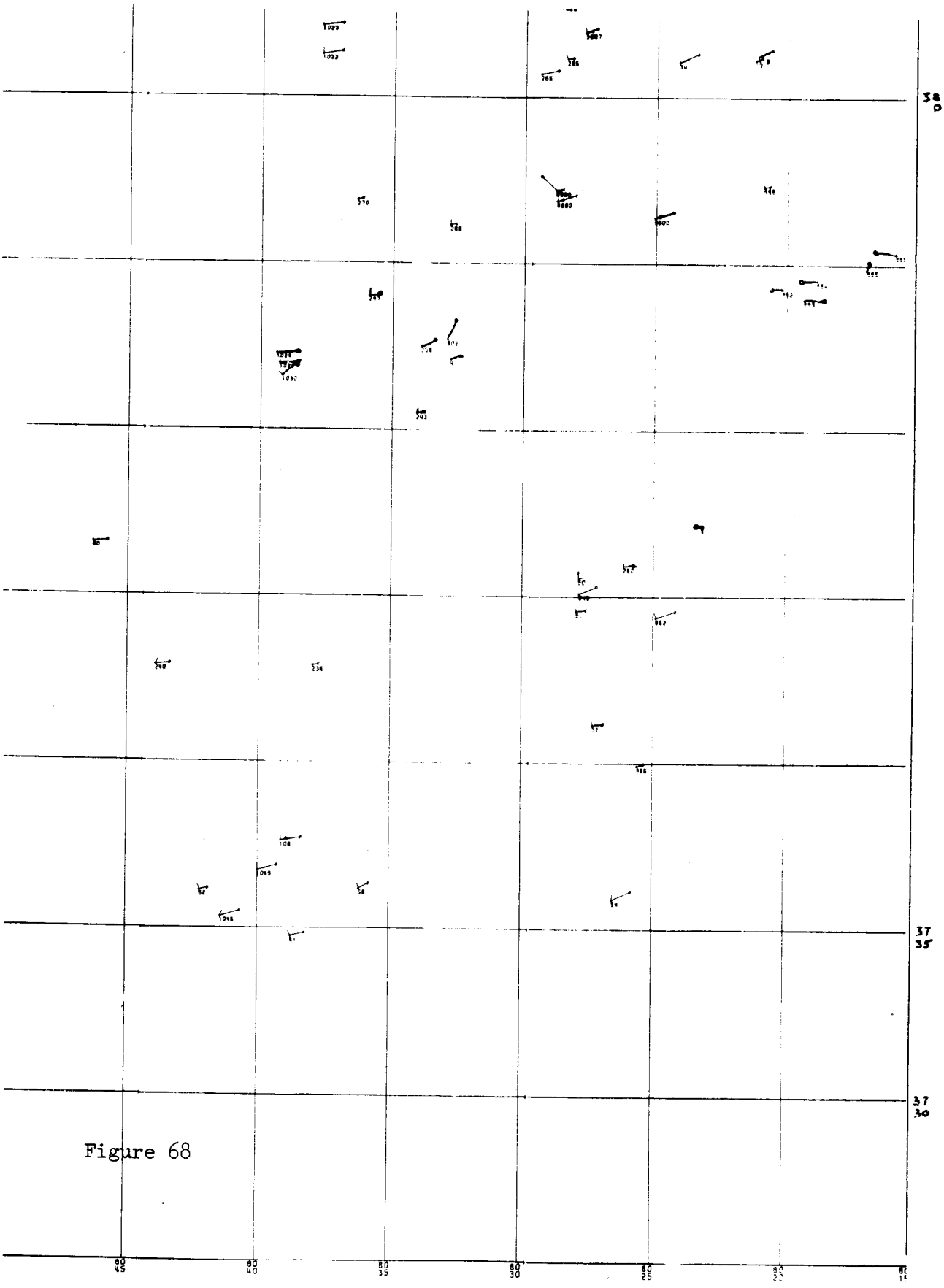
38
00
37
35
37
30
80
45
80
40
80
35
80
30
80
25
80
20
80
15
SYSTEMATIC & NONSYSTEMATIC FRACTURES

Figure 68

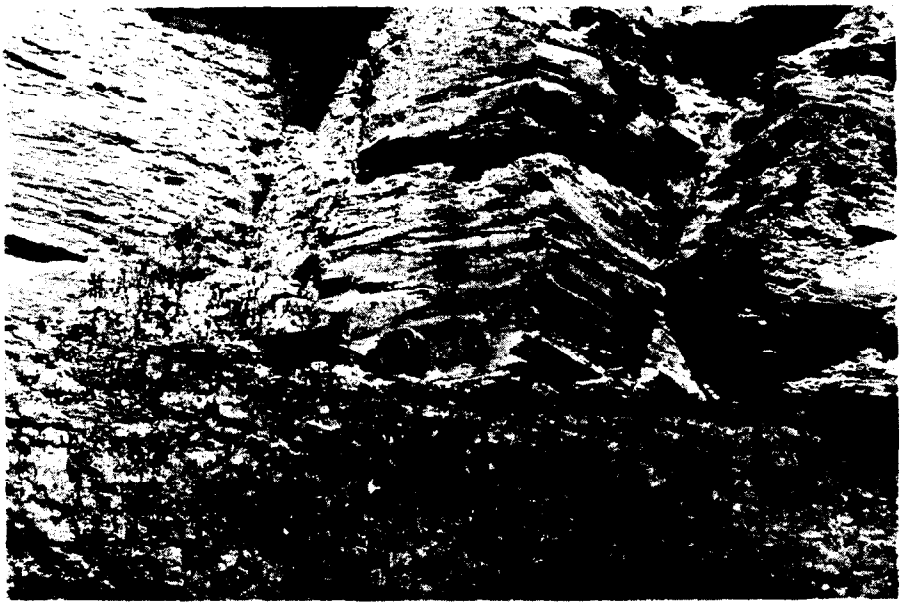

Figure 69, change of fracture trend and frequency in shale (systematic fractures parallel to compass) and coal (below compass).

Bedding thickness and other characteristics

For each different lithology at a particular outcrop, the bed thickness should be determined if possible. If fractures are consistently and uniformly developed throughout a lithology an average stratum thickness value will usually suffice. However, if close inspection shows that any fracture characteristics change, then these variations further restrict the limits of the assigned substation (figure 69).

Irregularities in bedding thickness and internal structures within the individual layer must also be taken into consideration because they may have influenced the propagation direction of a given fracture. Large-scale stratigraphic features such as channel and point bar deposits in sandstone, and reef deposits in limestone must be carefully noted at any observation station. Smaller features, usually within the domain of a given bed, such as cross bedding or soft sediment slump structures should also be recorded but are usually less significant in affecting large-scale fracture development. As a general rule small-scale fractures may be considerably affected by stratigraphic variations, whereas large-scale fractures may cross these features and maintain the same orientation. This statement is attributed to the fact that if a fracture is allowed to grow considerably larger than the variations within the fractured medium, the fracture may continue to spread around local stratigraphic variations.

Standard fracture data

Type of anisotropy

Before fracture orientations are recorded other pervasive and non-pervasive anisotropy planes must be distinguished. Of principal concern here are planes of cleavage in moderately to intensely folded rocks (figure 70). Included within this designation are any planes within the rock body that are defined by aligned planar rock components. In moderately folded rocks this type of anisotropy may be poorly developed and difficult to determine by field observation, but may nevertheless influence later fracture development. Even essentially horizontal strata, especially limestone, must be carefully examined where small flexures of low dip show well-developed fractures. If these fractures are parallel to, or fan about, the axial plane of the fold then they may represent fractures that have developed parallel to incipient flow cleavage formed under the inner arc of a buckle fold. In rocks where folding has been more intense, the detection of cleavage planes is not difficult. Where bedding planes are the major anisotropy at the inception of folding, resulting fractures formed during folding in thinly bedded rocks will generally break across a stratum by the shortest path.

In recording fracture data it is important to recognize all fractures that are locally developed or manmade in origin. These fractures include those that are clearly caused by local stress release or by blasting. Next, it is necessary to isolate all phenomena associated with a single fracture event. For example, fractures may change trend, hook, fork, or break into twist hackle depending upon the particular orientation of principal stresses, the propagation velocity of the fracture through the rock mass and internal rock anisotropies (figure 70). Such changes in fracture attitude must not be interpreted or recorded as different fracture sets attributed to separate stress events. Unfortunate observations of this nature can lead to erroneous assumptions about nonexistent stresses, conjugate "shear" sets and the like. The outcrop must be thoroughly examined before any joint data are taken. Statistical analysis of dozens or even hundreds of blindly taken fracture measurements recorded at a particular outcrop do not necessarily provide for a more meaningful interpretation of fracture orientation or tectonic relationships. This is especially true if a large number of fracture orientation readings are taken on non-natural fracture or on forking or hooking fracture surfaces. It is important to realize that at many outcrops, the major fracture sets present may be represented by only one or two natural fracture events. However, fracture faces of many orientations may be observed.

Figure 70, locally developed cleavage in moderately folded Mississippian limestone, Allegheny Plateau, West Virginia. Solution, aided by closely spaced cleavage planes, is responsible for linear series of sinks from observation point to barn in distance. The resulting lineament is easily visible on aerial photographs and cannot be attributed to systematic fracturing.

Fracture terminology

Fracture analysis terminology is essentially that adopted by Hodgson (1961) and Dennis (1967). Systematic fractures (joints) are those that are repeatedly found in a common orientation. Those of any specific orientation are said to be in the same set (figures 71 through 75). They exhibit planar or gently curved surfaces. Systematic fractures are typically regional in nature. However, local systematic fracture sets can be related to various local structures (figures 60, 61). Nonsystematic fractures generally display a more curviplanar surface and terminate at systematic fracture faces or at the faces of earlier formed fractures. Although nonsystematic fractures can show considerable variance in strike at any given station, they generally fall into distinct sets and they may be regional in nature. The particular type of nonsystematic fracture termed "cross joint" by Hodgson (1961) is not used by the authors because of possible confusion with fractures in igneous rocks (Balk, 1937; Hutchinson, 1956) and those perpendicular to fold axes (Badgley, 1965) that have been given this same designation by other workers. The nonsystematic cross joints of Hodgson are essentially perpendicular to, and also terminate at, systematic fracture faces.

It is generally not desirable to use fracture terminology that implies the origin of that particular fracture unless field evidence is exceptionally strong. Therefore designations such as shear or tension fractures based strictly on the geometric relationship of these fractures to regional or local fold structures is generally unwarranted. In many cases the fractures predate or postdate folding, and their symmetry with the fold axis is merely fortuitous. Also fractures in brittle rocks form as a direct response to applied tension at the spreading fracture front.

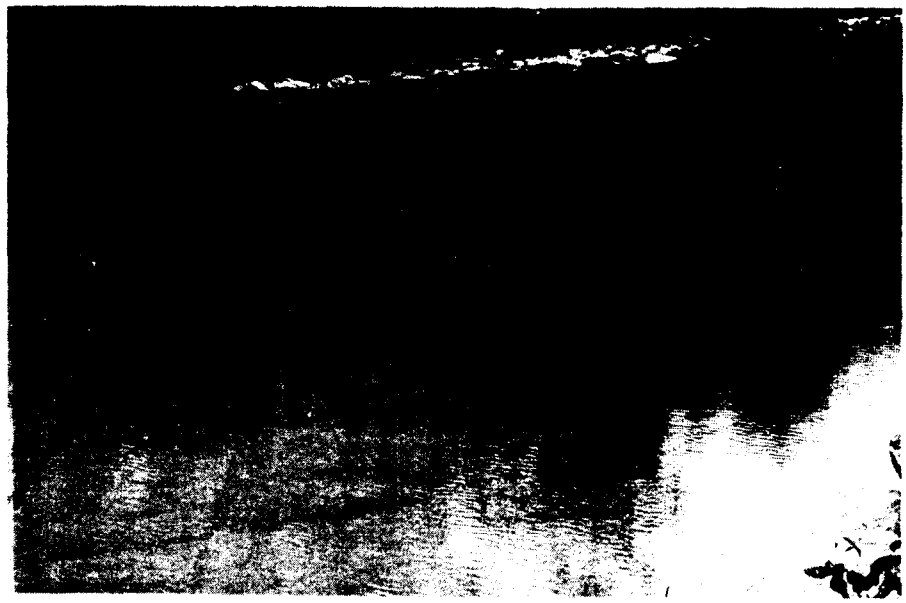

Figure 71, geometrical fracture pattern in sandstones of the Bluefield Formation in Elk River east of Webster Springs, West Virginia. Fractures have segmented the sandstone into polygonal blocks.

Figure 72, systematic-nonsystematic fractures in Pennsylvanian sandstone, West Virginia.

Figure 73, systematic-nonsystematic fractures in Mississippian limestone, West Virginia. Here systematic fractures control stream flow. Surface flow is intermittent above point where underground flow along systematic fractures emerges as a spring (spring emerges at geologist).

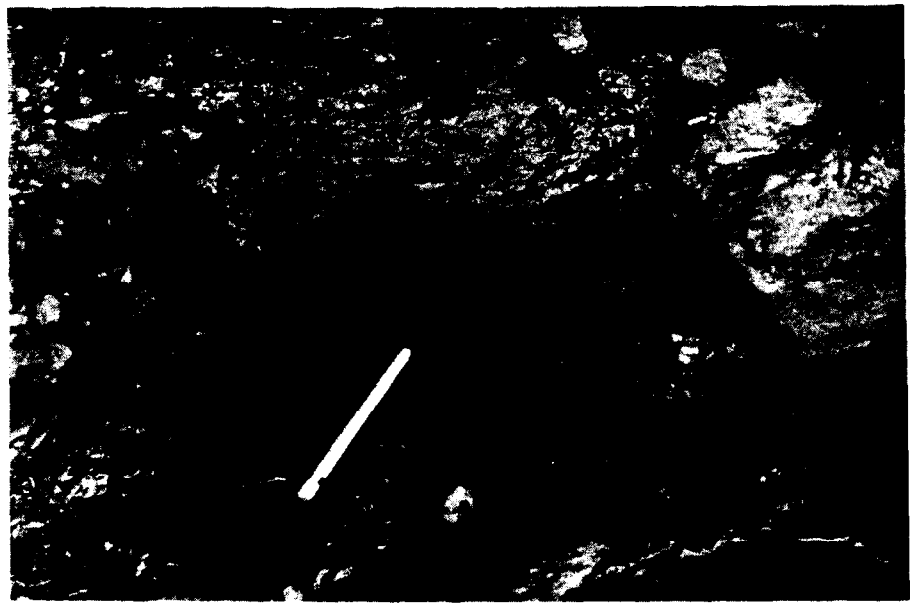

Figure 74, regional systematic fractures parallel to pen developed in local coal lens.

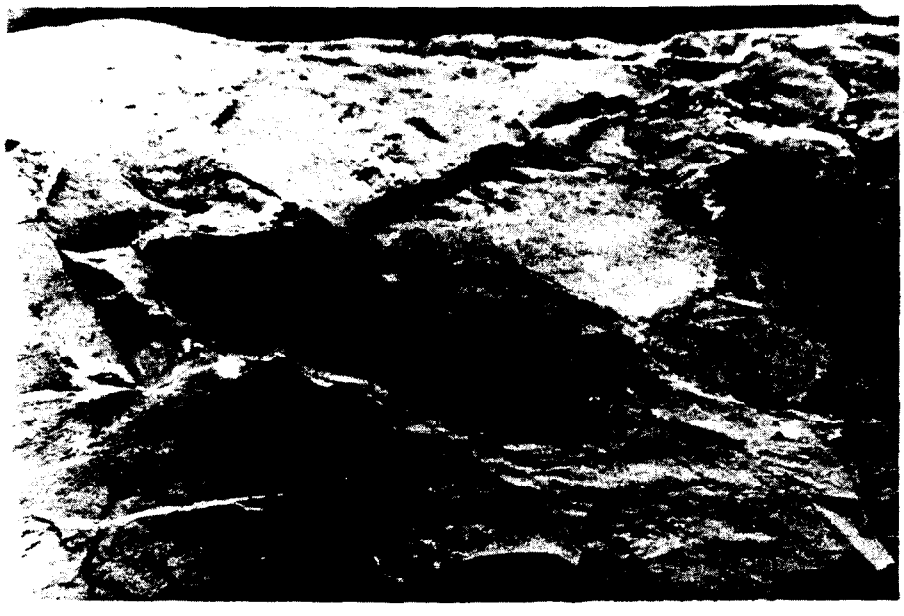

Figure 75, tendential penetration view of closely-spaced regional systematic fractures developed in chert nodule. Systematic fractures are not well-developed in the surrounding limestone.

A regional systematic fracture pattern for any given rock type can generally be broken down into distinct fracture domains. These fracture domains are generally, but not always, distinguished by the presence of a predominant fracture direction that can be pervasive for thousands of square miles. However, several fracture sets can persistently occur in the same domain. Fracture domain boundaries, marking zones where regional fracture trends change, can be abrupt or gradual. Figure 76 is an example of an abrupt coal fracture domain boundary. This boundary is exceptional because it lies over a pronounced zone of basement faulting (Kulander, Dean, Williams, in press).

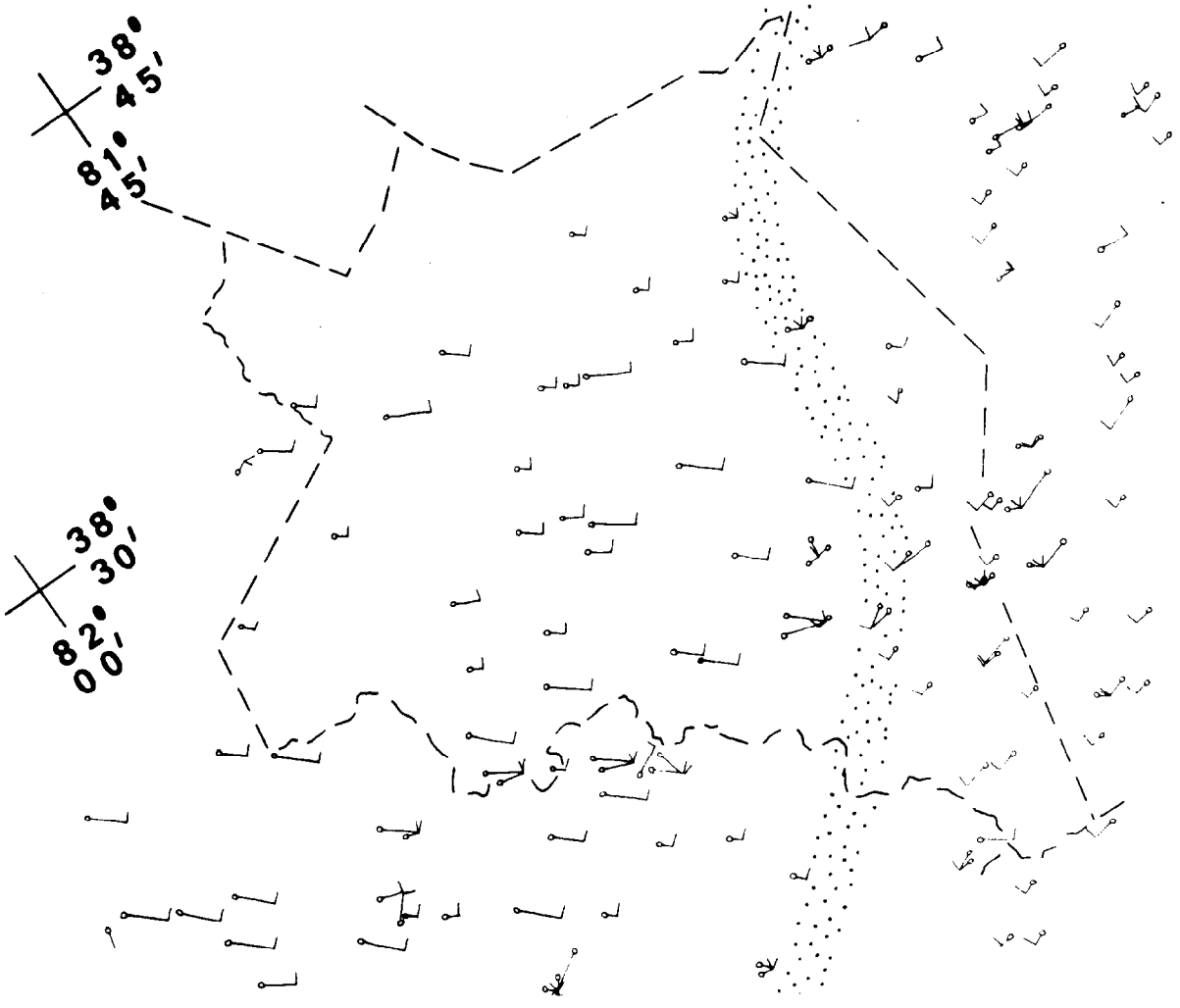

Figure 76, systematic-nonsystematic fracture trends in coal delineating a domain boundary. Barb with ball indicates mean systematic fracture trend. Naked barb indicates mean nonsystematic trend. Systematic barb length is inversely proportional to the standard deviation of ten fracture set azimuth bearings taken over each outcrop extent. Systematic-nonsystematic barbs originate at station locations. Stippled band indicates zone of subsurface basement faulting. Scale = 1:560,000. Kanawha County, West Virginia.

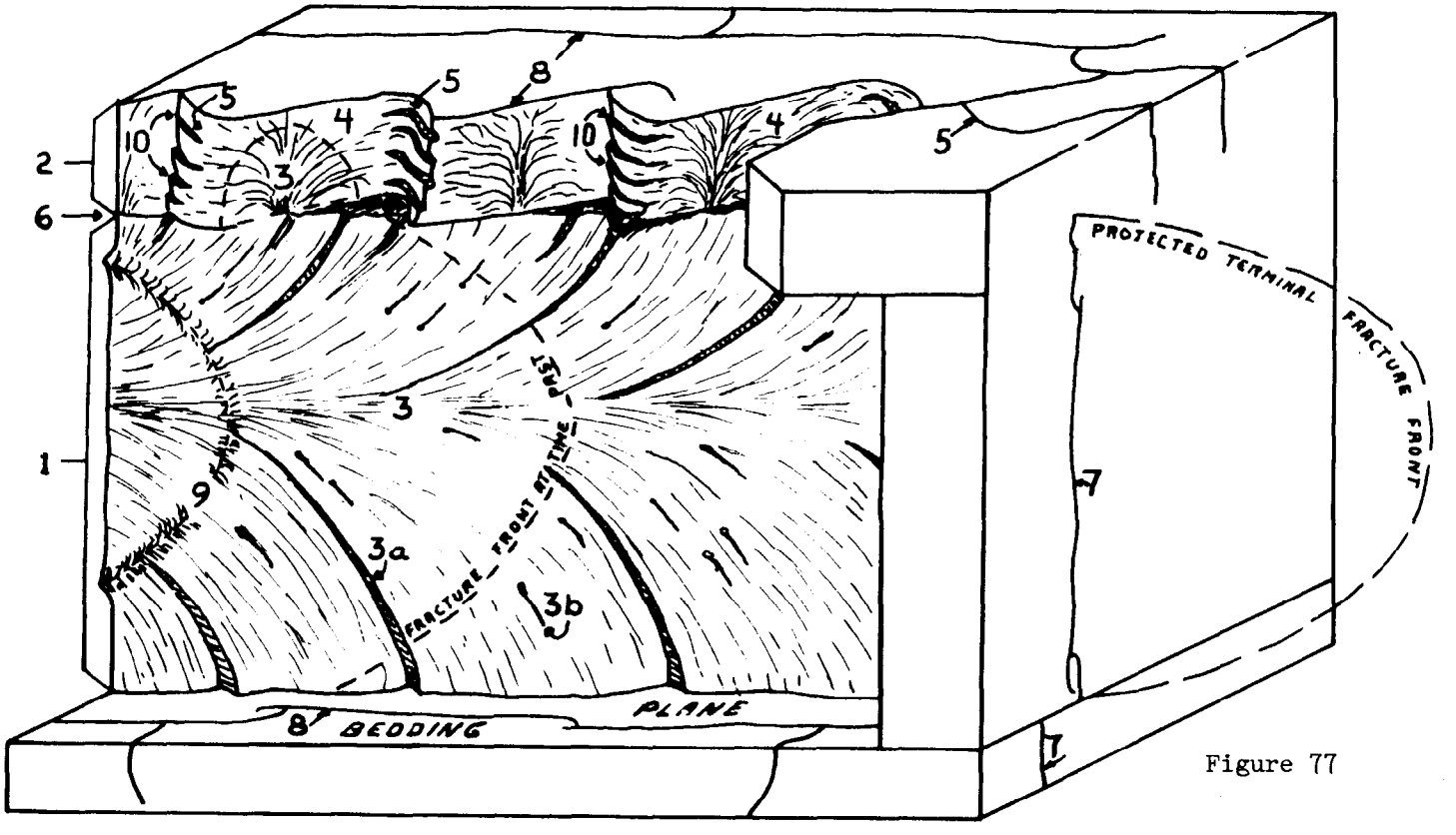

Figure 77

Descriptive classification after Hodgson (1961)

1. main joint face
2. fringe
3. plumose structure
4. F-joints (B-planes)
5. C-fractures (straight-medial)
6. shoulder
7. trace of main joint face
8. undescribed
9. conchoidal ridge

Genetic classification

1. main fracture face
2. twist hackle fringe
3. fracture plume, 3a = twist hackle component
   3b = inclusion hackle component
4. twist hackle face
5. twist hackle step
6. plumose-coarse twist hackle boundary
7. tendential penetration -- in vertical plane or perpendicular to bedding
8. tendential extent -- in horizontal plane or parallel to bedding
9. arrest or Wallner line depending on morphology
10. second order twist hackle

Fracture face terminology - a proposed new classification

Hodgson has developed a detailed descriptive classification of the markings visible on and adjoining a typical fracture face. This classification is shown in figure 77 (Hodgson, 1961, figure 1). The authors would like to introduce a genetic classification based on our understanding of the origin of these fracture markings as related to velocities, stress conditions, and material properties existent at the time of fracture propagation. The proposed classification is also given in figure 77. The classification is based on terminology abstracted from the ceramics, glass technology, physics and metallurgy literature. The usefulness of the reclassification has been verified through several field seasons in the Appalachian Plateau and Valley and Ridge. The proposed genetic classification has several advantages. Understanding and correct application of the terminology applied to the transient and tendential features greatly reduces the possibility of collecting erroneous and meaningless fracture data. It permits easy determination of single fracture events and fracture origins, and shows the direction(s) of fracture propagation at any point on the face. It has direct implications in many cases for the discernment of the local stress intensities and configurations that have created the fractures.

Gross fracture characteristics

After determining whether the particular fracture event is to be classified systematic or nonsystematic, and is regional or local in nature, the attitude of the fracture is recorded. Only a few such observations need be recorded for each fracture set (no more than ten) to give some indication of maximum variance at that outcrop. The nature of the fracture face is also noted with regard to whether it is planar, curviplanar, possesses megascopically visible transient markings, or passes into various fringe features. On a broadly curved fracture the average orientation is recorded. If the fracture face is strongly curved (figures 78, 79) into two or more curviplanar segments, the average strike and dip of each segment is recorded in addition to conclusions concerning whether or not all segments can be attributed to a single fracture event.

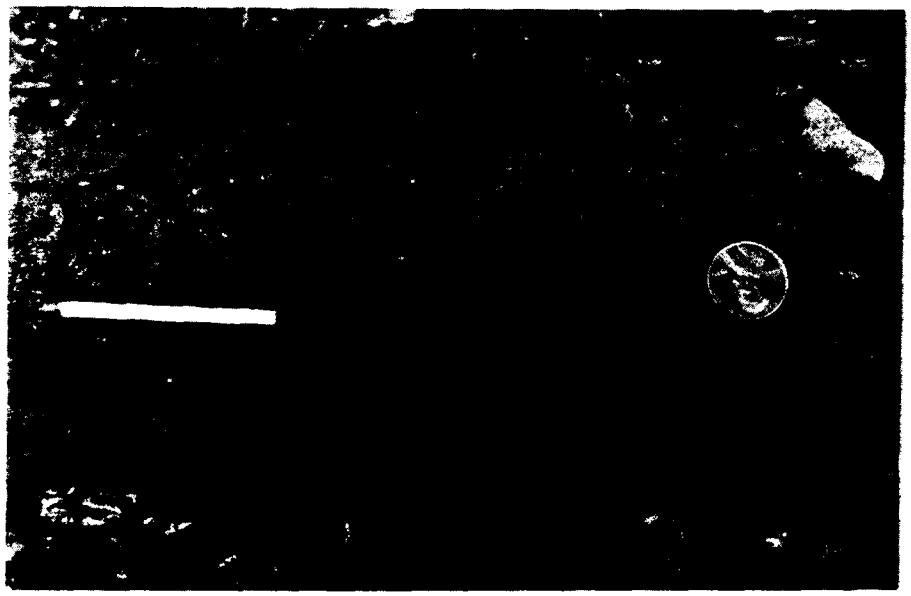

Figure 78, tendential view of systematic fracture in coal (parallel to match) that swings abruptly to new fracture trend (below penny). If the zone of curvature were not evident, two separate fracture sets would be recorded. In reality there was only one fracture event.

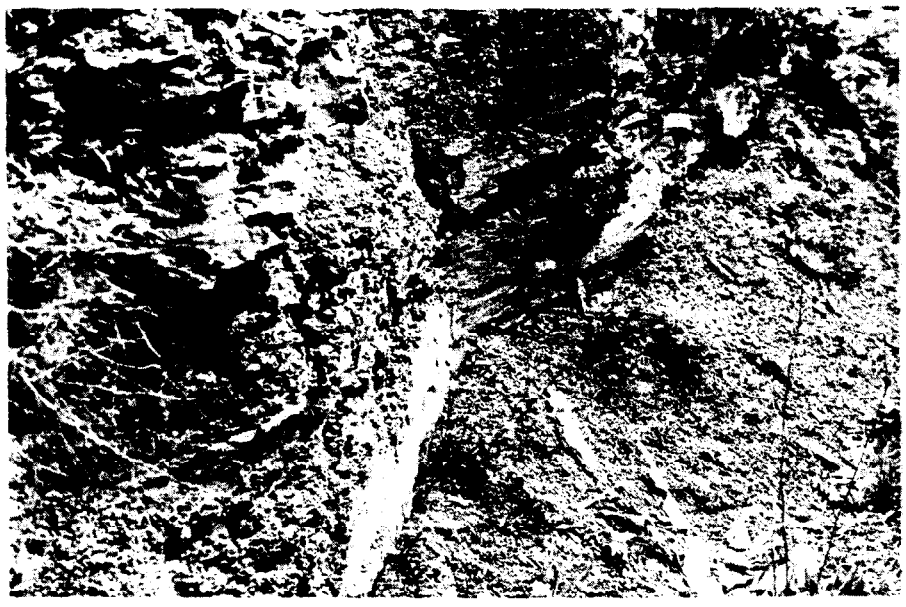

Figure 79, transient view of systematic fracture in Mississippian shale, West Virginia, that curves abruptly at pen to new fracture trend. Both trends are the result of the same fracture event.

Fracture frequency must also be determined and recorded. Frequency is measured in terms of the number of fractures of a given set that are present per linear foot (meter), measured perpendicular to the fracture face. Fracture frequency is generally a function of bedding thickness. Harris et al. (1960) also conclude that for a given lithology the concentration of fractures is inversely related to bed thickness. Massive and thick-bedded units of the same lithology generally show a lower fracture frequency, than most thin-bedded units which have a large number of fractures. In interbedded rocks of different ductility, the brittle lithologies generally show a higher fracture frequency than the more ductile units. Local increases in fracture frequency along an outcrop must also be recorded because they may be indicative of large-scale fracture zones extending for thousands of feet (figure 80). In some cases these zones may be correlated between different fracture stations (Plicka, 1976).

The penetration of the fracture face is the distance it extends across bedding. At most exposures fracture faces with large penetration generally belong to the regional systematic set for that area. The degree of penetration of joint faces is related in a general way to the bedding thickness. Massive and thick bedded units of sandstone and limestone and continuous shale sequences often show fractures of large penetration. On the other hand, fractures in thin bedded strata of high ductility contrast (Donath, 1970) have less penetration. In some cases this may be due to traction at bed interfaces between rigid and ductile strata . At some homogeneous shale outcrops regional systematic fractures penetrate the entire thickness of the exposure (figure 81). If cohesion is low across bedding anisotropies, the bedding plane may act as a free surface. In this case the tensile stress at the fracture tip cannot be maintained and the fracture is terminated. Also in interbedded strata of high ductility contrast, ductile units may dissipate crack tip stresses by local plastic flow.

The extent of a fracture refers to the distance it can be traced along its strike. Unfortunately at many outcrops, especially vertical or steep faces when the fractures trend into the cut, the fracture extent can only be estimated. Under these circumstances a minimal extent can be obtained by assuming the fracture surface to be equidimensional, that is the extent equals the penetration. In many layered rocks where bedding has served as a major anisotropy, the fracture is confined to an individual layer and generally bears well-developed hackle plumes with plume axis parallel to bedding. The extent of the fracture in this case may be considerably greater than its penetration.

Figure 80, tendential view of a local increase in systematic fracture frequency, Mississippian sandstone, West Virginia. Penny left of photo center is for scale.

Figure 81, view of tendential penetration, systematic fractures in Mississippian shale, West Virginia. Systematic fracture frequency is 1 per 4 meters. Poorly formed transient structures indicate that the nonsystematic fractures (facing observer) propagated generally from the bottom up.

Figure 82, abrupt change in fracture frequency from shale to underlying sandstone. Fracture frequency in the shale is fifteen times larger than sandstone fracture frequency.

Mesoscopic structure associated with the fracture

In addition to various types of fractographic markings commonly developed on the fracture face, a variety of mesoscopic structures may be associated with the fracture. When observed, these mesoscopic structures should be carefully noted because of the implications for interpretation of fracture origins and sequence of fracture development.

Slickenlines are present on many fracture faces and represent movement of one face past another (figure 83). The attitude of slickenlines must be recorded because they may reveal information about tectonic events subsequent to or synonomous with fracture formation. If the fracture formed in response to the stresses that ultimately caused slickenline development, the slickenlines may yield information about the approximate orientation of the principal stress responsible for the fractures. However, caution must be exercised in interpreting such faces as "shear" joints, even though these are strongly slickenlined. The fracture may have long predated the tectonic event responsible for the slickenlined surface and was merely favorably oriented for shear displacement in response to the later tectonic stress. The observer should be extremely cognizant of this sequence of events in any section of tectonically disturbed rock no matter how small the dip of the bedding. If slickenlines are present on bedding planes, then slip on early formed fracture faces is a good possibility.

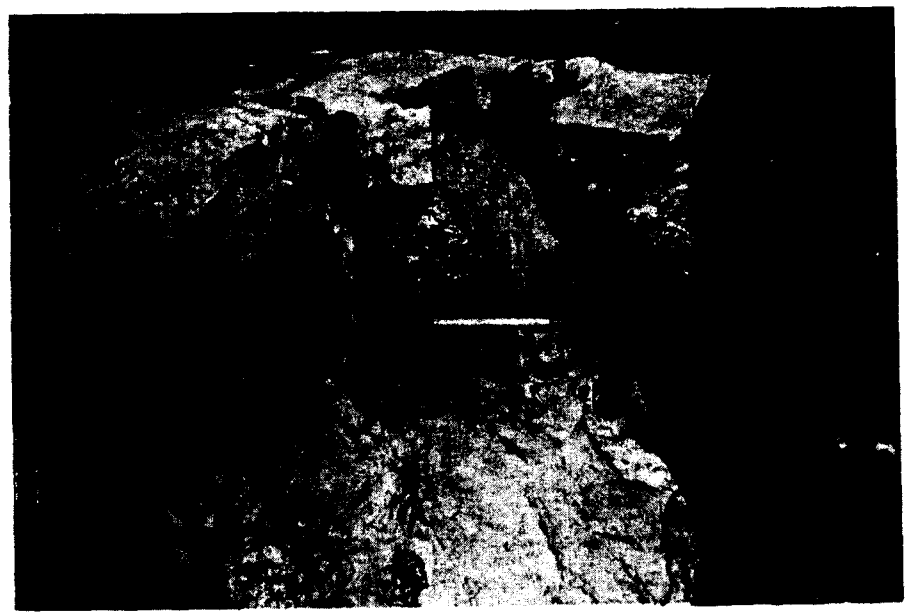

Figure 83, slickenlines (parallel to pencil) on systematic fracture face in Mississippian limestone, West Virginia.

Careful notation should also be made of all types of mineralization present on fracture faces or in the voids between the faces. Mineral growth fibers, such as calcite or quartz, perpendicular to the fracture may imply fracture development where mineralization has occurred parallel to the principal acting tension as the fracture opened (Durney, Ramsay, 1973). However, it must be remembered that mineral growth may have occurred long after fracture development and merely filled the void space, with no relation whatsoever to the original stress. A not atypical situation is the development of fractures in horizontal strata which were subsequently folded, resulting in opening of the early fractures. Mineralization may have occurred during folding and opening of the fractures, or at any later time. Where mineralized fractures show a cross-cutting relationship, the sequence of fracture development and mineralization is easily determined. Fibrous mineral growths may also be kinked in response to shear movement parallel to the fracture faces (figure 84). In this sense, the kinked growths may be used in the same fashion as drag features, although the curvature of the mineralization fibers may be growth phenomena related to a change in the principal tension direction rather than actual shear bending. In this regard, many so-called slickensided surfaces are actually mineral growths parallel or subparallel to the fracture face and approximately parallel to the principal tension during shear displacement. Mineralized en echelon tension gashes are associated with some fractures, principally in limestone terrain, and may be used to determine the slip direction, which enters the acute angle between the major fracture and the tension gashes. Under most circumstances these fractures probably originated by shear related tension. However, it must be re-emphasized that under conditions where an original fracture was oriented at a high angle to a later principal tectonic compression, tension gashes may develop associated with shear movement along this early surface.

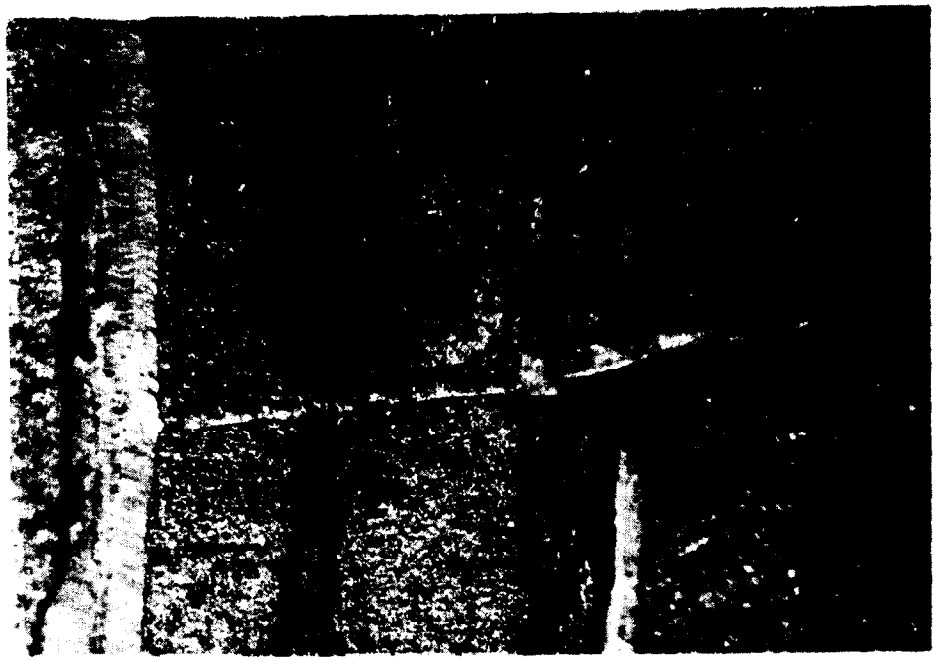

Figure 84, fibrous mineral growth in fractures cutting Cambrian shale, Alberta, Canada. Crosscutting and truncated mineral growths can be used to derive fracture chronology. Horizontal fractures formed first, vertical fractures formed second. Fibers are curved indicating a change in principal tension direction during fracture separation. Optical micrograph, 7X magnification.

Offset features and drag phenomena may be used to verify slip along a fracture face. Here again, evidence of drag or offset simply reveals the last event. The fracture may have originated under tensile stress and was favorably oriented for shear displacement in response to later compressive stress. Some features may be erroneously interpreted to be the result of slip along fracture faces. For example, hooking fractures may curve into another fracture with an apparent drag configuration in the hook zone. Similarly, nonsystematic fractures with a regular frequency may terminate on opposite sides of a systematic fracture face, indicating tendentially an apparent offset along the interval where the nonsystematics are separated.

The fracture face should also be carefully examined for local variations in lithology or grain size. Clasts, pebbles, nodules, fossils, etc. should be noted as well as changes in cement or degree of induration of the bedrock, assuming minimal lithification alteration after fracturing. These features may well affect the mechanical properties of the rock. Fracture face characteristics associated with these features should be recorded. For example, it is important to establish whether or not the fracture broke through or around a clast. Systematic fractures generally break through these features whereas nonsystematic fractures have a tendency to break around clasts (figures 85, 86).

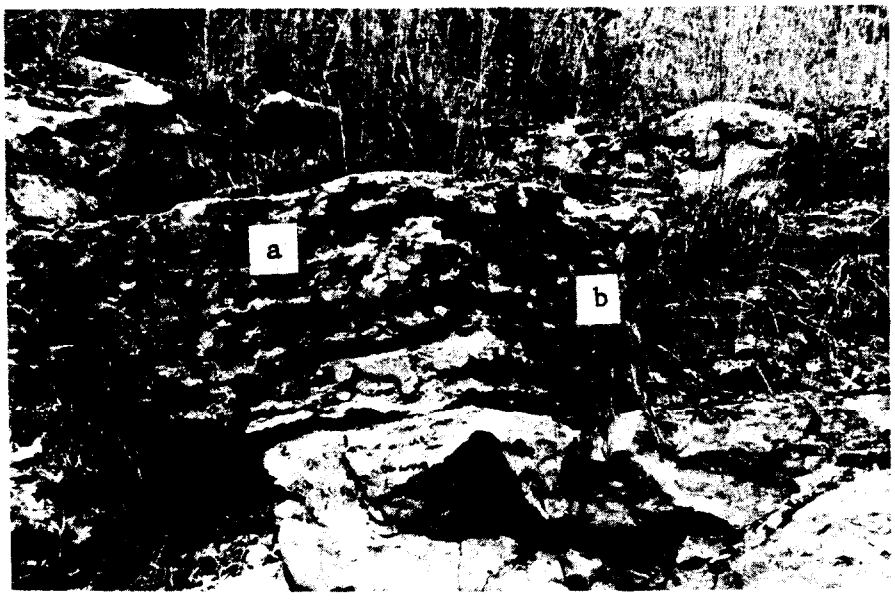

Figure 85, systematic fracture "a" breaking through chert nodules in limestone. Nonsystematic fracture "b" breaks around chert nodules.

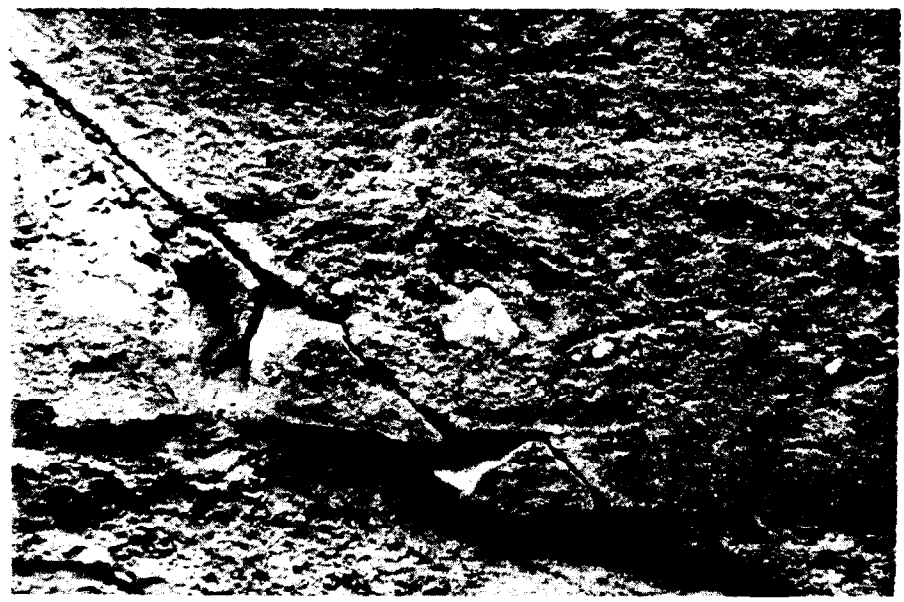

Figure 86, vertical systematic fracture breaking through a quartz pebble (one cm. diameter) in Mississippian quartz sandstone, West Virginia. The fracture trends N 60° - 70° E, as do others within this systematic set throughout the region. Surrounding fold axes would tempt many geologists to attribute the fractures to shear stress. However, a scanning electron micrograph (figure 41) of the pebble surface reveals twist hackle showing that the fracture front progressed perpendicular to some past acting principal tension.

Transient and Tendential Rock Fracture Features

For each fracture set visible at a given station particular attention is focused on all types of fractographic features that are developed on the major fracture face and in the fringe zone. Transient markings are those present on the fracture face. Tendential features represent the appearance of the fracture trace on another surface, usually perpendicular to the major fracture face.

Origin

All rock fractures begin at a distinct origin, which may take the form of a well-marked point or a broad zone, depending on the type of flaw in the rock which served as the fracture-causing stress concentrator.

The types of origin flaws in sedimentary rocks have been discussed previously and may be easily observed on the fracture face. However, in many cases the flaw is not discernible megascopically and the origin may only be located within a limited zone with the aid of other transient features. Where well-developed

hackle plumes are visible on the fracture face, the origin may be located approximately by the point of convergence of the plumose hackle markings and Wallner and arrest lines (figure 35). Establishment of the origin point of a fracture is critical in ascertaining the stresses or mechanisms responsible for fracture inception. Various workers, including Hodgson (1961) and Gay (1973) have advanced the theory that most fractures propagate upward through the sedimentary column, with Hodgson advocating a fatigue mechanism through tidal forces and Gay propounding a "bridging" mechanism caused by minor Precambrian basement vertical faulting. If fractures propagate solely upward as suggested by Hodgson then statistical analysis of origin points on regional fractures should show fractures originating consistently at the bottoms of any individual stratum with opening directions upward and outward. The fractures should also consistently lead on the bottoms of the beds. If, as advocated by Gay, a bridging mechanism is responsible related to vertical faulting in the underlying basement, then fractures may advance upward through the rock section, but not by continual upward propagation. Fractures in extended rocks on the upthrown side of the buried fault may originate at the top of individual beds and open downward. Conversely, fractures in rocks over the downthrown side of the fault, should originate on the bottoms of the beds and open upward. In the first case, fractures should lead on the top of the bed, and in the second case the fractures should lead on the bottom of the bed. In any event, whether or not the theories of any previous workers are correct, a proper procedure for the elucidation of regional fracture genesis must be in a systematic study of 1. origin point location, 2. location within a fractured stratum of the leading fracture front and 3. overall propagation directions. Light may also be shed on the origin of joints by other mechanisms. For example, fractures caused by buckling of rigid competent rock layers may fit an overall tension plan and strike parallel to the hinges of associated folds. On anticlines such fractures should originate about the outer arc of the buckled layer (crest) and propagate downward and subsequently in a lateral direction, with the fracture leading on the upface of the bed in which it originated. Fractures originating from, and striking parallel to, a lateral principal compressive stress should show less locational preference for origin points at either the top or bottom of fractured beds. Stress distribution in this case would permit a much higher percentage of origin points within the bed proper, assuming that buckling did not predate fracture inception. In addition, these fractures should show a greater tendency to lead outward through the middle of the bed.

Mirror and mist

Mirror and mist regions circumscribe the origin zone in fractured rocks. The mirror region is the extremely smooth surface surrounding the origin on may fracture faces (figures 9, 14). In coarse grained rocks the mirror region may be that portion of the fracture surface free of any sharp velocity hackle undulations larger than the grain size itself. Radially outward from the mirror lies the mist region which is slightly more rough and irregular and is attributed to velocity hackle development at some critical crack tip stress and propagation velocity. Mirror and mist are generally not well developed or are not easily discernible in coarse polycrystalline rocks. However, they may be well developed on the fracture surfaces

of coal, chert, and fine grained sedimentary and igneous rocks such as micritic limestones, dolomites and basalts. Delineating the mirror and mist region roughly locates the origin point, and the shape of the mist-mirror envelope may establish the principal propagation direction of the fracture.

Wallner lines

Wallner lines are transient features generally possessing low amplitude and rounded crests in contrast to the more striking and cusped arrest lines. In glass they are generally best observed in the otherwise featureless mirror region. In rocks, as well as in glass, the half wavelength and amplitude of Wallner lines is related to the size of the sonic wave generating flaw, which may be quite large (figure 87). One of the principal values of Wallner lines in fractography lies in their curved shape on the fracture plane which takes the form of a general convexity in the direction of fracture propagation. In addition, the intersection point of two Wallner lines, if observed on a fracture face, may be used to determine rock fracture propagation velocities (chapter 5). Small scale and subtle Wallner lines are not common megascopic features in rocks because of the overall coarse polycrystalline nature of these materials. In contrast, Wallner lines are best developed in fine grained rocks, and on some fracture faces broad, large amplitude Wallner lines are locally abundant. The absence of megascopic Wallner lines on many pervasive fracture faces again indicates that rock fracture velocities were not high and in many cases may have been far below the critical velocity necessary for velocity hackle and forking. In the field Wallner lines seem to be most abundant on artificially induced and natural release fractures.

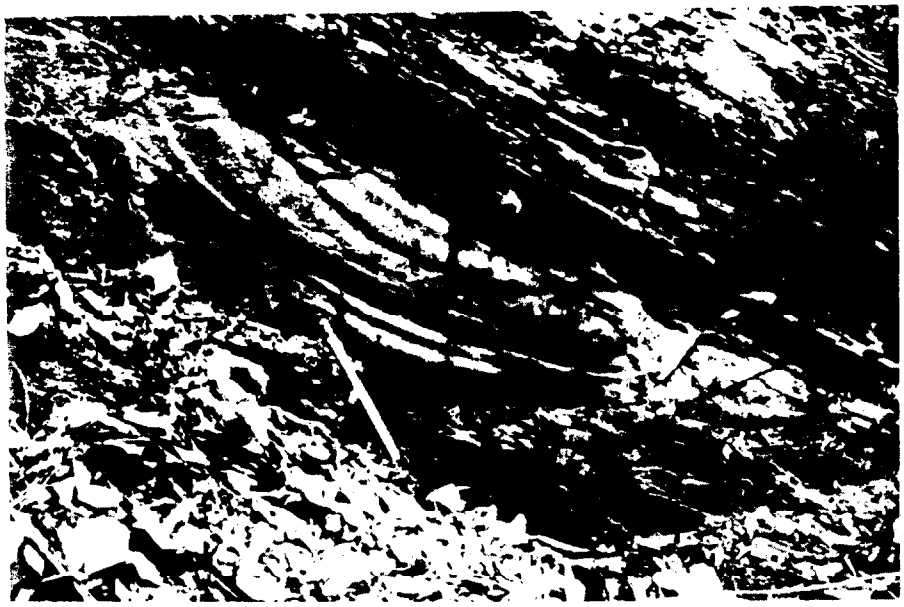

Figure 87, Wallner lines on fracture in folded Devonian shale, Maryland. Hackle marks are oblique to Wallner lines. Fracture originated at the stratum top (arenaceous shale layer) then spread downward and laterally leading at the fractured stratum top (off photo). Note pencil for scale.

Arrest lines

Arrest lines, commonly called rib marks, are best represented by the virtually omnipresent curved markings on fracture faces of fine grained natural materials where the term conchoidal fracture is often applied. Arrest lines can be used in the same fashion as Wallner lines for fractographic purposes because their convexity in almost every case indicates the direction of fracture propagation. However, arrest lines are much more commonly seen on fractured rock faces because they generally possess a much higher relief than Wallner lines. In profile they resemble a cusped wave. Parabolic-shaped arrest lines are useful in fracture analysis because the axis of the parabola indicates the region of greatest crack tip tension and concomitant leading portion of the fracture front (figures 34, 35). Also the curvature of an arrest line is convex in the direction of fracture propagation. This observation is strengthened by the fact that hackle marks are always perpendicular to arrest lines.

Hackle marks

Megascopic inclusion and twist hackle marks are very common transient features of fracture faces in all rock types. Hackle can be a valuable field tool for any geologist studying outcrop fracture characteristics, trends, and modes of formation. All hackle types, if interpreted correctly, can be used to:

1. determine fracture propagation directions (figure 88, 89);

2. determine the relative fracture velocity from place to place on the fracture face at any time during the history of fracture growth (figure 29);

3. reconstruct the general shape of the fracture front at any time during the history of fracture growth (figure 28);

4. determine whether or not the relative tension promoting fracture growth was uniform or unevenly distributed throughout the fractured stratum at the time of failure. If fracture sets geometrically related to folds are also genetically related (Stearns, 1968) observations of this nature could prove critical.

Unfortunately, twist hackle can also be easily misinterpreted by the untrained field geologist. For example, gross planar twist faces are often oriented at a high angle to the major fracture plane (figures 89 90, 91). The twist hackle face and step fractures and the main fracture plane are a product of the same fracture event. However, all planar fracture faces may be mistakenly interpreted as up to three individual fracture sets. If only the two dimensional tendential extent of twist hackle faces is observed on a bedding surface (figure 77), misinterpretation of fracture sets derived from observed fracture trends might easily result. One could attribute the en echelon fracture traces to a simple shear couple, or interpret the main face and twist hackle trends as a conjugate shear set. The latter error is easily committed if a large number of "statistically valid" but blindly taken fracture trends are later analyzed by a selected statistical procedure in the laboratory.

Velocity hackle has not proved to be a common feature on rock fracture faces. However, velocity hackle has been observed on fractures attributed to blasting that cut chert beds or chert nodules. If correct, the observation that velocity hackle is not prevalent on a regional scale can be interpreted as further evidence that less than critical propagation velocities existed during the development of natural systematic fractures.

Figure 88, large scale twist hackle in massive sandstone, Arizona. Closely spaced twist hackle has controlled the formation of the sandstone cave to right of photo. Twist hackle steps increasing in relief upward, and arrest lines at photo's left margin show the systematic fracture propagated from the bottom up. The photograph was supplied by Dr. V.D. Frechette, N.Y.S. School of Ceramics, at Alfred University.

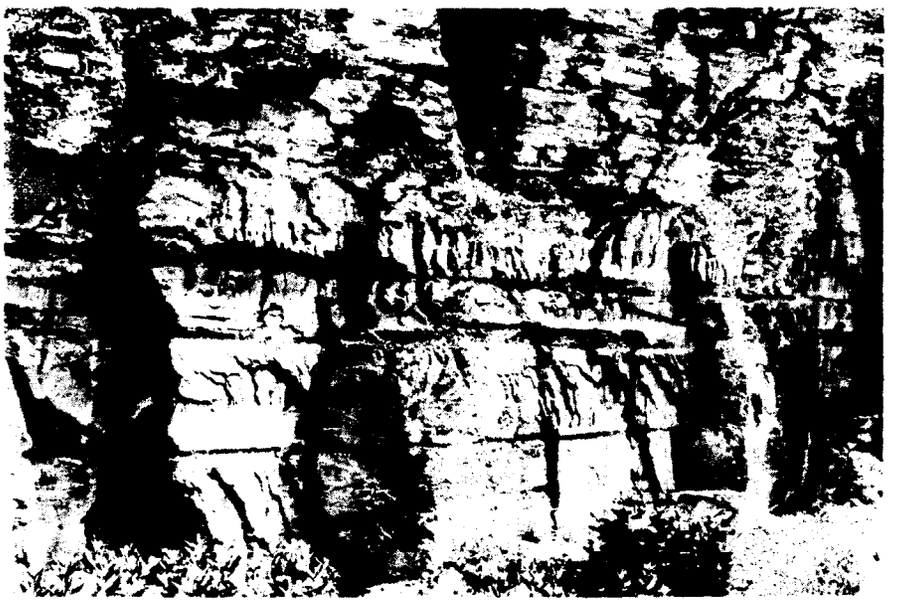

Figure 89, twist hackle faces and steps on a systematic fracture in Mississippian shale, West Virginia. The systematic fracture developed from right to left with the fracture front at any time past leading in the photo center and lagging at the photo top and bottom. A line drawn perpendicular to vertical sections of twist hackle steps shows that the lagging fracture section spread vertically downward in lower photo section. All faces related to the systematic fractures (hackle faces and steps) are the result of a single fracture event.

Figure 90, twist hackle faces and steps in Devonian shale, West Virginia. Here twist hackle faces are at a high angle (approximately 60°) to the systematic fracture face. The fracture developed generally from right to left. Note pencil in lower twist hackle fringe (arrow) for scale. Large arrow indicates twist hackle face enlarged in immediately following photo.

Figure 91, enlargement of twist hackle face shown in immediately preceding photo. Pencil points to the fracture origin location of the twist hackle face. The twist hackle face fractures spread from bottom to top. All fractures depicted are the result of a single fracture event.

Forking

If fracture velocity and crack tip stress reach critical proportions, or a propagating fracture encounters large favorably oriented anisotropies, the fracture may bifurcate or fork into a number of radiants. A forking fracture can provide the following fractographic information:

1. a rough approximation of the ratio between the two principal stresses within the bedded stratum (figure 43);

2. tendential determination of fracture propagation direction (figure 40);

3. a rough approximation of fracture propagation velocity (.5 V_t), if the forking event can be attributed to a critical fracture velocity; if the propagation velocity was at a critical value a zone of chaotic velocity and twist hackle should be evident in front of the radiant.

With regard to item three, it should generally be suspected that fracture forking in rocks of low tensile strength is attributed to factors other than critical fracture propagation velocities. One must also be cautioned against attributing an abutting fracture to forking. Generally if it can be determined by study of transient features that fracture propagation directions are similar before and after the radiant point on all forking fractures, and no origin is evident at the radiant, then all fractures can be attributed to the same fracture event.

Obviously, fracture forking, regardless of its initiation mechanism, can be attributed to a single fracture event. Here again the opportunity for misinterpretation through the formulation of different fracture sets and nonexistent conjugate shear relationships exists.

Hooking

The tendency for a fracture to hook into a free surface or neutral plane within a flexed object can be useful for determining the following fracture characteristics:

1. the fracture propagation direction;
2. the sequence of fracture events;
3. location of the greatest tension that existed along a fracture plane at the time of fracture.

The abrupt hook into a free surface will obviously form in the direction of fracture propagation. This relationship can be useful for determining fracture sequence, even at the intersection of two fracture faces bounding a single block of strata. The intersection, upon casual observation, forms a nearly orthogonal join, much like the edge of a brick, rendering abutting relationships difficult to ascertain. However, the abutting fracture will possess a hook. This hook may be so small that it must be determined by rubbing the fingertips along the fracture faces where these faces join. The first formed fracture will be smooth; however, the abutting fracture should possess a hook.

Any brittle fracture formed at the inception and as a consequence of folding, especially fractures trending parallel to the fold axis, may display well-defined hooks. Fractures forming parallel to and along the crests of incipient anticlines will generally initiate at the top of a given stratum and hook towards the bottom, depending on the position(s) of the neutral surface(s) in the sequence of layered rocks. The opposite situation can be expected in synclines. Hooking, in both instances, would indicate that bedding anisotropies acted as free surfaces. Torsion fractures should also have a tendency to hook toward the stratum face opposite their point of origin (figure 44).

Fracture intersection relationships

Fracture intersection relationships with various other anisotropies, including other fractures, should be studied and recorded with particular care. The most thorough examination can be accomplished if both the tendential and transient features of the abutting or interpenetrating (crossing) fractures can be observed.

Fractographic information that can be gained from fracture intersection relationships, if adequate data are available, is three-fold.

1. relative age and sequence of formation of individual fractures and fracture sets (see figures 45 through 53 for details).

2. relative age of fractures as compared to related or unrelated nearby structures. Examples would be previously existing fractures that have controlled stylolitization or have been consistently offset by bedding plane slip.

3. rough estimate of principal stress relationships at failure; as in the case of intersecting torsion and point load fractures.

CHAPTER 7

LABORATORY FRACTURE EXAMINATION PROCEDURES

The examination and logging of fractures in oriented core samples is most conveniently done in the laboratory away from the drill site. In some circumstances where field studies deal with microfractures, a geologist may need to take oriented samples back to the laboratory for further examination under proper illumination and magnification.

Laboratory investigation of fracture initiation and propagation, and the resulting transient and tendential features, can be an involved and complicated process, utilizing equipment of a very sophisticated nature. Descriptions of various specialized investigatory procedures are contained in several of the works cited in the bibliography. The basic techniques described in this chapter have proven useful to the authors and can be completed in even a minimally equipped laboratory.

Microscopy and illumination

The optical equipment used for the examination of a given fracture surface is dependent upon the shape, size and transparency of the fractured specimen. The most versatile tool for fracture surface study under reflected light has proven to be a binocular microscope attached to a firm base (figure 92). The adjustable boom permits examination of very large specimens. If the specimen must be viewed under high power, or must be held stable for photography, the sample can be placed in a sand-filled container that permits an adjustment to the proper position. Small specimens can be viewed by first placing them on a pedestal of modelling clay within an open hemisphere. The hemisphere is set in a ring to facilitate rotation to the proper orientation.

A simple magnification technique that also affords the most rapid overall view of a fracture surface is a large adjustable magnifying glass held within a frame.

The height and inclination of the glass should be adjustable. The availability of sophisticated optical devices and electron microscopes does not alter the fact that the simplest and most expedient examination procedure may involve nothing more than study of a hand-held specimen under a pocket lens.

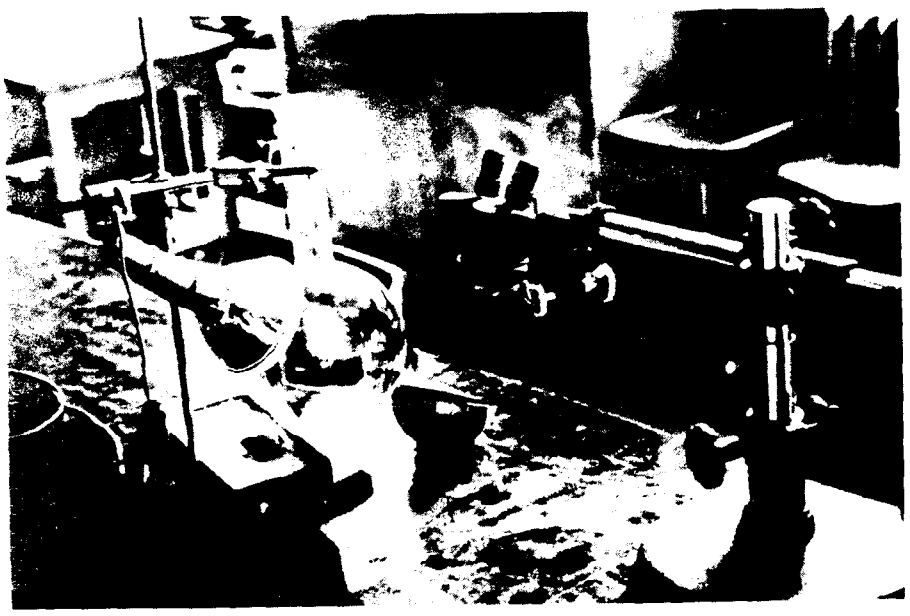

Figure 92, a convenient apparatus arrangement for examining fracture surfaces. The specimen, if not too large, can be oriented by placing it in the hemisphere and rotating the hemisphere in the ring upon which it sets. The bright light emitted from the high wattage lamp can be cooled and diffused by passing it through a flask of dilute copper sulphate solution.

Transparent and translucent fractured objects can often be better examined if the fracture surface is silvered to block subsurface reflections and refractions. The silvering process can also be used on opaque surfaces to enhance the surface albedo contrast under reflected light.

A fractographic analysis of transient features can often be accomplished without the use of a microscope. However, the success of any examination procedure will depend upon the proper source and arrangement of illumination and the orientation of the fracture surface in the field of light. It is generally best to allow the light to reflect obliquely from the surface and to view the fracture surface at a ninety degree angle to the line of light source. The fracture surface can also be manipulated within a stationary light source. Changing position of the specimen is essential when the fracture surface is highly irregular. Generally examination procedure requires light to be reflected to the eye from a well-defined source at an angle that permits slight undulations on the fracture surface to disrupt the light reflection. The disrupted and non-uniform reflection causes these regions to appear dark against a bright field or bright against a dark field. Oftentimes examination is facilitated if overhead lighting is extinguished, thereby enhancing bright and dark fields.

The authors have found that the availability of several light sources is beneficial. One light source should emit a high intensity beam and be small enough to be hand held to permit flexibility in choice of conditions for optical or naked eye examination. A large light source, such as a 160 or 200 watt flood bulb provides the best illumination in most instances. This is the case when examining extensive relatively flat surfaces. The harsh white light emitted by the high wattage bulbs can be cooled and diffused by passing it through a flask of dilute copper sulphate solution.

Fracture surface replication

The following replication methods have been developed by Professor V.D. Frechette (1973a)to facilitate the study of fractured surfaces in glass and ceramics. All procedures are adapted from his report.

The use of replicas to replace direct examination of fracture-generated surfaces will most likely not become a common laboratory procedure for fractographic investigations. However, the replication of rock fracture surfaces does offer some advantages that may prove useful in the following situations.

1. The replica is an easily catalogued record of a fracture surface on a specimen that is only a small part of a large, perhaps immovable, object. Also fracture surface replication on a specimen that must be destroyed for further testing may be necessary. The latter could be true of rock samples scheduled for later chemical and physical analysis.

2. Optical examination is facilitated by the thinness of the replica. This is true for oriented rock samples and core sections that are too large for convenient microscopic study. The absence of disturbing subsurface details afforded by a replica may prove beneficial when studying fractures in transparent or translucent material.

3. Highly curved and irregular surfaces are made more accessible to observation, since these can be flattened in mounting the replica.

4. Negative details (pores and cracks) are converted to positive in the replica, and may be more effectively examined at high magnification.

Disadvantages include the loss of optical characteristics, including color information, which could be used to identify mineral and fossil constituents. This loss could prove critical when the fracture originates from a foreign inclusion. Replication irregularities caused by the replication procedure itself or irregularities inherent in the replicating material itself must be avoided.

The replica surfaces may be made more reflective by any metallizing process to enhance reflected-light examination.

Polyvinylchloride (PVC)

The preparation requires melting PVC at a temperature of 250° - 290° C. Specimens that may degenerate with heating or specimens scheduled for later chemical testing which may lose volatiles when heated may make heating impractical. However, contact time of hot PVC with the surface may be short, and provided that the mechanical details of manipulation can be solved, the PVC technique can be used on almost all rock fracture surfaces.

The PVC remains pliant, elastic, strong and tough after the replication process. However, there is a slight yellowing and embrittlement. PVC works well even with very porous rocks provided they are well cemented.

Technique: In general, the specimen is heated on a hot plate or in an oven, with smaller specimens requiring higher temperatures because of their rapid cooling during replication. The specimen is then set with the fracture surface horizontal and facing up. The PVC sheet is placed on the fracture face and bubbles are worked to the side using a teflon rod. The replica is stripped with a quick pull after the temperature has dropped to approximately 60° C. The peel is laid on a glass mount, replication side up, and may be trimmed with a razor if necessary.

If the specimen is exceptionally large or stationary, it may be necessary to heat the PVC and press it against the cold fracture surface. Figure 93 outlines both procedures.

Please note that PVC vapors are harmful if inhaled. Therefore all PVC replications should be prepared under adequate ventilation.

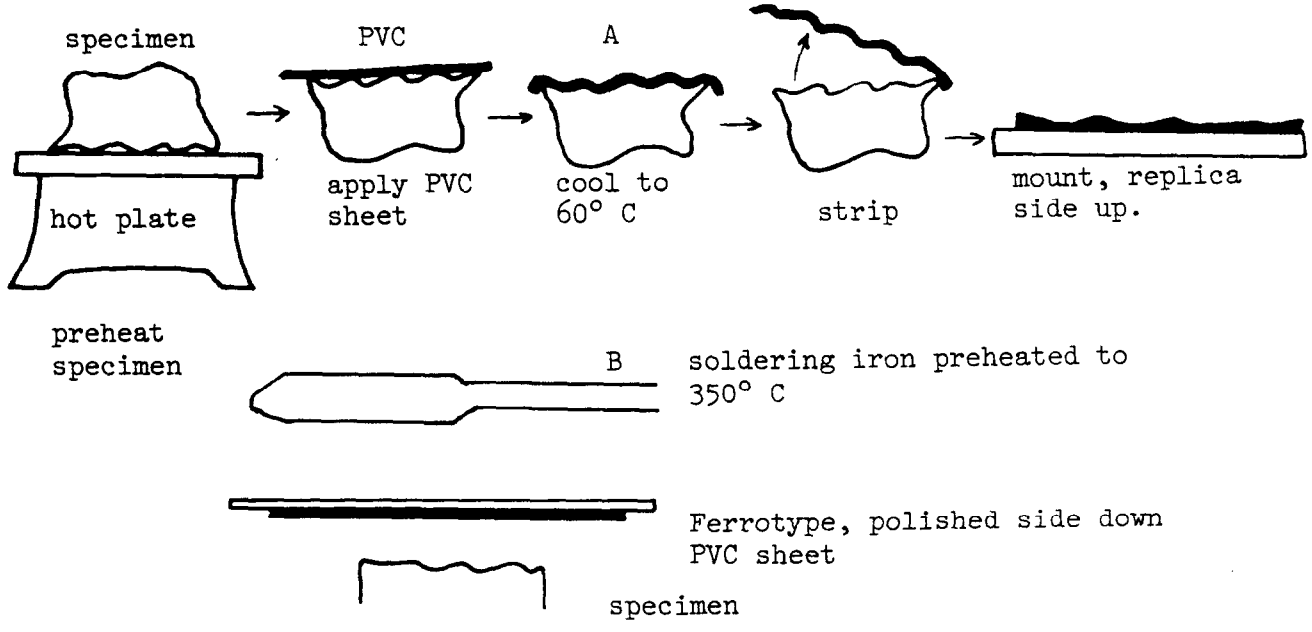

Figure 93, A, normal procedure for PVC replication. B, PVC replication procedure for large or immovable specimens. Preheat PVC for 5 seconds with hot iron, then press the iron and PVC against the specimen for one second. Finally remove and strip PVC after it has cooled.

Faxfilm (cellulose acetate)

Cellulose acetate replicas are stiffer, more brittle and weaker than PVC peels. Also, faxfilm rigidity makes mounting difficult, and tears or breaks may resemble natural fractures. Their special advantages lies in the fact that no specimen heating is required.

Technique: Press the faxfilm sheet into contact with a PVC strip of the same size, and immerse both in acetone for fifteen seconds. Next, place the sheets on the acetone -- flooded fracture surface (faxfilm down), and roll into place with a pliable silicone rubber roller. Repeat the rolling every fifteen seconds for three minutes. After an additional five minutes, strip the faxfilm from the PVC and specimen. The specimen can now be mounted with scotch tape to a glass plate and trimmed to size (figure 94).

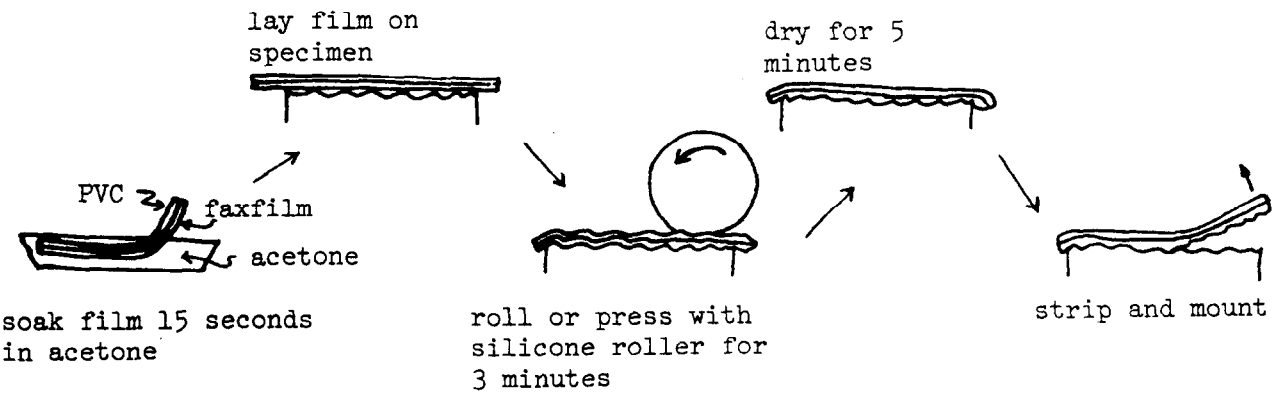

Figure 94, replication with faxfilm (cellulose acetate).

Silicone rubber

Cold and warm setting silicone rubber is elastic, quickly mounted and trimmed, and is easily stripped provided the fracture surface is not highly irregular. However, experience has shown that the cold-setting type is especially weak and has a short "pot life" after mixing.

Technique: Mixing of monometer and hardener is done in the proportions specified by the manufacturer (2 - 3% for cold-setting, 10% hardener for warm-setting types). After mixing, bubbles are drawn from the solution by evacuating two or three times.

The mixture is applied cold to the specimen by allowing it to flow over the surface thereby avoiding trapped air bubbles. After the fracture surface is coated, it is covered with a thin glass sheet and cured. Cold-setting types require 24 hours curing time before stripping. The hardening time at various temperatures for warm-setting types is described in the manufacturer's specifications. However, hardening can be accomplished in several minutes at about 200° C.

Plastisol

Plastisols are convenient because they require no mixing and provide a strong, tough, elastic, easily-stripped replica. However, the liquid is milky and viscous and requires evaporation for at least several hours to eliminate bubbling during curing. After curing, the plastisol is applied to the specimen surface, covered with nickel foil and warmed overnight at 165° C. The plastisol is then stripped from the specimen and foil and mounted.

Fracture orientation measurements

The orientation of fractures within a core sample or properly sized field sample can be measured rapidly and accurately by a number of procedures. The simplest method utilizes only a metal ring marked in 360°, a sand bucket the same diameter as the ring, a straight edge, and an inclinometer. The core section containing the fracture to be measured is placed in the center of the sand bucket with the core axis vertical (assuming the core was drilled vertically). The calibrated ring is then oriented on the lip of the bucket so that the north-south, east-west directions of the ring coincide with those of the core. The strike of the fracture is then easily determined with two taut parallel wires, larger than the ring and attached to a rigid frame. One wire is movable, the other stationary. The stationary wire is placed tangent to the fracture surface and the frame is held so that the wires are horizontal. The movable wire is passed upward along the frame and over the core until it lies over the upward projected core axis center (the core and ring center coincide). The strike of the fracture is then read from the calibrated ring where the movable wire lies over the ring. If parallax appears to present a problem a weighted string can be dropped to the calibrated ring for a more precise measurement. Slickenline bearings can be read by placing either wire over that feature and parallel to slickenline trend. A simple inclinometer, constructed from a protractor, string, weight and piece of rigid cardboard, can be used to ascertain fracture dip or slickenline plunge.

The orientation of any planar or linear feature on an oriented field sample is obtained in a similar manner. In this case, the sample is positioned horizontally in the sandbucket (with respect to its pre-collection horizontal field orientation). The calibrated ring is then situated on the sand bucket rim so that sample north coincides with north on the ring.

Unfortunately, hairline fracture traces on some core walls or other sample surfaces may be difficult to see. Also the tendential features at the feather ends of visible fracture traces may be difficult to ascertain. Overall, the omission of a few fractures may not be significant. However, there is the possibility that

critical tendential features may be missed. In addition, hairline fractures may impair some velocity measurements in core samples, or bias breakage directions and stress values in point or directionally loaded failure tests. These hairline cracks can be rendered more visible by spraying the core area under study with methyl alcohol. The alcohol evaporates quickly from the noncracked surfaces. However, alcohol drawn into the fractures remains briefly, causing tendential features to be darker and more discernible. Photographs can be made and the fracture trace outlined with chalk while it is still moist. Distilled water may be used in place of alcohol if cores are to be chemically tested for organic content.

Core logging technique

A logging procedure that facilitates rapid examination and recording of core fracture orientations and fractographic features was developed in a prototype study of a core section from the Nicholas Combs well, Hazard, Kentucky (Kulander, Dean, Barton, 1977). The following description is modified from that study.

It is convenient to first arrange in order, side by side on a long table, all core boxes containing rocks to be examined. Then each individual core sample within a given box is reconstituted into its proper place in that core section. Highly fragmented core sections can be taped with a strong transparent mending tape. The reconstructed core is then marked off into feet and tenths of feet using convenient foot marks already on the core. Each individual fracture can then be assigned a logging number. The number is written on the fracture face or along its tendential trace with a marking pencil. Care must be taken not to obscure important transient markings. Fractures within each box are numbered in an upcore to downcore direction with each core section box being lower in the section. A single fracture that is separated, but continuous into a number of core sections is assigned the same number. All planar and semi-planar fractures large enough to permit an accurate orientation measurement are numbered. Smaller fractures, if deemed important, can be numbered and described without orientation measurements. The number of core sections that can be reconstructed at the same time is limited by available work space.

Center-cored specimens and slabbed four inch cores, subjected to experimental fracturing, are assigned numbers followed by an upper case letter; for example, 553A. Occasionally in sequential numbering, a fracture is inadvertently omitted. This oversight is corrected by later assigning the slighted fracture a non-integer number.

After the core section has been marked into tenths of feet and the fractures numbered, each individual fracture is examined. First the orientation of the fracture is measured and recorded. Following this, the transient and tendential features are studied. It is often possible to complete the fractographic examination without the use of a microscope. However, as previously described, the success of the examination depends upon the proper arrangement of illumination and on the orientation of the fracture surface in the light.

A log sheet has been designed to facilitate the recording of pertinent observations (figure 95). No horizontal lines divide the log rows because fractures may require different amounts of description space. The log can be completed in the following manner.

1. The pre-designated fracture number is recorded.

2. The depth and total extent (if inclined) for the fracture is noted in the column, foot and extent. For example, "from 2600 feet to 2603.7 feet, entirely across the core," or "2607 feet, abuts against vertical fracture 266."

3. The orientation of the fracture is recorded.

4. All tendential and transient features observed are listed under the column, fractography markings. For example, "hackle meets core boundary orthogonally," "arrest lines are symmetrical downcore."

5. The location of the fracture origin is noted along with initial and final opening directions. For example, "origin immediately off core center, fracture initially opened toward center, then spread laterally to core margin." This data is recorded under the column, origin phenomena-location-opening direction.

6. Mineralogical or structural indicators of tectonic fractures are described, and linear feature orientations are listed under the column, tectonic indicators.

7. The column labeled, noteworthy features, is used to record any pertinent observations not covered by previous entries, or lists significant features to be subjected to later detailed study. For example, it is often possible, after a number of consecutive fractures have been examined, to determine the sequence of fracturing within a particular core section. The sequence can be recorded in this manner utilizing fracture numbers, $515 \rightarrow 514 \rightarrow 516$. Also included in this column are extraneous descriptions and a notation of any fracture deemed suitable for later photography. Polaroid picture examples of fractures characteristic of a given core may prove useful, especially since many cores are later used in destructive tests.

8. After thorough examination and notation of all transient, tendential, and structural features, a judgement is made determining whether a given fracture is coring-induced (CI), naturally induced (NI), experimentally induced (EI), or handling induced (HI). The conclusion is placed in the column headed, fracture classification. Experimentally induced fractures are obvious. However, it is important that EI fracture data are recorded. The data may be needed for further analysis.

When logging for all core fractures within a given box is completed, the samples are placed in the box in proper order. The box is then returned to its original position on the table.

The procedure described above best fits the authors' plans and facilities. However, the method is flexible and can be modified to any investigator's convenienc

SAMPLE CORE LOG

fracture number	foot & extent	orienta-tion	fracture classif.	fractography markings	origin phenomena location/opening direction	tectonic indicators	noteworthy features

Figure 95

NI = naturally-induced
CI = coring-induced
EI = experimentally-induced
HI = handling-induced

CHAPTER 8

FRACTOGRAPHIC CHARACTERISTICS AND FORMATIONAL MODES OF NATURAL, CORING-INDUCED, AND HANDLING-INDUCED FRACTURES

Any natural, coring-induced, or handling-induced core fracture is a direct result of the fractured material's mechanical properties, anisotropies, and complex internal and external stresses. Generally, the stress distribution responsible for natural systematic fractures is regional. Stress release or unloading fractures bear a direct relationship to topography and are, in this respect, caused by more local variations in stress. However, the most localized superposed stress systems of major interest in this chapter are generated about the drill bit during a coring operation.

A knowledge of fractography indicates that fractures produced regionally, by drilling, or by action near the ground surface should each possess characteristic transient and tendential features. If the investigator can interpret these fractographic events accurately, the separation of core-induced and handling-induced core fractures from natural fractures is facilitated.

This chapter is based largely on the author's experience with Devonian shale core from the Nicholas Combs well, Perry County, Kentucky (Kulander, Dean, Barton, 1977), the Reel Energy well, Mason County, West Virginia (Dean, C. and Kulander report in progress) and other selected Appalachian basin shale cores.

Natural core fractures

Natural core fractures are those produced by regional tectonic or non-tectonic stresses. Megascopically they are generally pervasive, large in penetration and extent, and occur with a well-defined frequency. A wide spacing of vertical natural fractures could, in some cases, render them difficult to detect in a vertically drilled well. The origin region of any natural fracture may be far removed from the cored area. Transient features on cored natural fracture faces should reflect this large origin separation distance. For example, oversize arrest ridges and hackle marks trending straight across the cored fracture face would be expected. Furthermore, fracture surface structure geometry would not be related to core geometry. Obviously, any fracture opening filled with secondary mineral matter would be judged natural.

Natural fractures are arbitrarily divided into three general categories to facilitate discussion.

Horizontal natural fractures

Horizontal to subhorizontal natural fractures in shale core samples studied to date are relatively simple to identify and often show indications of past tectonic activity. These tectonic indicators generally take the form of slickenlines and/or secondary fibrous or nonfibrous mineral growths (figure 96). Some slickenlines (slip lines) consist of mineral fibers subparallel to the fracture face indicating a fiber growth rate commensurate with rate of shear movement. Horizontal fractures may also contain secondary mineral growths of vertical fibers oriented perpendicular to the fracture faces. The vertical fibers suggest that abnormally high fluid pressure existed to separate the fractures. These horizontal fiber-filled fractures show that vertical and horizontal movements have occurred, and indicate that the interval has acted as a decollement to one degree or another.

Tectonically induced slip directions on the horizontal fracture surfaces in the Nicholas Combs and Reel Energy wells have several consistent trends throughout cored sections. Several prominent slip directions are present. In contrast, subhorizontal to horizontal slickenlines attributed to differential compaction show random orientations even on a single cored fracture.

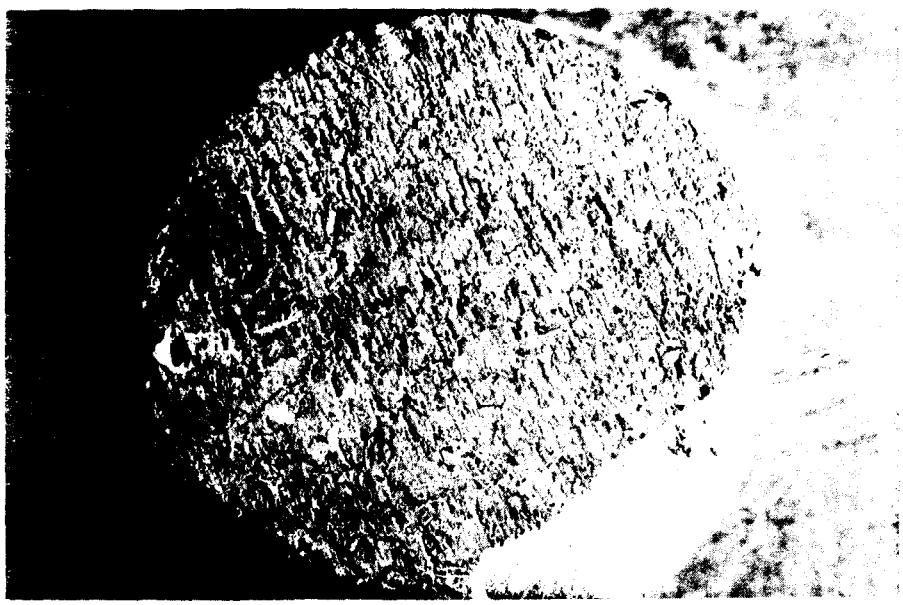

Figure 96, a horizontal, natural core fracture that has been mineralized and slickensided.

Vertical and subvertical natural fractures

Vertical natural fractures are difficult to penetrate by a conventional well because these fractures are parallel to the drilling direction and may be widely spaced. These fractures possess transient markings that are generally not symmetrical to the core dimensions. This nonsymmetrical relationship is attributed to the fact that the natural fracture origin is located away from the cored section. Where fractures have originated offcore, and before the coring operation, transient features on fractures penetrated by the drill show short segments that are often nearly straight lines. Arrest lines show a very large radius of curvature and hackle marks do not spread from a core-related origin (figure 97).

Figure 98 shows a mineralized natural fracture that terminated within the to-be-cored section. The resulting terminal arrest line is immediately preceded by a well-developed twist hackle fringe along much of the front. Terminal arrest line and hackle plume asymmetry show fracturing stresses and propagation velocity were greatest in the upper fracture section. The fracture beyond the terminal arrest line was laboratory induced to expose the natural fracture surface.

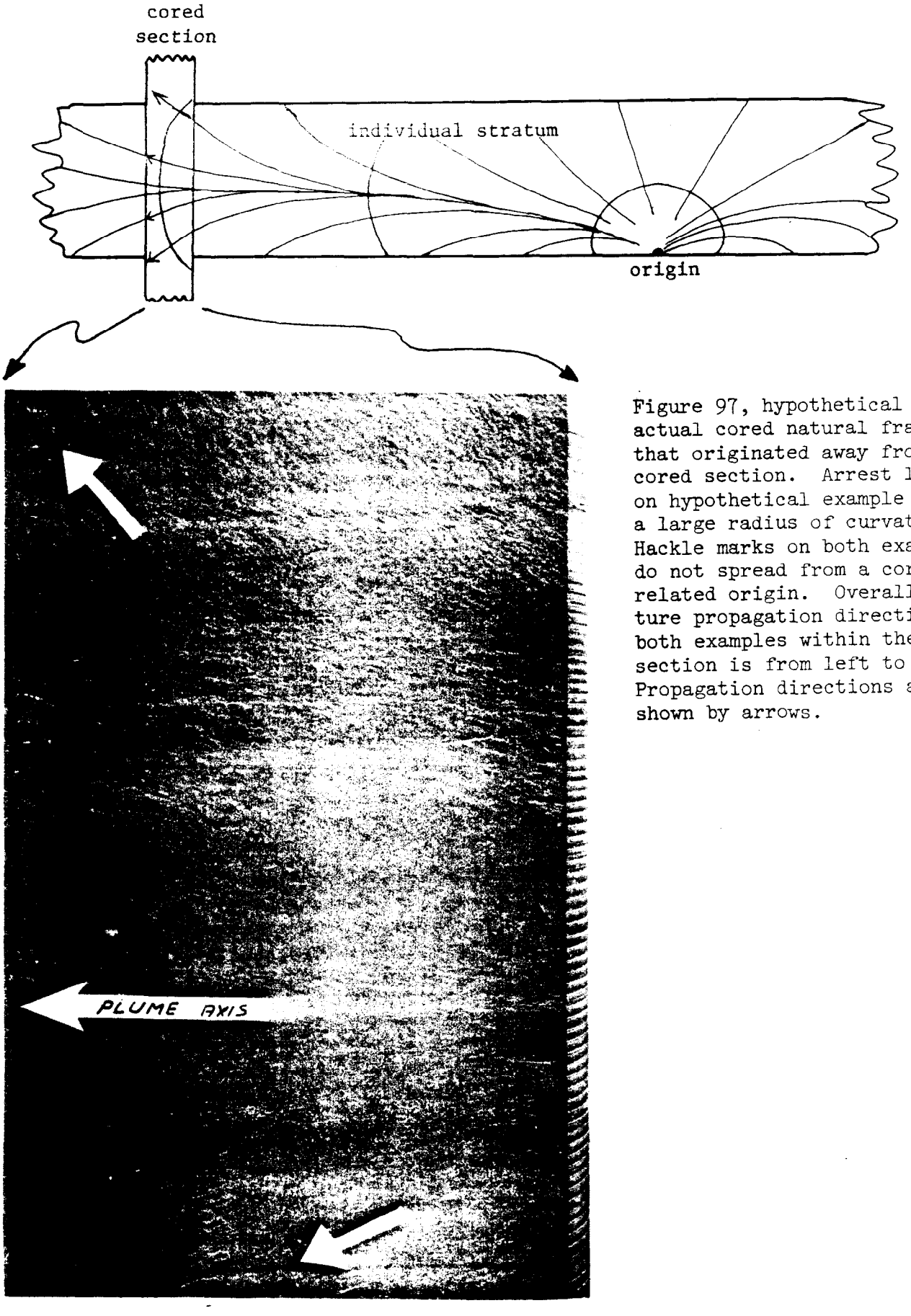

Figure 97, hypothetical and actual cored natural fracture that originated away from the cored section. Arrest lines on hypothetical example show a large radius of curvature. Hackle marks on both examples do not spread from a core-related origin. Overall fracture propagation direction on both examples within the cored section is from left to right. Propagation directions are shown by arrows.

Figure 98, natural vertical fracture terminating within the core. The mineralized fracture has a well-developed twist hackle fringe at its lower terminus. Some twist hackle faces in the fringe have been subsequently chipped. These hackle step-face traces may not meet the arrest line orthogonally. Note hackle on induced fracture section (right of terminal arrest line) does not meet the arrest line orthogonally: a further indication that the induced fracture postdates the natural fracture.

Subvertical natural fractures may cut diagonally across a vertical core at a small angle to the core axes. However, fractures in this category need not entirely transect the core and may not extend down the core center (as with most coring-induced centerline fractures). A natural fracture inclined 88° from the horizontal, with large vertical penetration, may cut diagonally entirely through the core for a length of 9.5 feet (2.91 meters). The fracture would obviously not be core-induced. Another diagnostic feature on fractures of this category are small conchoidal chips along the right-hand margin (fracture surface facing observer, downcore direction pointed down). These conchoidal chips are caused by the plucking action of a clockwise turning drill bit. Obviously the fracture predated drilling. However, the investigator should be warned that conchoidally chipped intersections at fracture-core boundaries need not prove a natural fracture origin.

Opened vertical or subvertical fractures may also be filled with secondary mineral matter (figure 99). Mineralized fractures in outcropping Devonian and Mississippian rocks are not uncommon. However, slickenlines (slip lines) are seldom found in outcrop on vertical systematic Plateau or western Valley and Ridge fractures, and accordingly may not be common on cored natural fractures in relatively undeformed Plateau rocks.

Figure 99, tendential view of two vertical systematic fractures connected by a nonsystematic fracture. All natural vertical fractures are mineralized. The mineralization in the nonsystematic fracture has enhanced fracture porosity.

Inclined natural fractures

Inclined natural fractures are those loosely grouped between approximate boundary inclinations of 10° and 80° to the horizontal. In contrast to the vertical natural fractures, these features often bear slickensides (figure 100). In fact, most slickensided inclined fractures are small faults, although it is not possible to determine relative displacement. For example, in the Nicholas Combs well, a number of these fractures were encountered in a 75 foot logged section. Here, all inclined fracture planes struck north-south, cut the entire core, dipped between 20° and 60° to the west and were slickensided (Kulander, Dean, Barton, 1977, figure 22).

Transient features on inclined natural fractures do not include an origin point within or on the cored fracture circumference. In addition, hackle marks trend straight across the fracture section and do not curve in an attempt to meet the then nonexistent core boundary orthogonally (figure 101). Also, natural inclined fractures generally do not hook into the core boundary. They have a tendency to remain planar across their cored extent. The more steeply inclined fractures in this category may possess chips along the right hand fracture-core boundary (as with vertical natural fractures).

Considering the paucity of regional systematic inclined fractures in outcrop across the Allegheny Plateau (work in progress, Kulander, Dean, Williams), it can tentatively be postulated that these fractures in Devonian rocks from the Plateau may be rare unless related to local vertical tectonism or a decollement mechanism. The absence of evidence of extensive tectonism in a stable Plateau region would suggest that regional stresses at depth were oriented horizontal and vertical. However, mineralized inclined fractures are present in surface rocks across the Allegheny Plateau and western Valley and Ridge provinces, and there is no reason to believe they would not exist at coring depth especially in decollement zone rocks.

Figure 100, a slickensided inclined natural fracture.

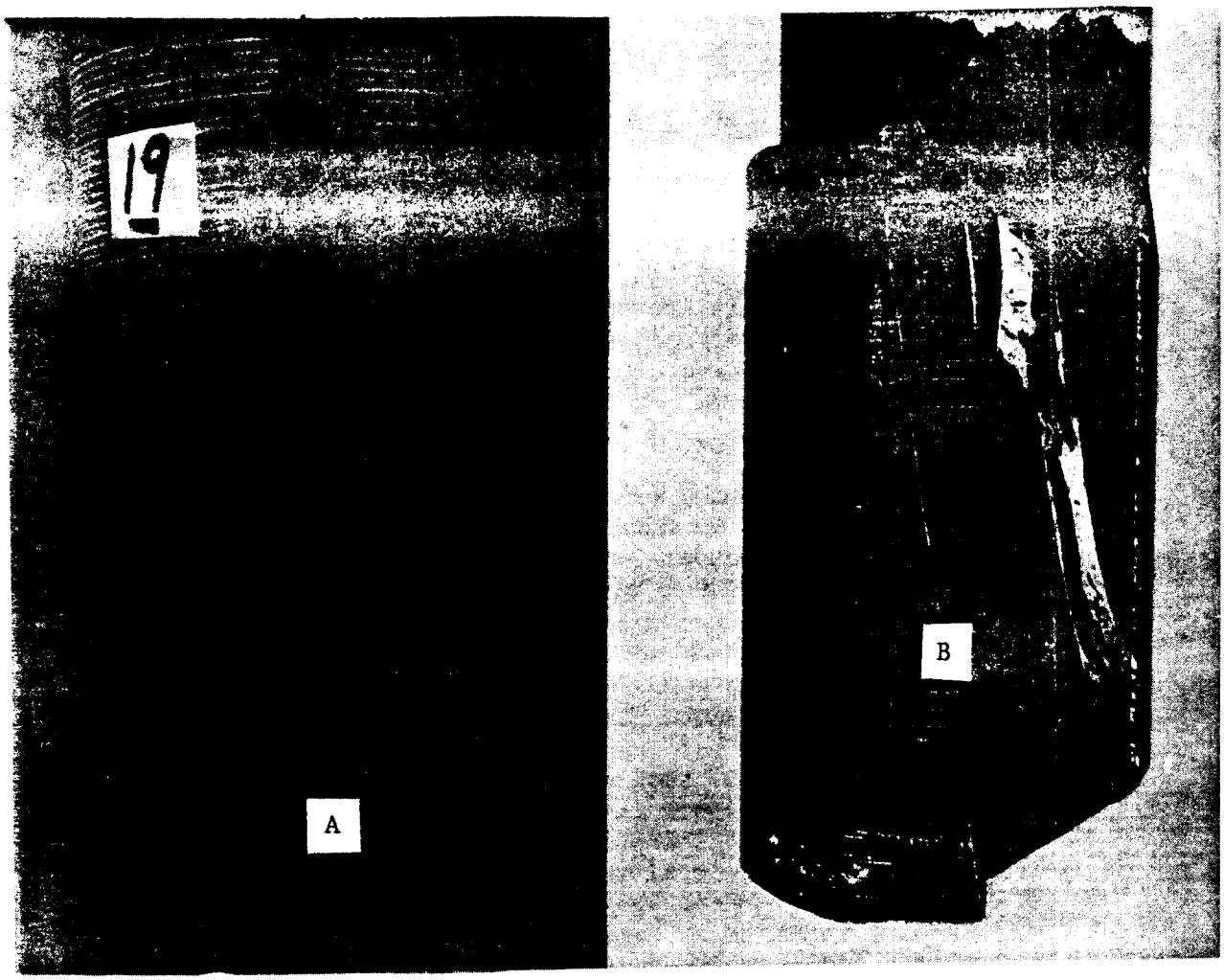

Figure 101, two inclined natural fractures. Drilled fracture A possesses hackle plumes that do not spread from a core-related origin. Natural fracture propagated from left to right. Drilled fracture B is mineralized. Note petal fracture initiating at left hand core margin strikes parallel to natural fracture B.

Coring-induced fractures

Coring-induced fractures are those that develop during the actual process of coring and are initiated by stresses directly related to coring. Furthermore, superimposed and intrinsic body stresses in the drilled column vary about the core bit. In addition, the drilling procedure itself leaves characteristic marks on the core and fracture surfaces. This stress variance and presence of characteristic marks make possible three important observations:

1. the relative timing of core-induced fracture occurrence during the drilling process;

2. the position of origin of a particular set of core-induced fractures in relation to the bit;

3. the orientation of the principal tension responsible for the initiation of a particular set of core fractures.

The three preceding observations lead to the conclusion that coring-induced fractures will possess a unique geometry directly related to, and symmetrical with the cylindrical core section.

Disc fractures

Horizontal and sub-horizontal disc fractures form in direct response to vertically acting principal tensile stress. These fractures are invariably inclined at less than 15° from the horizontal. However, non-horizontal bedding (cross bedding) or a large origin flaw may control the orientation of these fractures, because bedding planes, or laminations often represent a primary anisotropy across which rock cohesion may be markedly reduced. Consequently, even if beds are slightly inclined to the principal tension the resulting fracture may follow bedding anisotropy and be subhorizontal. Horizontal coring-induced fractures generally cut entirely across the core or abut against earlier-formed natural or coring-induced fractures.

Transient morphology on disc fracture surfaces is quite distinctive, and individual markings are almost always well-formed. The origin is always present on disc fracture surfaces, even though not always megascopically apparent, and it is generally located within the core interior. However, the disc origin flaw may be quite large, and may lie along the core boundary or along the line formed by the intersection of the disc fracture and an earlier formed fracture. Disc fracture origins are located at flaws consisting of fossils, mineral nodules, clasts, large grains, voids, and surface chips and cracks. Coarse and fine twist and inclusion hackle diverge from these origins and curve to meet the core boundary and pre-existing fracture surfaces orthogonally. Twist hackle steps often increase in relief towards these pre-existing boundaries. In some cases hackle plumes spiral from the fracture origin indicating an active torsion stress at time of failure (figure 102).

Disc fracture interpretation may be complicated where a disc surface consists of several coalescing disc fractures. In such cases one or more disc fractures generally hook conchoidally into a pre-existing disc surface (figure 103). In almost all cases the origin point on each disc lies within the core interior. It appears that several fracture origins in close proximity occurred almost simultaneously to produce the disc chips.

Figure 102, hackle on a disc fracture radiating from the fracture origin (fossil) and curving to meet the core boundary orthogonally. Spiral radiating pattern indicates a torsion stress component. Note the inclusion hackle spiraling from the edge of the fossil.

Figure 103, two distinct pyrite nodule origins on separate fracture chips forming a disc fracture surface. Hackle radiates from both origins and curves to meet the core boundary and earlier formed petal fracture (next section) orthogonally. Note the discontinuity of hackle across the fracture intersection separating the two origins. The intersection line is concave toward the second formed fracture origin. Inclusion hackle from nodule to core boundary and hackle pattern about origin indicate that stresses peaked at the nodule edge facing the inner core at crack inception. A slight fracture hook exists along the entire core margin, petal fracture intersection boundary.

Disc fracture frequency proved to be highly variable in previously examined core, ranging megascopically from one per inch to one per foot. This observation is corroborated by investigators working with other core samples.

The primary stress responsible for disc fracturing is attributed to unloading and bit pressure assisted by vibrations and torques inherent in the drilling process. The unloading is achieved by rapid removal of the above-lying cored column. For example, a vertical 3000 foot rock column with an average density of 2.60 gms./cm^3, exerts a pressure at the bottom of that column of 3880 lbs./in^2. Overburden and bit pressure may promote disc fracture development by two related mechanisms. First removal of above lying strata would permit underlying rocks to expand, thus contributing to a vertical tension component. Also removal of overlying core creates a void. Rocks immediately below the bit reacting to pressure exerted by surrounding strata would attempt to expand into the void, thereby creating a vertical tensile stress component. The tensile stress does not necessarily have to be high at the core center and may well peak near the core or to-be-cored margin where the radius of curvature, however slight, of any given stratum surface moving into the core barrel would be greatest. Second, bit pressure of up to 15,000 - 18,000 lbs./bit area is compression in comparison to the tension caused by the removed overburden pressure. The stress field would change from vertical tension beneath the cored column to compression beneath the bit. A stress field altered in this manner would necessitate a vertical neutral surface between the inner bit radius and the core interior. The neutral surface would promote hooking toward the bit commonly observed around the disc fracture margins. These hooks may extend up to three quarters of the distance around the core's circumference and cannot be attributed to cross bending (figure 104).

Origin flaws within the core interior on most disc fractures serve as evidence for peak tensile stress location. Also the inception point of the disc fracture is invariably located on the side of the origin flaw facing the core center, and the initial spreading direction of the fracture is into the central core region (figures 105, 106).

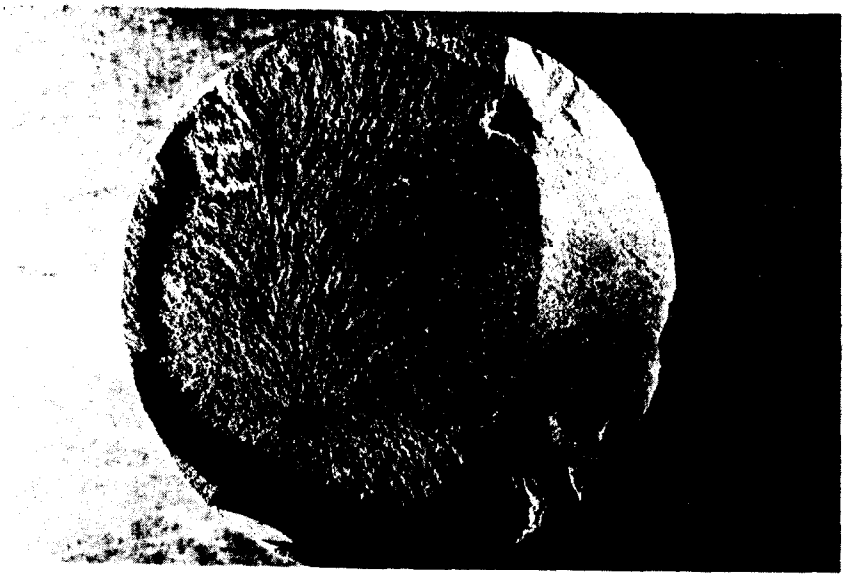

Figure 104, circumferential hook toward the core boundary that extends almost entirely around the core. A lingula brachiopod acted as the origin flaw. Hackle plumes radiate from the origin to meet an arrest line and core boundary orthogonally. Note that hackle and the arrest line are continuous across the tendential trace of an experimentally induced fracture through the approximate core center.

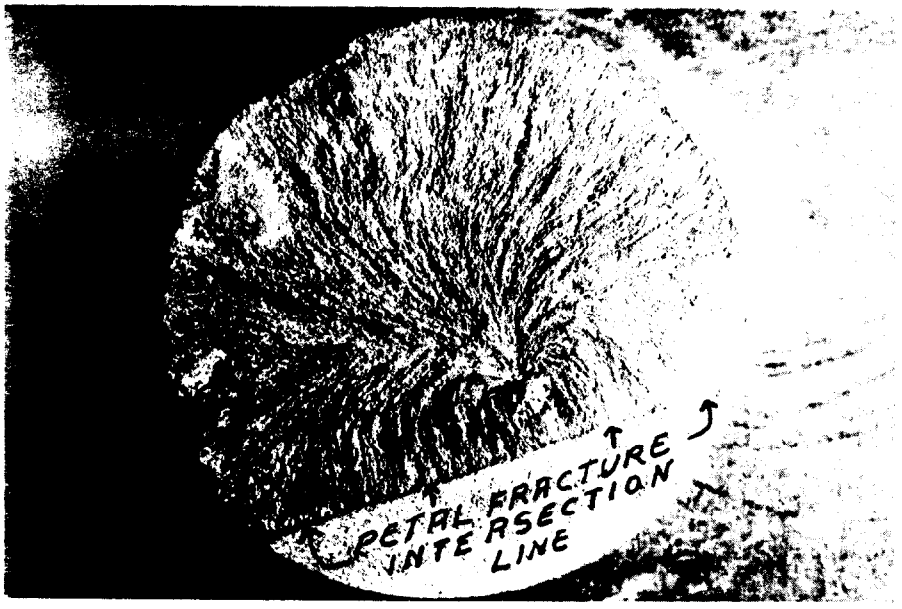

Figure 105, pyrite nodule that served as a disc fracture origin flaw. Hackle radiates from the origin and curves to meet the core boundary and earlier-formed petal fracture (see next section) intersection line orthogonally. Hackle pattern about the origin indicates that tensile stresses peaked at the nodule boundary that faced the core center at time of fracturing.

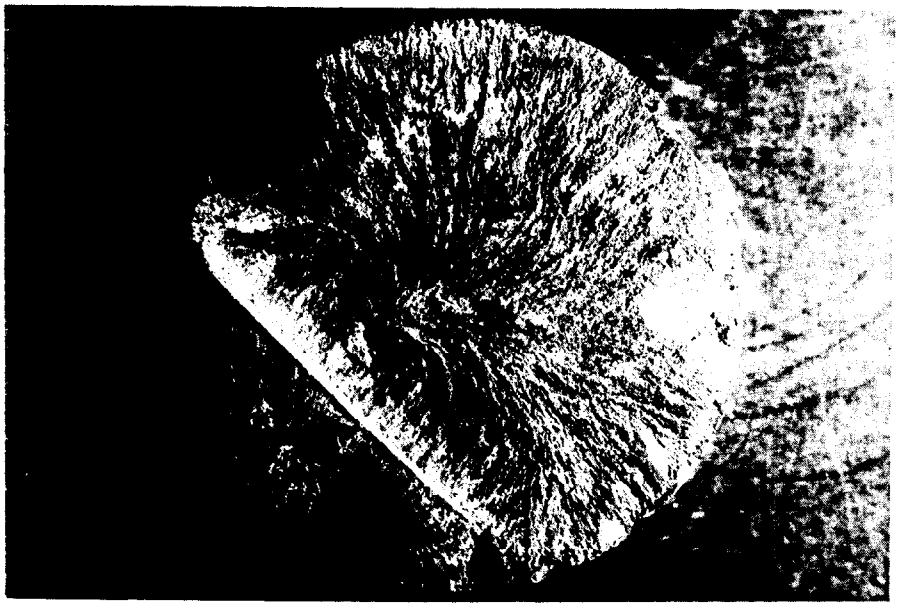

Figure 106, separate origin points on two disc fractures. Hackle plumes radiate from both origins to intersect an earlier-formed petal-centerline fracture and the core boundary orthogonally. The hackle pattern about the origin on the larger fracture indicates that stresses peaked, and the fracture began, at the nodule boundary facing the core interior.

Additional evidence for the presence of high interior core stress differences is indicated by relative disc fracture velocities. Relative fracture spreading velocities increase toward the core center and decrease at the core margin, perhaps in response to an increase and decrease in tensile stress toward these regions. Figure 107, drawn from an actual disc fracture surface, depicts this proposed relative velocity relationship. Lines constructed perpendicular to hackle show the fracture front at successive times during fracture growth. These lines diverge in the core center and converge along the core margin, thereby supporting the propounded fracture velocity relationship. Arrest lines, where present on a disc fracture, verify this construction. Obviously the fracture will initiate at the largest, properly shaped, and best situated origin flaw. This flaw is not always located toward the core center and may be located at the core boundary.

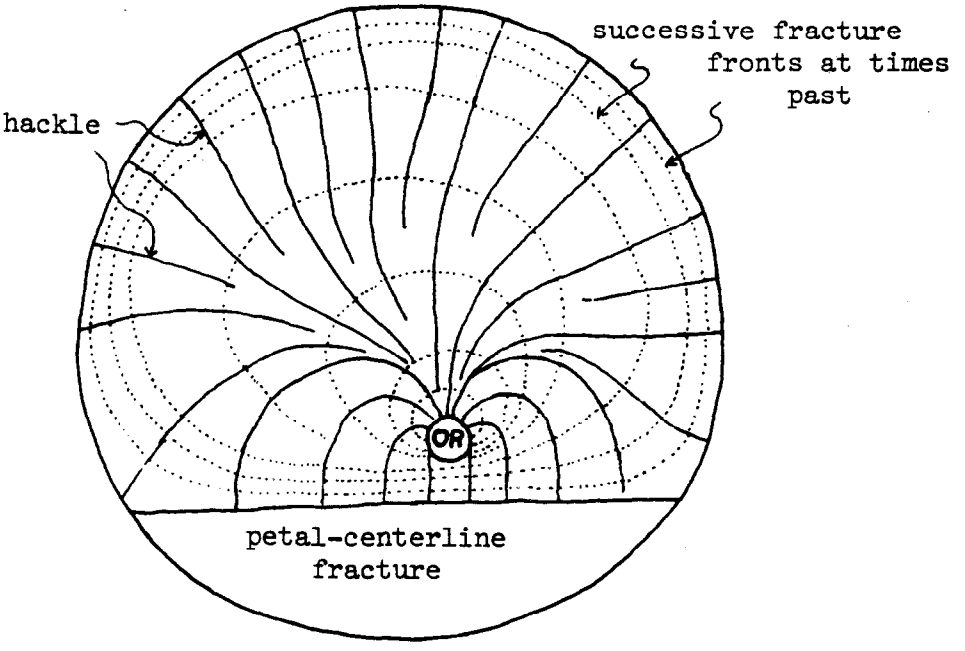

Figure 107, diagram of a disc fracture surface showing hackle relationship to constructed successive fracture fronts at times past. Distance between dotted fracture front lines becomes greater where fracture velocity increased. "OR" marks the fracture origin. See figure 37a through f.

It is believed that most disc fractures form in the space between the drill bit and the scriber blades located within the core barrel and used to incise orientation grooves. Hackle marks generally curve to meet the pre-existing core boundary orthogonally, and the fracture plane often hooks into the core boundary. However, disc fracture-core boundary intersections can be chipped and scalloped indicating some may have formed immediately before the bit. Formations of disc fractures before the scriber is indicated by the fact that the passage of the scriber often plucks a small chip from the upper pre-existing disc fracture face and gouges the lower face. Also, no disc fracture origins were found at the induced scriber flaw as would likely be the case if the scribe mark existed before the disc fracture. However, all disc fractures may not completely form before the scriber. Stored strain energy in any core section might be relased anywhere in the core barrel, perhaps aided by vibrations and impact shocks. Finally, all centrally located origins on disc fractures cannot be attributed to cross bending because, as previously mentioned, disc fractures occasionally possess small core boundary hooks that extend one-half to three-quarters of the distance around the circumference. Likewise, peripherally located origins not showing a shatter zone in many cases cannot be attributed to a sharp blow.

Occasionally, several disc fractures will originate, most likely at the same time, in close proximity to each other. Generally, only one will pass entirely through the core, thereby dissipating tensile stresses and arresting the progress of any nearby fracture. However, if a pre-existing vertical fracture serves as a free surface, two closely spaced disc fractures, at slightly different levels, on either side of the vertical fracture may be necessary to relieve the tensile stress (figure 106).

Petal-centerline fractures

Vertical and inclined sections of petal-centerline fractures form in response to a core-induced principal tension that rotates downward in a vertical plane from an inclined orientation to horizontal. The petal section of these fractures is that portion that curves in a downcore direction from a dip angle generally between 30° and 75° at the core boundary to a vertical inclination within the core and parallel to the core axis. The petal fracture may occur without the centerline section. However, the centerline fracture must develop from a pre-existing petal section. A petal-centerline fracture, where both portions exist, is continuous and attributed to a single fracture event.

Petal-centerline fractures are generally smooth, curviplanar to planar and, if continuous for any length (seldom over several feet in the Nicholas Combs well), curve in a downcore direction to a vertical inclination while maintaining a constant strike. Frequencies of one inclined petal fracture per inch of core length are not uncommon (figure 108). However, only one vertical centerline fracture is necessary to relieve horizontal tensile stresses and complete separation in any small volume of rock. Incipient petal fractures can exist alongside a centerline fracture indicating that stresses initiating the petal fracture are affected by only a small component of any existing horizontal in situ stress. No petal-centerline fractures were seen to cut entirely across the core. The centerline fracture section simply ceases to propagate downcore and terminates within the core or at a pre-existing

fracture. It would be expected that a downward propagating centerline fracture would terminate if the drill encountered an uncemented vertical natural fracture. Under these circumstances any stress release would simply separate the natural fracture. Petal-centerline fractures can transect natural fractures if the latter are recemented by secondary mineral matter. It follows that several vertical fractures side by side, without symmetrical arrest lines, and perhaps hooking into one another, are most likely natural fractures.

Downward propagating centerline fractures should not be expected to curve outward in a downcore direction away from the line of core advance unless an altered stress configuration is encountered. Therefore, any join completing the fracture separation with juxtaposed petal-centerline fractures or from petal-centerline to core boundary is generally a post-core event that spreads from the terminal front of the centerline fracture to the outer core or to a pre-existing fracture (figure 109). The later-forming petal or core boundary join is usually without symmetrical arrest lines. If a petal fracture consistently curves to meet an immediately adjacent lower petal fracture or the core boundary, a scalloped core section results (figure 110). Scallops can occur singly or in a group.

Figure 108, closely spaced petal fractures (frequency = 1 fracture/2 inches) that have inhibited the development of the centerline fracture section. Downcore direction is to the right.

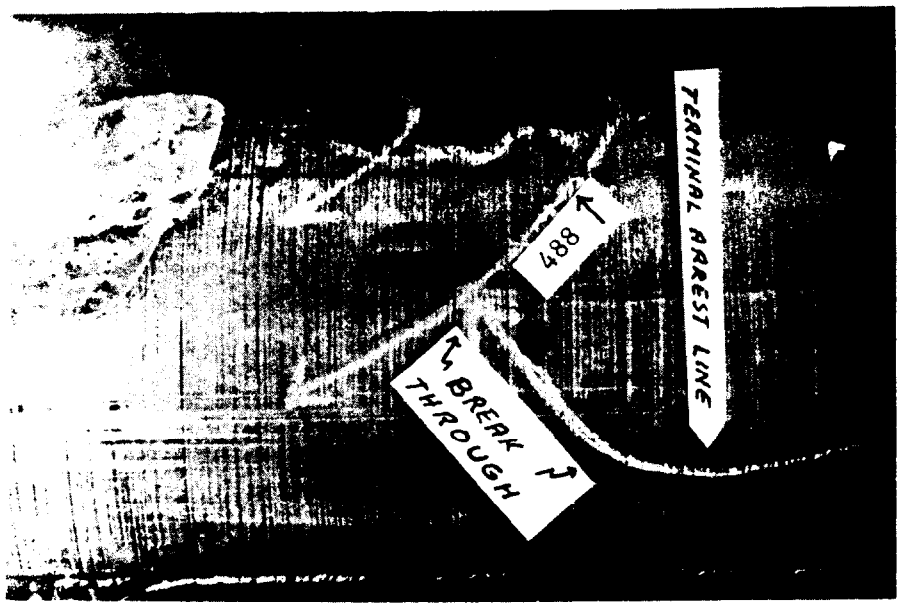

Figure 109a, tendential view of the apparent intersection of two petal-centerline fractures. The chalked lines highlight the fracture traces. Arrows point in the direction of fracture propagation. The fracture intersection gives the unfortunate impression that fracture 488 formed first.

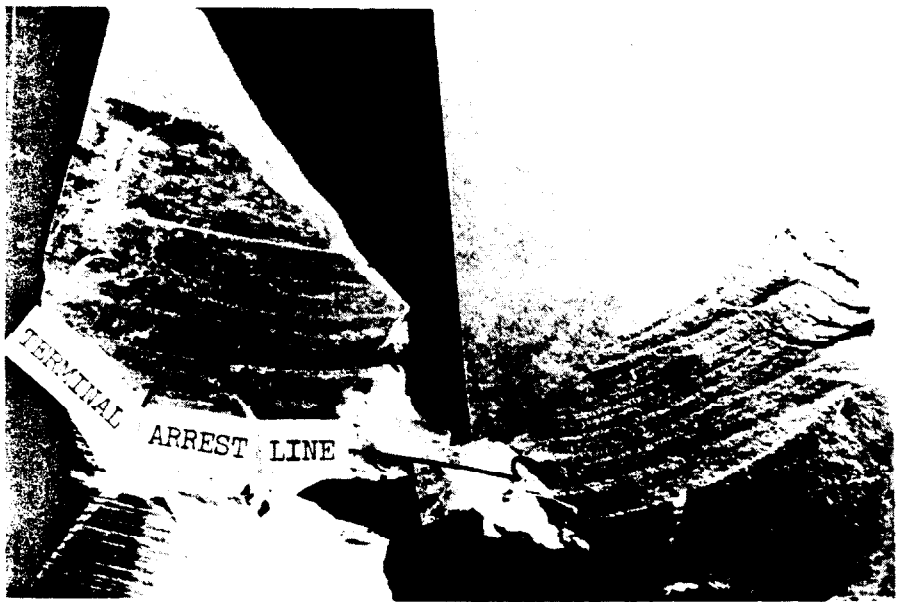

Figure 109b, fracture abutting orthogonally against 488 separated from the core, thus exposing transient features. An absence of arrest lines on the join between the two surfaces shows it did not form during drilling. Note the sharp terminal arrest line marking the lower boundary of the petal-centerline fracture. Therefore the vertical petal-centerline fracture formed first, the inclined petal 4ôô formed second and the breakthrough from the terminal centerline fracture arrest line to 488 formed last.

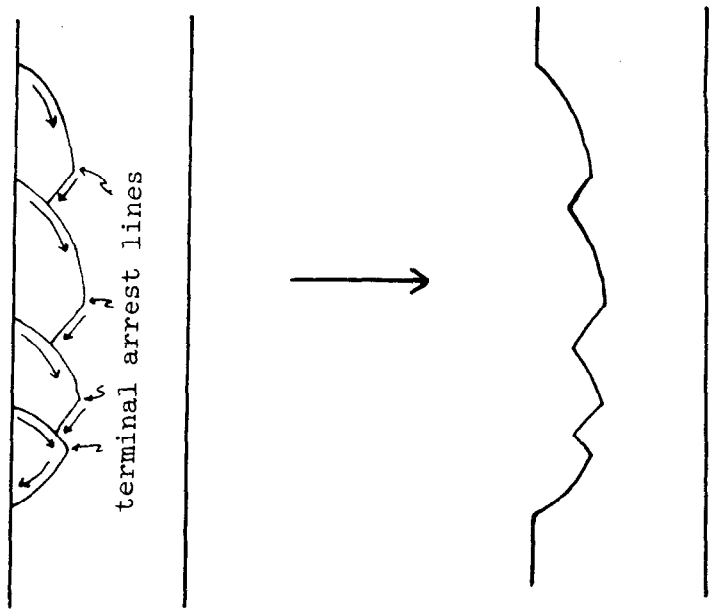

Figure 110, petal sections of petal centerline fractures breaking through downcore from terminal arrest lines to produce a scalloped core section. Arrows indicate directions of fracture propagation.

The exact origin is rarely discernible on petal-centerline fractures. However, the origin area is always located near the uppermost (upcore) inclined section of the fracture surface in proximity to the core boundary. It is likely that those origins formed below the cutting edge of the drill bit and have been subsequently drilled away. The origin may rarely be associated with a large pre-existing flaw on the subsequently drilled core face.

Closely spaced arrest lines (approximately four per centimeter megascopically) are common and are arranged in a symmetrical fashion about the fracture origin location (figure 111). The closely spaced arrest lines indicate a slow propagation rate of a fracture that developed during drilling. The arrest lines are convex in a downcore direction, and symmetrical about an imaginary vertical line bisecting the fracture face. These arrest lines always lead downcore in the fracture face center, and possess a constant curvature radius of approximately six inches (15.2 cm). Cyclic variations in drill stem rotation, bit pressure, and vibrations produced by drilling caused the tensile stress across the developing fracture plane to vary in direction and magnitude. This would cause the fracture to move forward in steps, thus producing the symmetry and uniform frequency of the arrest ridges visible on the majority of petal-centerline fractures. These well-defined cusped features must never be interpreted as Wallner lines. Several sets of symmetrical Wallner lines, convex downcore, and intersecting along the fracture center, would be evident if generated by sonic waves originating behind the fracture front at pre-existing circumferential core boundary flaws (assuming erroneously that they formed behind the bit). In addition, Wallner lines on a continuously advancing front, if caused by sonic vibrations, would not possess the observed constant radius of curvature.

Hackle marks diverge downcore symmetrically about the center of the petal-centerline fracture, and maintain an orthogonal relationship with arrest lines. However, only rarely does the hackle meet the later-formed core boundary orthogonally, because here again the hackle propagated before the drill and has been cored through. The vertical fracture faces can, in some core sections, be traced upward from their terminal arrest lines continuously through the inclined section to the core boundary and probable vicinity of the fracture origin.

The transient and tendential features described show that petal-centerline fractures are core-induced. The closely spaced symmetrical arrest lines with a nearly constant radius of curvature, plus symmetrically diverging hackle that seldom meets the core boundary orthogonally, mandate that petal-centerline fractures formed during coring. They originated at or near the cutting edge of the drill and propagated downward before the advancing bit. The fracture cut diagonally downward into the area yet to be drilled, thereby forming the petal. The fracture then swung to a vertical orientation in order to remain perpendicular to the principal horizontal tension and thereby developed the centerline fracture section. This situation enables the fracture to exist immediately before it was drilled through, thus explaining the superimposed conchoidal chips concentrated at the right-hand edge of the fracture caused by the later clockwise drill motion (figure 112). The absence of discrete origins and the non-orthogonal hackle-core boundary relationship is also explained. A fracture curving away from the line of core advance, would be impossible to detect. Arrest lines indicate that petal-centerline fractures did not propagate smoothly, but grew in small increments below the bit. Because these fractures originated immediately before drilling, they should be present in the core hole wall. Any subsequent rubber impaction cast of the core hole should detect these fractures. The penetrative trace of these fractures on the core wall might be saw-toothed because of spreading twist hackle or sharply cusped arrest lines.

Well-defined but changing mean strike directions for petal-centerline fractures in the Nicholas Combs well, indicate that these fractures may follow some regional incipient fracture directions or other poorly developed rock anisotropy. Petal-centerline fracture propagation also could have been influenced by nonlithostatic stored strain energy released by drilling. Deviatoric stresses from both causes could be affected by excessive pore pressure. It seems reasonable to assume that preferentially oriented petal-centerline fractures may provide valuable information on rock anisotropies and in situ stresses throughout the drilled column.

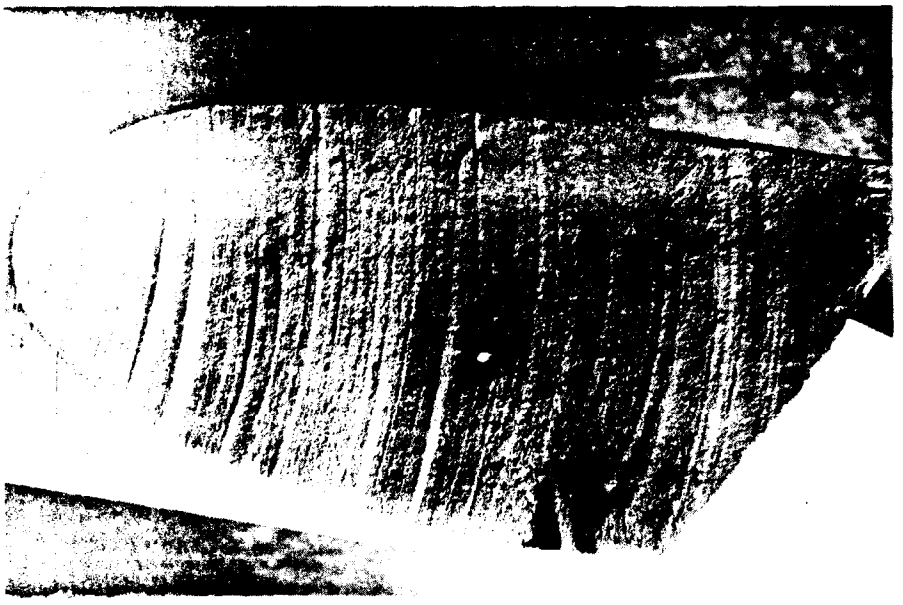

Figure 111, symmetrical circular arrest lines (note sharp ridges), convex downcore, and fine hackle plume - coarse twist hackle diverging downcore on a petal-centerline fracture.

Figure 112, symmetrical circular arrest lines, convex downcore, and fine hackle plumes - coarse twist hackle diverging downcore on a petal-centerline fracture surface. The fracture propagated in the direction of arrest line convexity. Note conchoidal chips preferentially located along the right-hand intersection of the fracture with the core boundary.

A fracture similar in many respects to the core-induced petal-centerline fracture has been observed in drilled and blasted road cuts through Devonian shales of western New York (figure 113). The road cut fractures originated and propagated immediately before the bit and were subsequently drilled through. These fractures possess symmetrical, closely spaced, convex downcore arrest lines and diverging hackle. The fractures are generally elliptically shaped with a long axis averaging one foot in diameter. The fractures form an angle of approximately 30° with the core axis where they first enter the drilled area, and tend to curve downward in an attempt to become parallel to the inclined drill axis. The fractures generally became inclined to an approximate vertical orientation and, therefore, cut entirely across the inclined drilled diameter. Where observed, the road cut drill-induced fractures have a preferred orientation parallel to vertical regional systematic fractures observed by Parker (1942) throughout western New York. If a detailed study proved this relationship to be regionally consistent, it could be interpreted to support an argument for the influence of directional rock anisotropies.

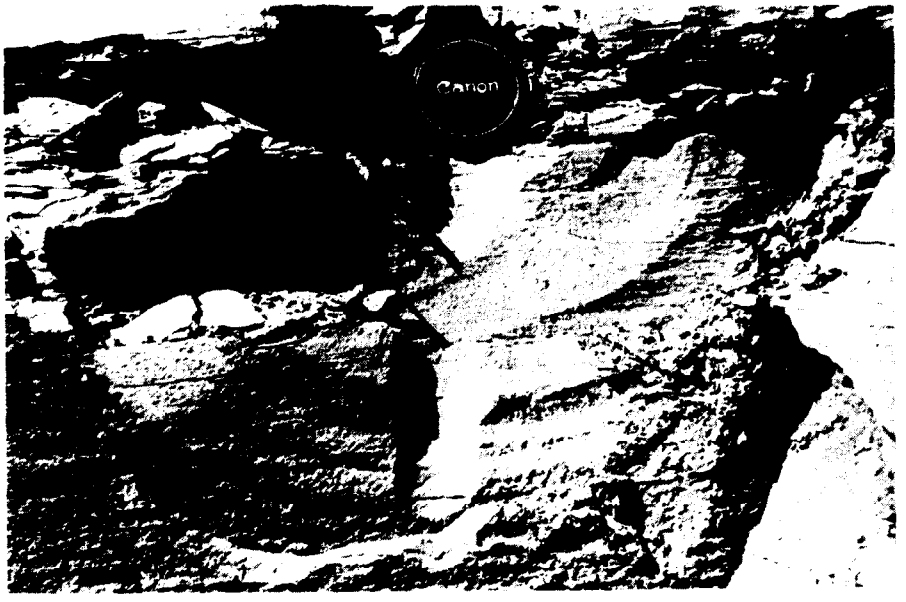

Figure 113, road cut fracture in Devonian sandstone, New York, that originated and propagated immediately before the drill bit. The fracture was subsequently drilled through. The drilled section would possess symmetrical arrest lines convex downcore and hackle diverging in a downcore direction.

In summary, all petal-centerline fractures are coring-induced and formed below the drill bit. Most possess symmetrical arrest lines indicating that they formed during drilling. All fractures in this category possessed hackle that diverged symmetrically downcore. Arrest lines and hackle indicate an upcore to downcore propagation direction. Several vertical fractures in the Nicholas Combs well possessing unusually smooth and planar fracture faces were marked solely by downcore diverging fine hackle that did not meet the core boundary orthogonally. Arrest lines were not observed on these faces even though they cut diagonally into the core in the same fashion as other petal-centerline fractures. The authors are inclined to believe that these fractures are coring-induced also.

Torsional fractures

Torsional fractures propagate in direct response to a torsion-induced stress. These torsion stresses can be viewed as simple shear and are generated behind the bit but generally before the scribing knives. The simple shear stresses acting on the core can be resolved into tensile stresses acting perpendicularly to any given 45° helical line along the core boundary (pure shear, figure 114). Compressive stresses act orthogonally to the tensile stress direction and parallel to the helical line.

Generally, torsional fractures originate on or in close proximity to the core exterior and penetrate into the interior toward the core axis. The resulting fracture surface can be approximately traced by an imaginary line penetrating the core exterior and fixed at the core axis. The line can be pictured as spiraling along the 45° helical trace at the core exterior (figures 114, 115). The torsion fracture will separate the core as the line, and related surface (fracture) generated by the line, approach the vertical and approximate parallelism with the core axis. A fracture similar in every respect to the coring-induced torsion fracture can be produced by twisting a piece of chalk.

Torsion fractures, after initiation, generally spread in up and down core directions defining the 45° helix. As the fracture spreads in the described surface it also penetrates towards the core axis. Fracture progress can be traced in shale cores by well-developed twist hackle and hackle plumes. Arrest lines are also common on these fracture surfaces.

The helical tendential trace of torsion fractures at the cylindrical core surfact permits their detection with little difficulty. On cores where the torsional fracture is poorly developed the following simple test may prove helpful. Place fragments of the fractured core together and twist clockwise and counterclockwise in an attempt to slide the fractured pieces along the major surface of disruption. If the canted or otherwise irregular fracture was formed by torsion, the pieces will generally slide much more easily in one direction than in another.

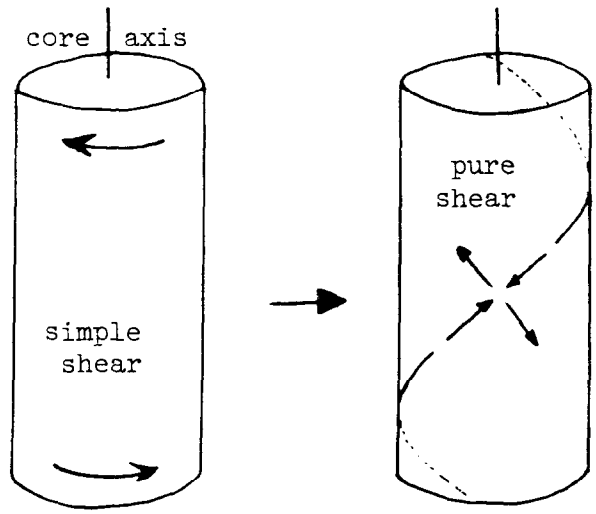

Figure 114, resolution of simple shear stresses produced by torsion into the compressive and tensile stresses responsible for torsion fractures. A torsion fracture in this hypothetical case would most likely initiate near the core boundary and propagate up and down core with its tendential trace forming the helical line perpendicular to the principal tension.

Figure 115, torsion fracture that originated at a centerline fracture face and spread toward the cylindrical core boundary.

Knife edge spall

The knife edge spall is a coring-induced fracture that is directly related to tensile stresses produced by the knives used to scribe orientation lines along the core perimeter. The initial fracture bounding the upcore margin of each spall is driven immediately before the knife, angling down and toward the core interior. As the knife continues to advance, the fracture may break abruptly to the core exterior along a planar fracture or bedding plane. A thin wedge-like fragment is thereby separated from the core leaving a notch concave in a downcore direction (figure 116). The concavity of the upper fracture bounding the notch is enhanced by the curvature of the cylindrical core wall. Where bedding anisotropies are not utilized to complete separation of the wedge shaped spall, the spall may form a broad shallow chip. The fracture separating the thin chip spreads downcore from the initial fracture, parallels the core axis, and then hooks abruptly to the core boundary. The chip boundary is, in this case, convex both up and downcore. However, hackle marks show that the fracture that creates the chip always spreads in a downcore direction. The hackle and lower chip boundary (convex downcore) are in turn scribed by the knife. The concave relationship of knife edge spalls can be used to determine the downcore direction for any core section containing them, regardless of the size of the spall itself.

Occasionally the initial fracture, that bounds a knife edge spall, may be driven quite deep (several centimeters) into the core interior. In this case it may resemble a petal fracture. However, the symmetrical relationship of the spall to the knife groove permits the proper identification of the fracture.

Knife edge spalls are very useful for determining fracturing sequence and approximate location of formation of coring-induced fractures. Any coring-induced fracture that is chipped by a knife edge spall must have formed before the core section passed the scriber (figure 118). Obviously any uncemented core fracture may be scalloped by a knife edge spall (figure 117).

Knife edge spalls resemble a series of chatter marks or more randomly oriented and singly-occurring lunate fractures commonly found on bedrock in glacial terrain.

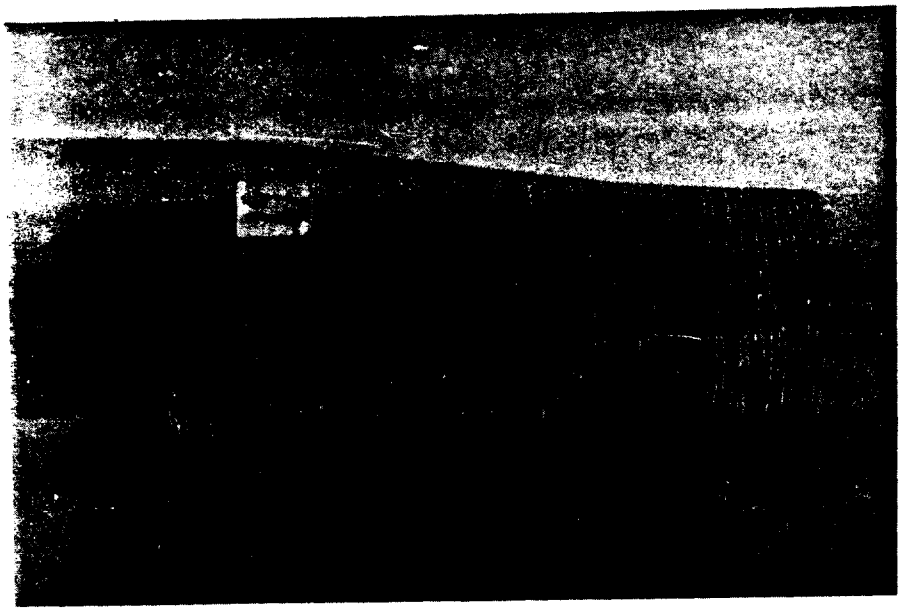

Figure 116, knife-edge spalls, concave downcore, formed around a scribe orientation line.

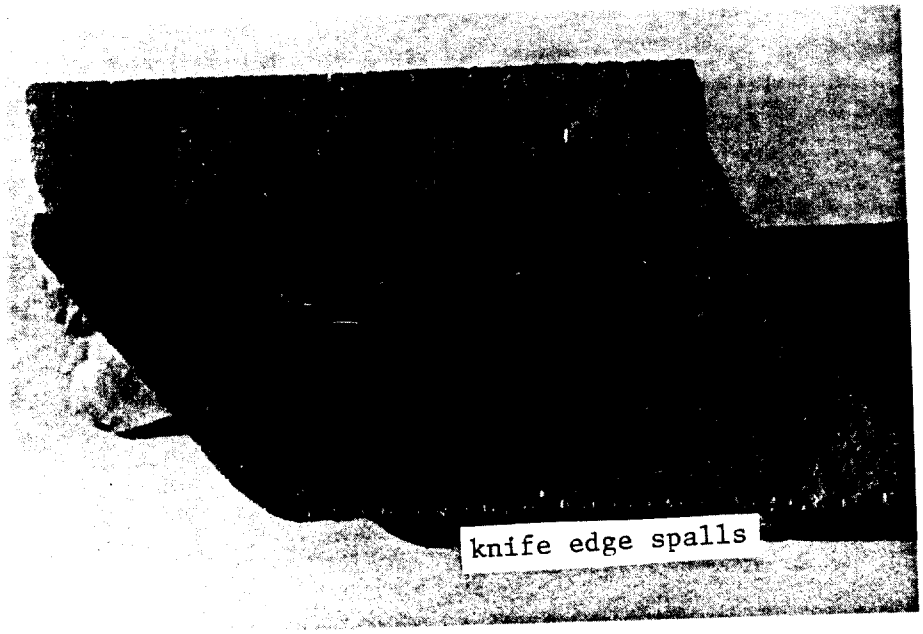

Figure 117, a coring-induced centerline fracture that has been chipped by knife edge spalls.

Figure 118, artificially-induced knife-edge spalls produced on a glass slide by dragging a file point from photo top to bottom. The moving file formed a conchoidal chip, originating at the upper surface of a pre-existing horizontal fracture. This chip is analogous to the chips formed on the upper surfaces of disc fractures by the scribing knife. Note the shattered compression zone on the bottom surface of the pre-existing fracture. Optical photomicrograph, 10X magnification.

Handling-induced fractures

Handling-induced fractures are those induced during or after removal of the core from the core barrel. These fractures are almost always caused by impact or cross bending. For example, a hammer may be used to break core sections into lengths suitable for sample boxes. A core may be dropped, resulting in both impact and cross bending. A core section might also be subjected to cross bending during removal from the core barrel.

Regardless of the method by which a post-core fracture is initiated, it should, in most cases, possess a distinctive surface morphology. A fracture generated by impact will have a powder or shatter zone on its outer circumference. The fracture origin need not coincide with the shatter zone and may in fact lie at the opposite side of the core fracture surface. In addition, the fracture may be located at some distance up or downcore from the impact point. A powder zone would not be obvious in this case. If all potential origin flaws in the vicinity of impact are small and properly oriented, a high impact stress is needed to cause failure within that vicinity. This situation may cause the core to break at another location. A higher initiation stress produces elevated fracture velocities and the resulting surface will tend to be rough and irregular. This irregular surface is readily apparent on fractures induced by experimental loading. Only a light tap is needed if the origin flaw is large. The low stress to failure, less chaotic vibratory

stresses, and slower propagation velocity, will produce a fracture that will be smooth and planar. In fact, an excellent procedure to induce a well-placed and smooth fracture would be to scribe a deep flaw with a rough file on the core circumference and then strike the core on the opposite side with a hammer.

A fracture initiated by cross bending has a tendency to hook into the surface opposite its origin point, especially if the stress to failure is high. Here again this type fracture is generally rough and irregular. The oftentimes high stress needed to initiate failure during point or directional loading perpendicular to bedding often causes the induced fracture to fork. A handling-induced core fracture will abut against all other coring-induced and uncemented natural fractures. Also, handling-induced fractures will not be chipped by the scriber or drill bit.

Summary of naturally-induced, coring-induced and handling-induced fracture characteristics

A summary of fractographic morphological features characteristic of natural, core-induced, and handling-induced fractures is given below. Transient and tendential features characteristic of the different fractures are listed under the appropriate category. It should be expected that many of the fracture features will be found on more than one type of fracture. The reader is referred to the previous chapter for more detailed discussion of each listed characteristic.

Natural fracture characteristics

1. Polished and slickensided fracture faces (almost always smooth and planar). Circular slickenlines caused by abrasion of rotating core sections are excluded.

2. Fractures filled by fibrous or non-fibrous secondary mineral matter.

3. Smooth fractures showing no hooking, especially those of high inclination, that extend entirely across the core and against which later fractures terminate. (Here it must be remembered that post core or disc fractures may abut petal-centerline fractures.)

4. Inclined to vertical fracture faces displaying small, often conchoidal chips at the fracture - drilled core boundary intersection. The chips curve to meet the inclined fracture orthogonally. Chips are preferentially located along the right hand edge of the fracture face at the core boundary (fracture face toward observer, downcore direction pointed down).

5. Conchoidal chips originating at the scribe mark and curving to meet a pre-existing fracture face orthogonally may indicate the pre-existing fracture face is natural.

6. Outsize transient markings and/or twist and inclusion hackle that do not curve to meet the core boundary orthogonally.

7. Several parallel to subparallel vertical or inclined fractures passing completely through the core.

8. Suspected natural core fractures that possess the same attitude as surface fractures measured at outcrops of similar lithology.

9. General lack of any diagnostic symmetrical correlation between fractographic markings, coring methods, and core geometry.

Coring-induced fracture characteristics

1. A fracture origin along or immediately outside the core circumference or within the core itself (it is highly unlikely that the drill would consistently capture the origins of natural fractures).

2. Hackle diverging to meet the core boundary or pre-existing fracture surface orthogonally (as on a horizontal disc fracture).

3. Inclusion and twist hackle becoming more coarse with the hackle steps increasing in relief in the immediate vicinity of an orthogonal join with the core boundary or pre-existing fracture surface (as on horizontal disc fractures).

4. Hackle marks on petal-centerline fractures that diverge downcore symmetrically about an imaginary line down the fracture center.

5. Closely spaced arrest lines with constant radii of curvature on petal-centerline fractures that are convex downcore and symmetrical about an imaginary line down the fracture surface center.

6. Any Wallner or arrest line megascopically possessing a smaller or only slightly larger radius of curvature than the diameter of the core.

7. Any Wallner or arrest line that megascopically undergoes an abrupt curvature change within the core; for example, an arrest line may curve to become tangent to the core boundary.

8. Fractures that hook abruptly towards the core boundary or a previously existing fracture surface, especially if the hook extends more than halfway around the core circumference.

9. Conchoidal chips originating at the scribe mark and curving to meet a pre-existing fracture face orthogonally.

10. Inclined to vertical fracture faces displaying small, often conchoidal chips at the fracture-drilled core boundary intersection. The chips curve to meet the inclined fracture orthogonally. Chips are preferentially located along the right-hand edge of the fracture face at the core boundary.

11. Vertical fractures consistently cutting the central cored region.

Handling-induced fracture characteristics

1. A powder zone at the point of impact anywhere along the outer core - fracture intersection.

2. Marked hooking at the fracture boundary - the powder zone may be on the same side of the core as the hook.

3. An unusually rough fracture surface (as compared to natural and coring-induced fractures).

4. Fractures that fork into the core boundary opposite the origin (generally displaying a rough fracture surface).

BIBLIOGRAPHY

Badgley, P.C., 1965, Structural and tectonic principles: New York, Harper and Row, 521 p.

Balk, R., 1937, Structural behavior of igneous rocks: Geol. Soc. America Memoir 5, 177 p.

Bankwitz, P., 1965, Über Klufte, beobachtungen im Thurinischen Schiefergebirge: Geologie, v. 14, p. 242-253.

Bankwitz, P., 1966, Über Klufte, II: Geologie, v. 15, p. 896-941.

Bieniawski, Z.T., 1966, Mechanism of rock fracture in compression: Report of the South African Council of Scientific and Industrial Research, No. MEG 459.

Bieniawski, Z.T., 1967, Mechanism of brittle fracture of rock, part I and part II: Int. J. Rock Mech. Min. Sci., v. 4, p. 395-423.

Bieniawski, Z.T., 1968, The phenomenon of terminal fracture velocity in rock: Felsmech. Ingenieurgeol., v. 6, p. 113-125.

Brace, W.F., 1964, Brittle fracture of rocks, in Judd, W.R., ed., State of stress in the earth's crust, New York, Elsevier Press, p. 110-178.

Brace, W.F., 1971, Micromechanics in rock systems, in Te'eni, M., ed., Structure, solid mechanics and engineering design, New York, John Wiley and Sons, p. 187-204.

Brace, W.F., 1972, Pore pressure in geophysics, in Heard, H.C., et al., eds., Flow and fracture of rocks, geophysical monograph 16, Amer. Geophysical Union, Washington, D.C., p. 265-273.

Cloos, E., 1955, Experimental analysis of fracture patterns, Geol. Soc. America Bull., v. 66, p. 241-256.

Cloos, E., 1968, Experimental analysis of Gulf Coast fracture patterns: Am. Assoc. Petroleum Geologists Bull., v. 52, p. 420-444.

Coble, R.L., 1958, Effect of microstructure on mechanical properties of ceramic materials, in Kingery, W.D., ed., Ceramic fabrication processes, Technical Press, Mass. Inst. Tech. and John Wiley and Sons, Ceramic Abstr., p. 123.

Congleton, J. and Petch, N.J., 1967, Crack branching: Phil. Mag., vol. 16, p. 749-760.

Coulomb, C.A., 1773, Essi sur une application des regles des maximis et minimis a quelques problemes des statique relatifs a l'architecture, Acad. Sci. Paris Mem., Pres. Divers Savante, v. 7.

Currie, J.B., and Reik, G.A., 1977, A method of distinguishing regional directions of jointing and of identifying joint sets associated with individual geologic structures: Canadian Jour. Earth Sci., v. 14, p. 1211-1228.

Dean, S.L., and Kulander, B.R., 1977, Kinematic analysis of folding and pre-fold structures on the southwestern flank of the Williamsburg anticline,, Greenbrier County, West Virginia abs : Geol. Soc. America Abs. with programs, v. 9, p. 132-133.

Dean, S.L., Kulander, B.R., and Williams, R.E., 1979 (in press), Regional tectonics, systematic fractures, and photolinears in southeastern West Virginia, in Podwysocki, M., ed., 2nd International Conf. on New Basement Tectonics, Newark, Delaware, New Basement Tectonics Comm.

Dennis, J.G., 1967, International Tectonic Dictionary, English Terminology: Am. Assoc. Petroleum Geologists Bull., Memoir 7, 196 p.

Dennis, J.G., 1972, Structural Geology: New York, Ronald Press, New York, 532 p.

Donath, F.A., 1970, Some information squeezed out of rock: American Scientist, v. 58, p. 54-72.

Durney, D.W., and Ramsay, J.G., 1973, Incremental strains measured by syntectonic crystal growths, in DeJong, Kees and Scholten, eds., Gravity and tectonics, New York, John Wiley and Sons, p. 67-96.

Evans, A.G., and Tappan, G., 1972, Effects of microstructure on the stress to propagate inherent flaws: Proc. Brit. Ceram. Soc., v. 20, p. 275-297.

Field, J.E., 1971, Brittle fracture: its study and application: Contemporary Physics, vol. 12, p. 1-31.

Erdogan, F., 1968, Crack propagation theories, in Liebowitz, H., ed., Fracture: an advanced treatise, ed. by H. Liebowitz, New York, Academic Press, p. 497-590.

Frechette, V.D., 1972, The fractology of glass, in Pye, L., et al., eds., Introduction to glass science, Plenum Press, p. 432-450.

Frechette, V.D., 1973, Initiation and propagation of fracture in ceramics, Plenary lecture, in Proceedings of the Third International Congress on Fracture, Munich, PL IX - 132.

Frechette, V.D., 1973, A replication of fracture generated surfaces: New York State College of Ceramics Instruction Manual, Alfred, New York, 4 p.

Freminville, C. de, 1914, Recherches sur la Fragilite: Rev. de Metallurgie, no. 9, p. 971-1056.

Gash, P.J.S., 1971, A study of surface features relating to brittle and semi-brittle fracture: Tectonophysics, v. 12, p. 349-391.

Gay, S.P., 1972, Aeromagnetic lineaments, their geological significance and their significance to geology: Salt Lake City, Utah, American Stereo Map Company, 94 p.

Gay, S.P., 1973, Pervasive orthogonal fracturing in earth's continental crust: Tech. Pub. #2, Salt Lake City, Utah, American Stereo Map Co., 121 p.

Griffith, A.A., 1920, The phenomena of rupture and flow in solids: Phil. Trans. Royal Soc. London, A 221, p. 163-198.

Griffith, A.A., 1925, The theory of rupture, in Proc. First Internat. Cong. Applied Mechanics, Delft, 1924, p. 55-63.

Harris, J.F., Taylor, G.L., and Walper, J.L., 1960, Relation of deformational fractures in sedimentary rocks to regional and local structures: Am. Assoc. Petroleum Geologists, v. 44, p. 1853-1973.

Hodgson, R.A., 1961, Classification of structures on joint surfaces: Am. Jour. Sci., v. 259, p. 493-502.

Hoek, E., and Bieniawski, Z.T., 1965, Brittle fracture propagation in rock under compression: Int. Jour. Fracture Mechanics, v. 1, p. 139-155.

Hutchinson, R.M., 1956, Structure and petrology of the Enchanted Rock batholith, Llano and Gillespie Counties, Texas: Geol. Soc. America Bull., v. 67, p. 763-806.

Inglis, C.E., 1913, Stresses in a plate due to the presence of cracks and sharp corners: Trans. Inst. Naval Archit., v. 55, p. 219.

Irwin, G.R., 1960, Fracture mechanics, in Goodier and Hoff, eds., Structural mechanics, New York, Pergammon Press, p. 557-592.

Jaeger, J.C., and Cook, N.G.W., 1976, Fundamentals of rock mechanics: New York, Halsted (Wiley), 2nd ed., 575 p.

Kerkhof, F., 1956, Ultrasonic fractography, in Proc. 3rd Int. Congress High-Speed Photography, London, p. 194.

Kies, J.A., Sullivan, A.M., and Irwin, G.R., 1950, Interpretation of fracture markings: Jour. Appl. Phys., v. 21, p. 716-720.

Knudsen, E.P., 1959, Dependence of mechanical strength of brittle polycrystalline specimens on porosity and grain size: Jour. American Ceram. Soc., v. 42, p. 376-387.

Kulander, B.R., and Dean, S.L., 1976, Residual gravity signature of an Appalachian transverse lineament zone abs. : Geol. Soc. America Abs. with programs, v. 8, p. 213-214.

Kulander, B.R., Dean, S.L., and Barton, C.C., 1977, Fractographic logging for determination of pre-core and core-induced fractures -- Nicholas Combs no. 7239 well, Hazard, Kentucky: U.S. ERDA MERC/CR-77/3, 44 p. (Springfield, Va., U.S. Dept. of Energy, Morgantown Energy Research Center, Natl. Tech. Inf. Service).

Kulander, B.R., Dean, S.L., Williams, R.E., 1978, Correlation between outcrop fractures, geophysics, and Rome Trough structure in Kanawha County, West Virginia, in Schott, F.L., et al., eds., 1st Eastern Gas Shales Symposium Proc. Morgantown, W. Va., p. 484-495. (Springfield, Va., U.S. Dept. of Energy, Morgantown Energy Research Center, Natl. Tech. Inf. Service).

Lawn, B.R., and Wilshaw, T.R., 1975, Fracture of brittle solids: Cambridge Univ. Press, 197 p.

Love, A.E.H., 1920, A treatise on the mathematical theory of elasticity: Cambridge Univ. Press, 3rd ed., 619 p.

McClintock, F.A., and Walsh, J., 1963, Friction on Griffith cracks in rocks under pressure, in Proc. 4th U.S. Congress on Applied Mechanics, Am. Soc. of Mech. Eng., New York, p. 1015-1021.

Mohr, O., 1882, Uber die Darstellung des Spannungzustandes eines Korpelmentes: Zwil Ingenieure, v. 28, p. 113-156.

Mott, N.F., 1948, Brittle fracture in mild steel plates, Engineering, p. 16-18.

Murgatroyd, J.B., 1942, The significance of surface marks on fractured glass: Jour. Soc. Glass Tech., v. 26, 155T, p. 155-171.

Nickelsen, R.P., and Hough, V.D., 1967, Jointing in the Appalachian Plateau of Pennsylvania: Geol. Soc. America Bull., v. 78, p. 609-629.

Nickelsen, R.P., 1976, Early jointing and cumulative fracture patterns, in Hodgson, R.A., et al., eds., Proc. of the 1st International Conference on the New Basement Tectonics, Salt Lake City, Utah Geol. Assoc., publication no. 5, p. 193-199.

Orowan, E., 1949, Fracture and the strength of solids: Rept. Progr. Phys., v. 12, p. 185-232.

Parker, J.M., III, 1942, Regional systematic jointing in slightly deformed sedimentary rocks: Geol. Soc. America Bull., v. 53, p. 381-408.

Petch, N.J., 1954, Fracture in metals, in Chalmers, B., ed., Progress in metal physics, v. 5, New York, Interscience Publishers, Inc., p. 1-53.

Plicka, M., 1976, Observations on joint zones in Moravia, Czechoslovakia, 1974, in Hodgson, R.A., et al., eds., Proc. of the First International Conference on the New Basement Tectonics, Salt Lake City, Utah Geol. Assoc., publication no. 5, p. 193-199.

Poncelet, E.F., 1958, The markings on fracture surfaces: Jour. Soc. Glass Tech., v. 42, p. 279T-288T.

Poncelet, E.F., 1965, Modern concepts of fracture and flaw: Poulter Research Laboratories technical report 002-65, 160 p.

Preston, F.W., 1926, A study of the rupture of glass: Jour. Soc. Glass Tech., v. 10, p. 234-269.

Preston, F.W., 1935, Angle of forking of glass cracks as an indicator of the stress system, Jour. American Ceram. Soc., v. 18, p. 175-176.

Preston, F.W., 1939, Bottle breakage - causes and types of fractures: Bull. Amer. Ceram. Soc., v. 18, p. 35-60.

Price, N.J., 1959, Mechanics of jointing in rocks: Geol. Mag. v. XCVI, p. 149-167.

Price, N.J., 1966, Fault and joint development: Oxford, Pergamon Press, 176 p.

Pugh, S.F., 1967, The fracture of brittle materials: Brit. Jour. Appal. Phys., v. 18, p. 129.

Reches, Z., 1976, Analysis of joints in two monoclines in Israel: Geol. Soc. Amer. Bull., v. 87, p. 1654-1662.

Roberts, J.C., 1961, Feather-fracture and the mechanics of rock jointing: Am. Jour. Sci., v. 259, p. 481-492.

Schardin, H., 1959, Velocity effects in fracture, in Averbach, B.L., et al., eds., Fracture, New York, John Wiley and Sons, p. 297-329.

Secor, D.J. Jr., 1965, Role of fluid pressure in jointing: Am. Jour. Sci., v. 263, p. 633-646.

Secor, D.J. Jr., 1969, Mechanics of natural extension fracturing at depth in the earth's crust, in Research in tectonics, Geol. Surv. Canada Paper 68-52, p. 3-47.

Shand, E.B., 1954, Experimental study of fracture of glass: I., The fracture Process: Jour. Am. Ceram. Soc., v. 37, p. 52-60.

Shand, E.B., 1959, Breaking strength of glass determined from dimensions of fracture mirrors: Jour. Am. Ceram. Soc., v. 42, p. 474-477.

Shand, E.B., 1967, Weakening defects in glass: Am. Ceram. Soc. Bull., v. 46, p. 1111-1115.

Snowden, W.E., 1976, Crack growth in glass subjected to controlled impacts Ph.D. thesis : Univ. of California, Berkeley, Lawrence Berkeley Laboratory, LBL-5752.

Stearns, D.W., 1964, Macrofracture patterns on Teton anticline, northwest Montana abs : Am. Geophys. Union Trans., v. 45, p. 107-108.

Stearns, D.W., 1968, Certain aspects of fracture in naturally deformed rocks, in Riecker, R.E., ed., Rock Mechanics Seminar, v. I, special rept. pub. by Terrestrial Sciences Lab. Air Force Cambridge Research Labs., Bedford, Mass, p. 97-116.

Terao, N., 1953, Relation between resistance to rupture and mirror surface of glass: Jour. Phys. Soc. Japan, v. 8, p. 545-549.

Wallner, H., 1939, Linienstrukturen an Bruchflachen: Z. Physik, v. 114, p. 368-378.

Woodworth, J.B., 1896, On the fracture system of joints, with remarks on certain great fractures: Boston Soc. Nat.History Proc., v. 27, p. 163-184.

APPENDIX I

$$\frac{V_F}{V_S} = \frac{00'}{0P} = \frac{\cos\alpha}{\cos\phi} \; ; \frac{00'}{0P'} = \frac{\cos\beta}{\cos\psi}$$

N.B. $\cos\alpha = \cos(\omega-\beta)$

$$\frac{V_F}{V_S} = \frac{\cos(\omega-\beta)}{\cos\phi} = \frac{\cos\beta}{\cos\psi}$$

$$\frac{\cos(\omega-\beta)}{\cos\phi} = \frac{\cos\beta}{\cos\psi}$$

N.B. $\sin x \sin y + \cos x \cos y = \cos(x-y)$

$$\sin\omega\sin\beta+\cos\omega\cos\beta = \cos\beta\,\frac{\cos\phi}{\cos\psi}$$

N.B. $\sin x = (1-\cos^2 x)^{\frac{1}{2}}$

$$\sin\omega(1-\cos^2\beta)^{\frac{1}{2}} = \cos\beta\left[\frac{\cos\phi-\cos\psi\cos\omega}{\cos\psi}\right]$$

$$\sin^2\omega(1-\cos^2\beta) = \cos^2\beta\left[\frac{\cos\phi-\cos\psi\cos\omega}{\cos\psi}\right]^2$$

$$\sin^2\omega = \sin^2\omega\cos^2\beta + \cos^2\beta\left[\frac{\cos\phi-\cos\psi\cos\omega}{\cos\psi}\right]^2$$

$$\frac{\sin^2\omega}{\cos^2\beta} = \sin^2\omega + \left[\frac{\cos\phi-\cos\psi\cos\omega}{\cos\psi}\right]^2$$

$$\frac{1}{\cos^2\beta} = \frac{\sin^2\omega + \left[\dfrac{\cos\phi-\cos\psi\cos\omega}{\cos\psi}\right]^2}{\sin^2\omega}$$

$$\cos^2\beta = \frac{\sin^2\omega}{\sin^2\omega + \left[\frac{\cos\phi - \cos\psi\cos\omega}{\cos\psi}\right]^2}$$

$$\cos\beta = \frac{\sin\omega}{\left[\sin^2\omega + \left[\frac{\cos\phi - \cos\psi\cos\omega}{\cos\psi}\right]^2\right]^{\frac{1}{2}}} \leftarrow \text{Expand}$$

$$\cos\beta = \frac{\sin\omega}{\left[\frac{\sin^2\omega\cos^2\psi}{\cos^2\psi} + \frac{\cos^2\phi - 2\cos\phi\cos\psi\cos\omega + \cos^2\psi\cos^2\omega}{\cos^2\psi}\right]^{\frac{1}{2}}}$$

N.B. $\sin^2 x = 1 - \cos^2 x$

$$\cos\beta = \frac{\sin\omega}{\left[\frac{\cos^2\psi(1-\cos^2\omega) + \cos^2\phi + \cos^2\psi\cos^2\omega - 2\cos\phi\cos\psi\cos\omega}{\cos^2\psi}\right]^{\frac{1}{2}}}$$

THEREFORE:

$$\frac{\cos\beta}{\cos\psi} = \frac{\sin\omega}{\left[\cos^2\psi + \cos^2\phi - 2\cos\phi\cos\psi\cos\omega\right]^{\frac{1}{2}}}$$

SO:

$$V_F = V_S \frac{\sin\omega}{\left[\cos^2\psi - 2\cos\phi\cos\psi\cos\omega + \cos^2\phi\right]^{\frac{1}{2}}}$$

APPENDIX II

SELECTED LABORATORY EXPERIMENTS IN FRACTOGRAPHY

This appendix contains descriptions of selected fractography laboratory experiments that can be performed with the barest minimum of equipment. The exercises are classic in their simplicity, and most have been performed many times over in fractographic laboratories around the world. All outlined procedures and questions are designed to illustrate, in a qualitative way, transient and tendential phenomena previously described in the text. Each experiment involves the brittle fracture of glass rods and lathes by various stress applications. The authors realize that glass possesses unique strengths and mechanical and chemical properties that are not characteristic of rocks. For example, glass can generally be considered homogeneous to the atomic level. It follows that some transient and tendential features common to fractured glass surfaces may be obscure or absent on rocks. However, the well-formed fractographic features found on rock fractures can be produced on common glass objects where they can be studied with relative ease and rapidity. The examination of fractured glass surfaces produced under controlled situations should enhance the individual's ability to qualitatively appreciate the relationships between varying stress intensities and configurations and the origin flaw size, stress to failure, and varying fracture velocities. These simple laboratory tests provide the geologist with an opportunity to gain experience in the art of "reading" the fracture stress distributions and propagation history of a fracture surface.

Please note that due to the near non-existence of test controls, any given experiment may have to be repeated several times in order to attain the best results. Finally, the point is again emphasized that stress distributions responsible for failure undergo continuous changes in intensity and orientation as the fracture propagates.

EXPERIMENTS UTILIZING GLASS LATHES

1. Obtain a number of glass microscope slides, size 3 x 1 inch (2.54 x 7.62 cm) by 1.07 mm thick and a number of square microscope slides.

2. Place a strip of Scotch tape along the face of each microscope slide to be broken in the cross-bending exercise (do not tape the slides that will be subjected to thermally-induced stresses or torsion).

3. Always wear gloves and safety glasses when completing the following experiments.

CROSS-BENDING

1. Select six microscope slides.

2. Scribe two slides with a tiny origin scratch, two slides with a larger origin scratch and leave two slides blank. Place each scribe mark perpendicular to the long slide axis and on the side opposite the tape.

3. Break each slide by cross-bending that places the scratched slide face in tension. Make a mental note of the amount of pressure needed to snap the small flaw, large flaw, and no-flaw slides (figure 1).

4. Sketch the tendential fracture trace for each slide. Identify each sketch, for example, no scribe flaw, large scribe flaw, etc. (figure 4).

5. Expose the fracture surfaces by folding the slide along the fracture utilizing the tape as a hinge (figure 2).

6. Anchor the slide in a piece of modeling clay and place under the microscope (figure 92, in text). Use oblique illumination to enhance the transient features.

7. Study all fracture surfaces and sketch the transient morphology visible on the fracture surfaces (figure 3). Label representative transient features. Mark the side of the plate that was under tension and compression during fracture. Be sure to identify each sketch with the proper slide.

8. Show by arrows on your transient sketches the direction of fracture propagation from origin to microscope slide boundaries. Indicate, by Wallner line observation, whether the fracture front was leading during propagation on the slide face under tension or compression.

9. Indicate on your tendential sketches the fracture propagation directions for all fracture events including forking fractures in the radiants (figure 4).

QUESTIONS:

1. Was the fracture, during its growth, leading near the slide face under tension or compression?

2. Which slides (large flaw, no flaw, etc.) exhibit fracture hooks? Do the fractures in these slides hook toward the slide face under tension or compression?

3. Measure the angle between the outer fractures of any fracture radiant (figure 4). Is this measured forking angle consistent with that given in the text for cross-bending fractures?

4. Within which slides (no flaw, large flaw, etc.) do the fractures fork closest to the origin? Is there a relationship between the number of fractures within a radiant and the radiant's proximity to the fracture origin? Which one of these slides failed under the greatest applied stress?

5. Why did the fractures fork?

6. Considering the fact that rocks contain many potentially serious origin flaws, what is your opinion on whether or not velocity forking, evident within the glass slides, will be prevalent in rocks?

7. Referring to your sketches, why would the determination and statistical analysis of fracture opening directions measured away from the origins on a number of fractures in a given set be meaningless?

8. Why might it be important to determine origin locations and leading sections of past fracture fronts, in relation to stratigraphic bedding tops and bottoms, for a number of fractures in a given set?

9. Where are the Wallner lines on any examined fracture surface closer together and where are they furthest apart? Why is this so? Refer to figure 28 in the text.

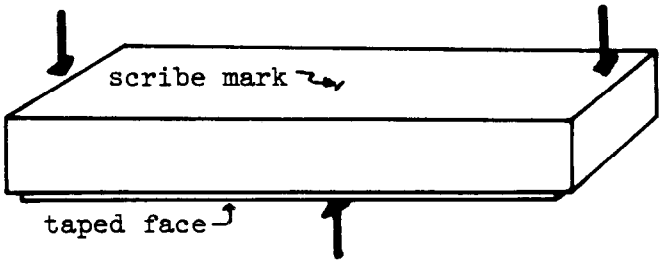

Figure 1

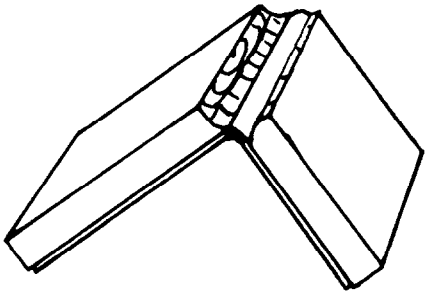

Figure 2

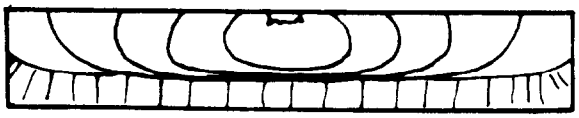

Figure 3, simplified sketch of transient fracture features

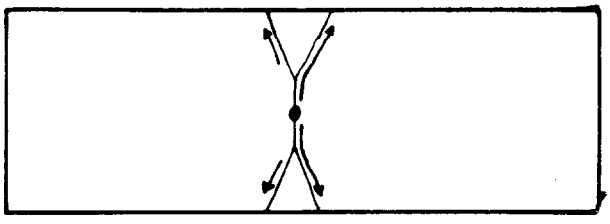

Figure 4, sketch of tendential fracture features, origin and fracture spreading directions

TORSION

1. Select three microscope slides. Using a circular motion, scour with fine sandpaper a single face of the first slide and both faces of the second slide. Do not sand either face of the third slide. It is advisable to prepare several slides for each set.

2. Place tape on the arbitrarily designated "up" face of each slide (figure 5).

3. Select a prepared slide and place four small wooden blocks, two to a face, with one on each side at the slide ends, as shown in figure 5.

4. Designate the ends of the slides that are to be twisted clockwise and counterwise: sinstral - S, dextral - D (figure 5).

5. Grasp the blocks firmly between thumbs and index fingers, with the taped side up, and twist in the previously noted clockwise and counterclockwise directions until the slide fails. Two fracture sets are usually formed.

6. Remove the wooden blocks and accurately trace on a piece of tracing paper, the tendential features on each slide. Relate each sketch to the proper slide. Note on the sketches the sides that were twisted clockwise and counterclockwise (figure 6).

7. Make note of any torsion fractures that fork. Does the forking angle agree with that given in the text for this test configuration?

8. Fold back along the tape and examine microscopically the transient features present on a number of fractures belonging to each set. Pay particular attention to fracture intersections and spreading directions. Accurately sketch the transient features of select fractures in each set (figure 7).

9. Indicate the spreading directions by arrows on all transient and tendential sketches. Show origins for examined fractures on tendential sketches by solid O's (origin on "up" face) and unfilled O's (origin on "down" face). Indicate on the sketches the slide face toward which the fractures had a tendency to hook. On the tendential sketches a solid arrow indicates an overall spreading direction and fracture leading on the "up" face. Conversely, dash-dot arrows indicate a fracture that led on the bottom face.

QUESTIONS:

1. Which slides (sanded, unsanded, etc.) are broken by fracture sets showing the greatest fracture frequency? Why is this observation so?

2. Determine from your tendential sketches the sequence of fracture set formation for each slide. Do the fractures originating on the sanded or unsanded slide faces generally form first or last? Why is this fracture sequence so?

3. Why do the fractures give the appearance of crossing each other?

4. Toward which slid face (taped "up" face or opposite) do the hooks (if formed) in each set propagate? Do the origin faces and hook directions of each fracture set agree with the pure shear stresses present on both slide faces during fracture?

5. How does the neutral surface affect hook formation?

6. Is hooking more predominant and does it occur closer to the fracture origin on fractures initiated on a sanded or unsanded face? Why is this so?

7. What geological settings might be conducive to the formation of torsion fractures?

8. Would you expect torsion fractures cutting a rock stratum to exhibit velocity induced forking and fracture hooking?

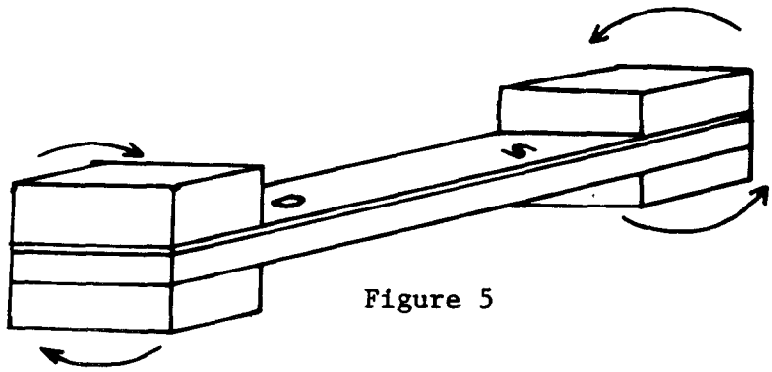

Figure 5

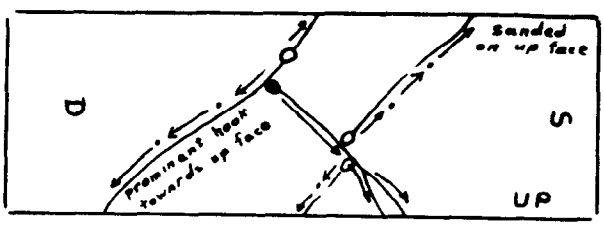

Figure 6

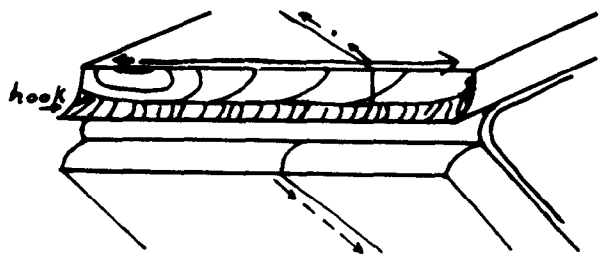

Figure 7

POINT LOAD

1. Using a circular motion sand one face of several microscope slides; sand both faces of several slides and leave several slides unsanded.

2. Place tape on one face of all slides.

3. Place an unsanded slide, tape face down, on a smooth table top. Apply pressure to the center of the slide with a hard rounded object, such as a BB, until the microscope slide fails (figure 8). Do this for several slides. Note the face to which pressure has been applied.

4. Place a slide sanded on a single face, sanded side down, on a table. Repeat step three for several slides. Note whether or not more pressure was needed to fracture the sanded as compared to the unsanded slide.

5. Place a slide, sanded on a single face, sanded side up and repeat step 4.

6. Place a slide, sanded on both faces, on the table and repeat step 4.

7. Trace the tendential fracture patterns formed on representative slides fractured in steps 3 through 7. Note on your sketch whether or not the slide was sanded and on what side (figure 9).

8. Examine the transient morphology on fractures in the sanded and unsanded slides. Locate origins, determine spreading directions, and indicate the fracture's leading edge on appropriate tendential fracture tracings as the transient features are examined. Use the previously described origin symbols and dashed or solid arrows. Sketch the transient features on representative fractures from the sanded and unsanded slide sets. Again pay particular attention to fracture intersections. See figure 50 in the text.

9. Sand a circular cover slide on one side and point load to failure with sanded face down. Are the fractures rectangular?

QUESTIONS:

1. How does the transient and tendential fracture morphology in the unsanded slides differ when compared to the sanded slides (sanded faces opposite pressured face)? Why is this so? Is the fracture morphology of the single-face sanded slides dependent on whether or not the sanded face was opposite the pressured face during fracture?

2. Are the fracture origins located on the pressured or opposite slide face? Did the fractures lead at the face opposite the applied pressure? Explain your answers, considering the relative tension and compression regions as dictated by the loading geometry.

3. Study the slides and your tendential and transient illustrations to determine the fracture chronology on all slides. Can the fractures on the unsanded slide be proven to represent a single fracture event (fracture with a single origin)?

4. Why should it require more pressure to break an unsanded slide?

5. Through which slides did the fractures propagate at the greatest velocity? Why is this so?

6. Why can the Wallner lines on the sanded slides be more pronounced?

7. What geological mechanisms could be invoked to explain natural point load fracture sets?

8. Break a previously fractured sanded slide by repeated point load applications (sanded face down). Record the relative chronology of these fractures. How do these rectangular fractures differ from systematic - nonsystematic fractures at any given location?

9. How do you explain the fact that the rectangular fractures generally form parallel to the slide boundaries?

10. How would you determine if intersecting fractures could be contributed to a central pressure or point load?

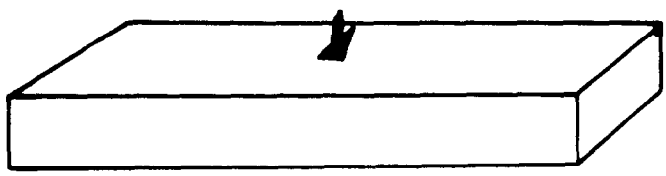

Figure 8

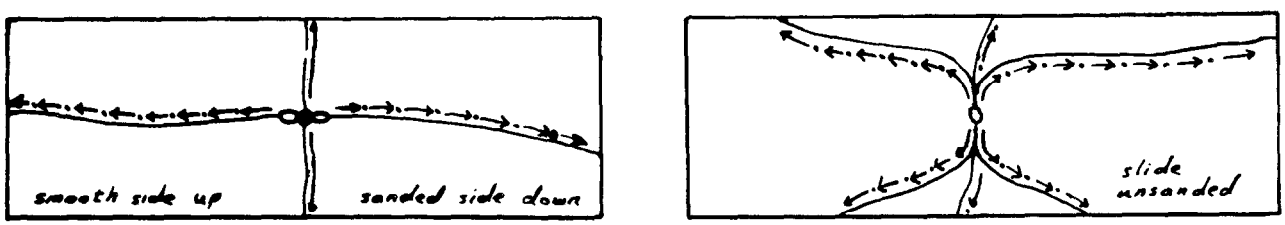

Figure 9

THERMAL FRACTURES ATTRIBUTED TO EXPANSION AND CONTRACTION

Thermal fractures can be produced in glass by applying heat from a Bunsen burner flame. The resulting fractures propagate perpendicular to the greatest principal tension and can be attributed to either expansion or contraction. For example, a fracture that initiates during heating is propagated by stresses produced by expansion. In contrast, a fracture that forms after the glass is removed from the flame must originate and grow by stresses related to contraction. Generally more heat is required to cause an expansion fracture than a contraction fracture. Consequently, the microscope slide that fails by expansion will do so explosively. The resulting tendential features will reflect a rapid fracture propagation. Expansion fractures can reach critical velocities necessary for the formation of mist, coarse velocity hackle and forking. On the other hand, contraction fractures may propagate slowly enough to allow observation of dynamic crack growth.

It has been implied that thermal cracks will have a transient and tendential morphology unique from fractures produced from other applied stress configurations. The thermal laboratory exercise will illustrate this contrasting morphology and should give added insight into the fracture propagation process. All thermal experiments should be attempted while wearing adequate face protection.

Figure 10 shows the explosive fracture patterns produced in several 3.5 x 3.5 cm x 1 mm glass plates. The plates were heated at their geometrical center and the fracture is produced by a relative tension in the immediate flame vicinity. Radial compression grows progressively less outward along any radius from the heated center. As the radial compression decreases, the circumferential stresses become tensile. This circumferential tension is maximum immediately away from the heated spot and declines toward the unheated margins of the glass plate. A fracture will originate at some pre-existing flaw in or near the zone of maximum circumferential tension. The origin is surrounded by an "ideal" fracture morphology - mirror, mist, coarse hackle, and generally exhibits 180° forking. The fracture velocity often slows immediately after forking and the fracture surface reverts from mist to mirror. Figures 10a and b illustrate that the higher the heat necessary to produce fracturing the more violent will be the fracture process. As a result the mirror will be stunted, coarse hackle will be more prevalent, and the 180° radiant will contain more forking fractures.

Several groups of thermal contraction fracture tracings are depicted in figures 11, 12, and 13. In all cases the microscope slides have been heated at a corner or edge to above the annealing point and then permitted to cool. The heated corner of a slide will at first be under great strain. However, the heated corner will become free of strain at the annealing temperature. Upon removal from the flame the slide corner becomes strained again, due to volume contraction, and a fracture, originating at the annealed - unannealed boundary, runs diagonally from one edge to another. If the slide has been heated to an adequate temperature, the contraction fracturing process can be semi-violent (less violent than an explosion fracture), and the corner will become separated. In contrast, if the slide is heated to just above the annealing temperature and allowed to cool the fracture or fractures, initiating at the annealed - unannealed boundary on the slide edges spread slowly and may not separate the corner. These slow-moving fractures follow a sinuous path as previously described by Preston (1926). The slow-moving fracture originates at

the slide edge and propagates, perpendicular to the greatest tension, along the annealed - unannealed boundary. However, away from the edges the tension can become a compression as indicated by the fractures in figure 12. This compression causes the fracture to veer toward the slide interior and stop or turn back on itself and propagate again towards the edge containing its origin point. The tensile and compressive stresses arise when the annealed corner attempts to become circular upon cooling (figure 14).

Thermal contraction fractures produced by heating a long edge form several characteristic tendential patterns illustrated in figure 13. It is not surprising that edge fracture paths are controlled by the same mechanical principles as corner fractures.

1. Place a Bunsen burner in a large open box to facilitate retrieval of broken fragments.

2. Hold a microscope slide (preferably a square one) over the Bunsen burner flame so that the reducing flame tip is in contact with the center of the slide. Hold the slide in the flame until it ruptures. Slide disintegration can be explosive. Therefore, the box should be large enough to catch the fragments.

3. Reassemble the microscope slide fragments on a piece of wide transparent tape.

4. Repeat step two with a slide that has been weakened with fine grit or sandpaper and reassemble the fragments on a piece of transparent tape.

5. Make an accurate tracing of the tendential fracture features; pay particular attention to forking and radiant locations.

6. Locate the fracture origin or origins and make sketches of select transient features. While examining the transient features, show fracture origin locations and spreading directions on your tendential traces.

CONTRACTION FRACTURES

1. Hold the corner of a microscope slide in the Bunsen burner flame until a yellow sodium flame is observed and/or the corner appears to soften.

2. Remove the slide from the flame. Failure should occur within approximately ten seconds. If failure does not occur, lightly scour the slide edges and repeat steps one and two.

3. If corner separation occurs, reassemble the slide and set it to one side.

4. Repeat steps one through three for several slides.

5. Heat the long edge of a microscope slide until a yellow sodium flame appears.

6. Remove the slide from the flame. Again failure should occur within ten seconds. Scour the slide edge and try again if there is difficulty in achieving failure.

7. If the slide becomes fragmented, reassemble the pieces on transparent tape. Repeat steps 5 and 6 with several slides.

8. Make accurate tracings of the tendential fracture morphology for all corner and edge heated slides.

9. Locate the fracture origins and spreading directions on all slides. Make sketches of transient features about select origins. Be aware that contraction fracture transient features are generally difficult to see even under proper lighting and high magnification.

QUESTIONS:

1. What transient and tendential characteristics make thermal fractures unique from fractures induced by the stress applications in previous (and following) experiments?

2. Why can expansion thermal fractures produce a 180° fork in contrast to the contraction fractures?

3. What is the ratio of the two principal tension stresses contained in the plane parallel to the long dimensions of the glass plate at the instant of expansion fracture initiation?

4. What criteria might be useful to determine whether a glass article failed by contraction or expansion thermal fracturing?

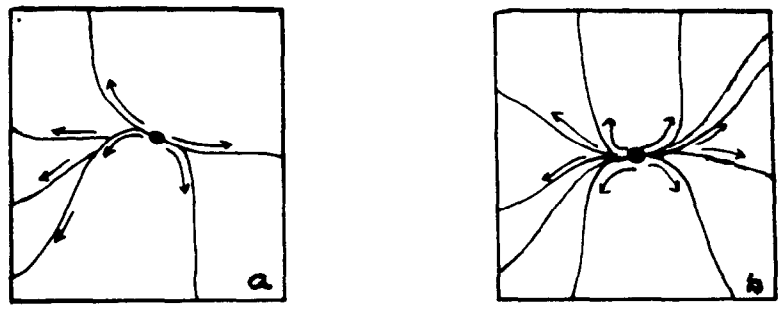

Figure 10, explosive thermal expansion fracture patterns in a glass plate.

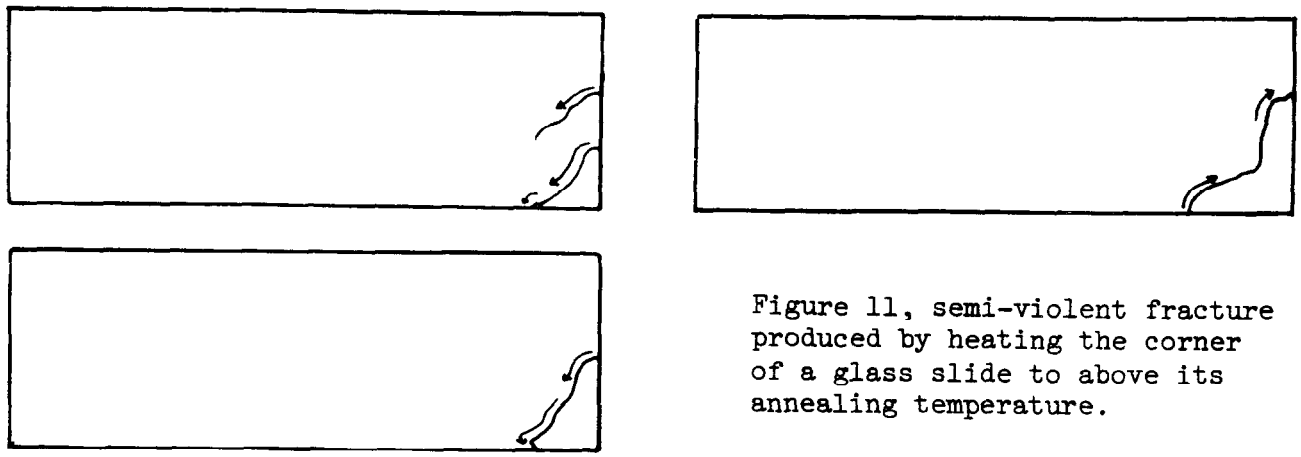

Figure 11, semi-violent fracture produced by heating the corner of a glass slide to above its annealing temperature.

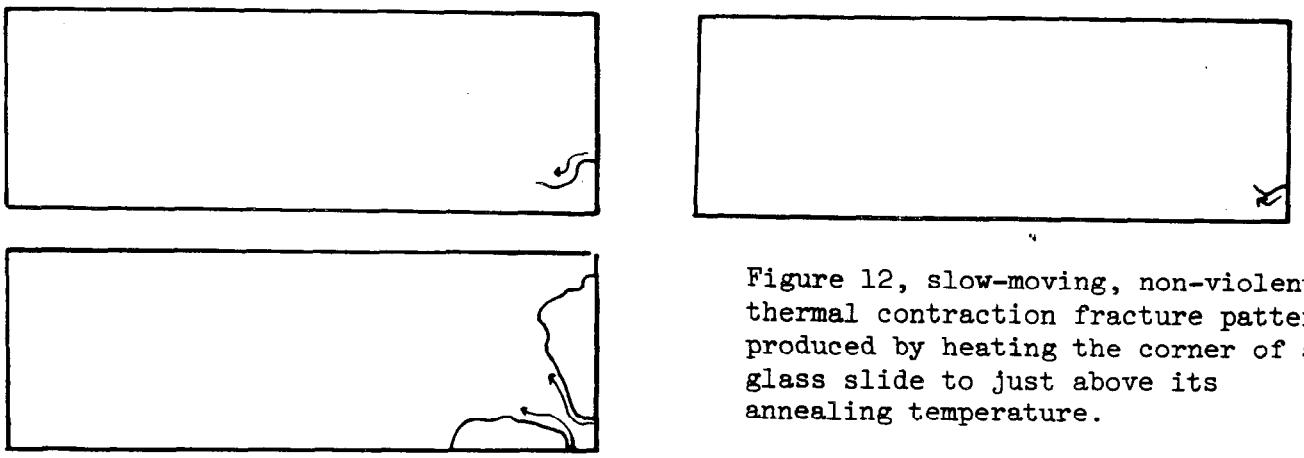

Figure 12, slow-moving, non-violent thermal contraction fracture patterns produced by heating the corner of a glass slide to just above its annealing temperature.

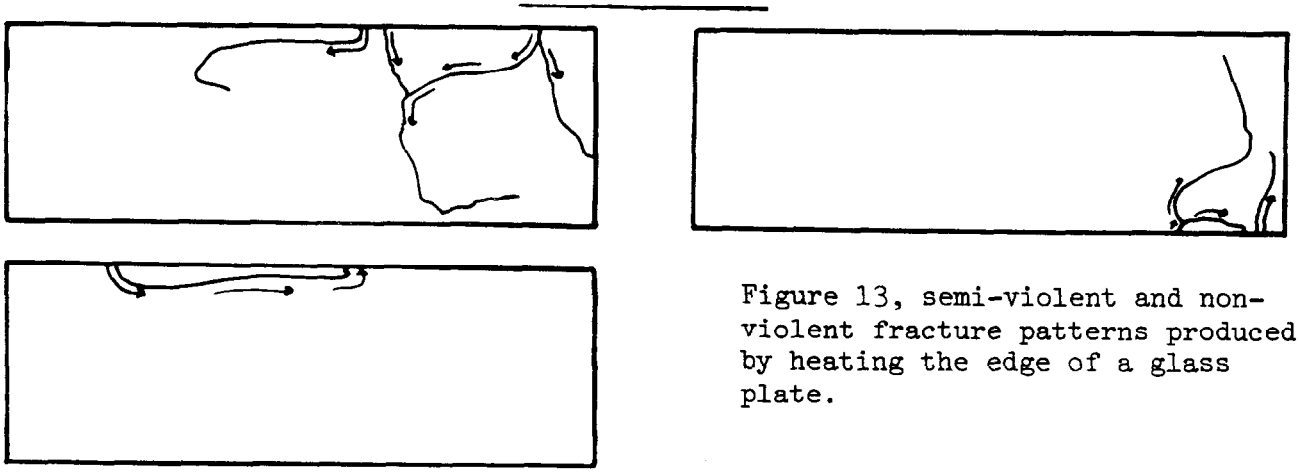

Figure 13, semi-violent and non-violent fracture patterns produced by heating the edge of a glass plate.

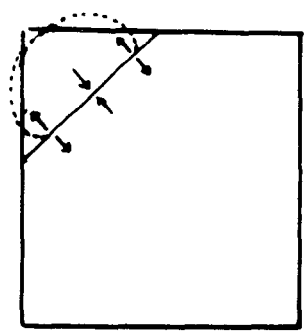

Figure 14, tensile and compressive stresses that result when an annealed corner attempts to become circular upon cooling.

EXPERIMENTS UTILIZING GLASS RODS

1. Obtain lengths of solid glass rods and fine bore (1 mm) glass capillary tubes. Rods 0.3125 in (.724 cm) in diameter work very well and can be easily broken by hand.

2. Obtain a small three-cornered file.

3. Perform all experiments using safety glasses and gloves.

CROSS BENDING

1. Select six 3-inch lengths of the solid glass rod.

2. Scribe two rods with deep origin flaws perpendicular to the rod axis. Approximately ten complete file motions are adequate.

3. Scribe two rods with shallow origin flaws perpendicular to the rod axis. One complete file motion is adequate.

4. Do not scribe the two remaining rods.

5. Break all six rods by cross-bending. Position thumbs opposite the scribe so bending will place the scribed flaw under tension. Note which rods required the greatest stress to failure.

6. Place each rod section in modelling clay and position under the microscope so that light reflection facilitates a study of the fracture surface.

7. Accurately sketch the transient fracture surface morphology. Label characteristic transient features (figure 15).

8. Sketch the tendential traces of the fractures through the rod sections. Indicate fracture propagation directions with arrows (figure 16).

QUESTIONS:

1. Which rod sections required the greatest stress to failure? Why is this so?

2. In which rods did the hooking initiate closest to the fracture origin? Why is this so?

3. If a fracture hooks and becomes parallel to a neutral surface, how must the greatest principal tension be oriented at the neutral surface?

4. Which rods contain the largest mirror surface? Why is this so?

5. What is the geometrical relationship between the pre-existing rod boundary and hackle marks?

6. How can fracture hooking, even if it does not occur at high velocities, be useful geologically in determining relative fracture chronology? How could hooking be used to determine which stratum face was under the greatest tension during fracture?

7. Calculate the fracture velocities from appropriate measurements made from intersecting Wallner lines immediately before the mist surface. What is the ratio between your calculated velocity V_c, and the bar velocity for the glass rod, V_b, (V_c/V_b)?

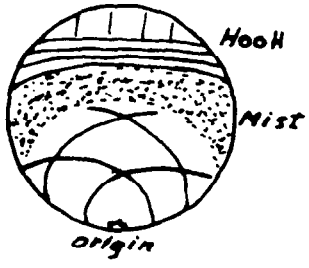

Figure 15, transient features on a fractured glass rod.

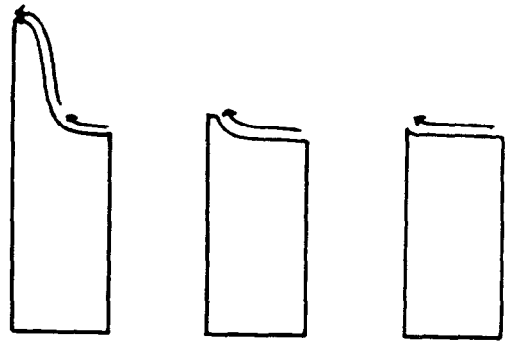

Figure 16, tendential features on fractured glass rods. Arrows indicate fracture propagation direction.

CAPILLARY TUBE

1. Select several three-inch lengths of capillary tubing.

2. Scribe the tubes with an origin flaw large enough to inhibit pronounced fracture forking.

3. Break the tubes by cross-bending in the same manner that the solid rods were broken.

4. Place each tube section in the modelling clay and position under the microscope in a manner that permits light reflection to facilitate a study of the fracture surface.

5. Accurately sketch the transient surface morphology on select fractures containing well-formed transient markings. Pay particular attention to the region around the capillary bore (figure 17).

QUESTIONS:

1. The capillary bore, acting as an "inclusion," has initiated the formation of what unique set of transient features on its "lee" side (side away from fracture origin point)? These features were not observed on the glass rod fracture surfaces.

2. Why are the winged-shaped features identified in question one actually a form of Wallner line? Why is the "tail" feature on the lee side of the inclusion actually a form of hackle? How is this feature formed?

3. Is there a relationship between the tail and the fracture propagation direction?

4. How must the principal stresses be situated about the free surfaces of the capillary bore?

5. What role might these inclusion-initiated features play in the formation of geological plumose structure?

6. Examine the transient features and form an opinion on whether or not the fracture velocity was altered about the capillary bore.

7. Calculate the fracture velocity, using intersecting Wallner lines, at:

   a. a pair of intersecting Wallner lines just before the inclusion.

   b. the intersection of the inclusion-related Wallner lines (gull wings).

   Has the capillary bore acted to slow down or accelerate the fracture process?

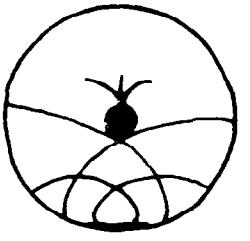

Figure 17, transient surface morphology of a fracture surface through a capillary tube.

TORSION FRACTURES

1. Select several glass rods approximately three inches in length.

2. Scour the rods with fine-grained sandpaper.

3. Wrap two bands of masking tape, each with approximately ten layers, around each glass rod. Place the bands approximately one-half inch apart (figure 18).

4. Using two pairs of pliers, grasp the rod with the pliers at the taped bands. Grip firmly enough to prevent the rod from slipping and apply a torsion stress to the rod until it fails. Note which rod end was twisted clockwise and which counterclockwise (figure 18).

5. Examine the torsion fractures under the microscope.

6. Select the best-formed spiraled torsion fracture and accurately sketch its transient morphological features. Mark the spreading directions with arrows.

7. Sketch the rod with its axis depicted parallel to the paper. Show the spiral tendential fracture trace and torsion stress directions at the rod top and bottom.

QUESTIONS:

1. Graphically resolve the simple shear stresses indicated by the torsion arrows on your tendential fracture trace sketch into a pure shear stress state. Are the resultant principal tension and compression directions in accord with the geometry of the fracture trace?

2. Was the tip of the torsion fracture propagated by the direct action of shear, tensile or compressive stresses?

3. Judging from your simple to pure shear stress resolution, what angle should the helical fracture trace make with the rod axis? Does this angle approximate the angle actually formed in the glass rod?

4. Why did the fracture originate at the exterior of the glass rod?

5. The outer core barrel, to which the drill bit is attached, turns to the right about a stationary inner barrel holding the core sample. Assume that for some unfortunate reason the inner barrel is forced to turn and the circular core section jams in the revolving inner barrel. How will the resulting coring-induced tension fracture be oriented with respect to the core axis?

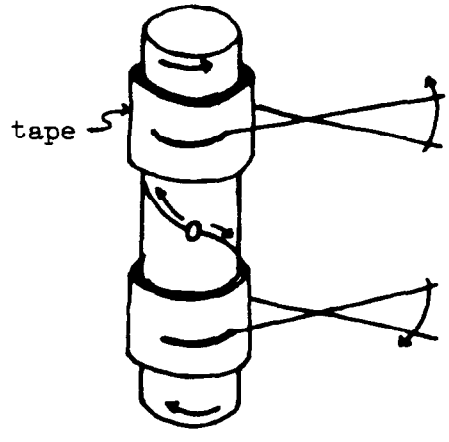

Figure 18, method for inducing torsion failure in a glass rod.

GLASS PLATE AND PROJECTILE

A projectile striking a glass plate initiates a unique fracture pattern familiar to everyone; especially those of us who, as children, owned or had access to a BB gun. This pattern is a composite of fracture events that affords the student a classic exercise in fractographic investigation. Projectile impact fractures possess a characteristic relationship to each other and the tensile stresses that initiated them. Also the chronology of fracture formation is consistent. All these sequential events can easily be deduced from transient and tendential fracture characteristics.

The cone with apex at impact point, and radiating fractures, are produced by tensile stresses initiated by the projectile. A compression exists at the point of impact. However, deflection of the glass produces a ring of radial tension around the impact point. On the side of the plate opposite the impact point the glass is subject to an outward deflection and concomitant tension. The first

fractures occur circumferentially around the impact point and spread inward initiating the cone. The cone fracture surface possesses a characteristic morphology progressing from mirror through mist to coarse hackle. A second fracture set radiates outward from the cone surface. These fractures originate mainly within the initial coarse hackle region on the cone surface. The radiating fractures propagate faster than the cone and cause distal cone sections to be truncated. A third radiating fracture set can be initiated at the point of maximum glass deflection and extension opposite the impact point. This set is propagated by a tension uniform along all radii and may form radiants forking at 180°.

A exceptionally thick piece of glass or glass plate backed by a rigid support, when struck by a high velocity projectile, can produce multiple cones giving rise to a cone-in-cone structure. Generally fracture effects attributed to projectile impact will vary with 1) mass and velocity of the projectile, 2) glass thickness and shape, 3) damping effect of edge clamping, 4) elastic properties of the backing material for cone-in-cone.

1. Place a one-quarter or three-eighths inch glass plate, approximately four by four inches on edge in a bucket of sand. Thicker glass generally allows for the formation of a larger, better preserved, cone. Scotch tape strips placed on the back of the plate will keep the glass from falling into pieces upon projectile impact.

2. Place the sand bucket and plate in a large box set on its side and open at the top. Hang a piece of heavy clear plastic or vinyl over the open box top. Cut a small hole in the plastic through which the BB gun barrel can be placed.

3. Shoot the glass in its center with a BB.

4. Retrieve the glass pieces, being especially careful to find the cone. Repeat for several glass plates.

5. Sketch the transient and tendential fracture results observed on the glass plate. Radial fractures can be folded back along the tape. If a complete cone is present, make detailed sketches of its fracture morphology.

QUESTIONS:

1. Why does the cone fracture originate circumferentially around the impact point instead of at the impact point itself?

2. Are the radial fractures propagated by a principal tension that is greatest on the impact face of the glass plate or the opposite side?

3. From your sketches, what evidence do you have to indicate that the cone fracture formed before the radial fractures?

4. From your sketches, what evidence do you have that indicates the radial fractures, once initiated, propagated faster than the cone fracture?

5. Explain how you might use fractographic features to determine if a geological cone-in-cone structure was caused by impact.

6. Why would forking of radial fractures, originating at the cone's coarse hackle shoulder, be more prevalent if a higher velocity projectile were used?

☆ U.S. GOVERNMENT PRINTING OFFICE: 1979—640-092/ 1276